

MANITOBA

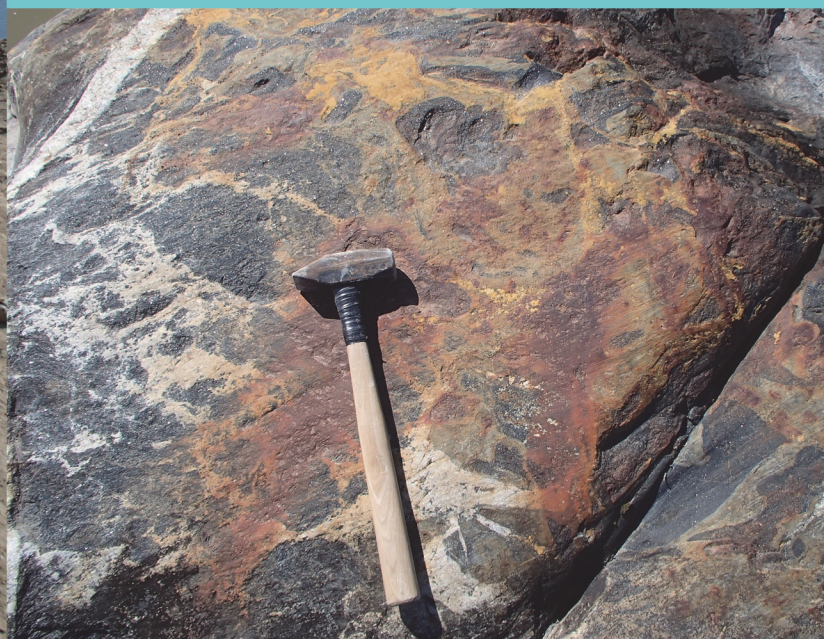
INVEST. BUILD. GROW



GEOSCIENTIFIC REPORT GR2019-1

GEOLOGY OF THE SOUTHERN
INDIAN LAKE AREA, NORTH-
CENTRAL MANITOBA
(PARTS OF NTS 64G1, 2, 7–10,
64H3–6)

Manitoba Geological Survey





Geoscientific Report GR2019-1

**Geology of the Southern Indian Lake area, north-central
Manitoba (parts of NTS 64G1, 2, 7–10, 64H3–6)**

**by T. Martins, P.D. Kremer, D. Corrigan and N. Rayner
Manitoba Geological Survey
Winnipeg, 2019**

©Queen's Printer for Manitoba, 2019

Every possible effort is made to ensure the accuracy of the information contained in this report, but Manitoba Growth, Enterprise and Trade does not assume any liability for errors that may occur. Source references are included in the report and users should verify critical information.

Any third party digital data and software accompanying this publication are supplied on the understanding that they are for the sole use of the licensee, and will not be redistributed in any form, in whole or in part. Any references to proprietary software in the documentation and/or any use of proprietary data formats in this release do not constitute endorsement by Manitoba Growth, Enterprise and Trade of any manufacturer's product.

When using information from this publication in other publications or presentations, due acknowledgment should be given to the Manitoba Geological Survey. The following reference format is recommended:

Martins, T., Kremer, P.D., Corrigan, D. and Rayner, N. 2019: Geology of the Southern Indian Lake area, north-central Manitoba (parts of NTS 64G1, 2, 7–10, 64H3–6); Manitoba Growth, Enterprise and Trade, Manitoba Geological Survey, Geoscientific Report GR2019-1, 51 p. and 4 colour maps at 1:50 000 scale.

NTS grid: 64G1, 2, 7, 8, 9, 10, 64H3, 4, 5, 6

Published by:

Manitoba Growth, Enterprise and Trade
Manitoba Geological Survey
360–1395 Ellice Avenue
Winnipeg, Manitoba
R3G 3P2 Canada

Telephone: 1-800-223-5215 (General Enquiry)

204-945-6569 (Publication Sales)

Fax: 204-945-8427

E-mail: minesinfo@gov.mb.ca

Website: manitoba.ca/minerals

ISBN No.: 978-0-7711-1596-7

This publication is available to download free of charge at manitoba.ca/minerals

Cover illustrations:

Left: Sandy beach at Southern Indian Lake.

Right: Altered and oxidized amphibolitic rocks in central Southern Indian Lake.

Abstract

The Southern Indian Lake project covers an extensive area of more than 3500 km² in north-central Manitoba. Field mapping took place between 2008 and 2016, and involved regional-scale geological mapping (1:50 000), sampling, and lithogeochemical, isotopic and geochronological studies of supracrustal and plutonic rocks. The northern portion of Southern Indian Lake, as well as Northern Indian, Gauer and Thorsteinson lakes, are dominated by granitoid bodies of different ages, including exposures of the Chipewyan-Wathaman batholith. The central portion of Southern Indian Lake, as well as Pine and Partridge Breast lakes, are dominated by supracrustal rocks.

Rock units were grouped according to their lithogeochemical and isotopic characteristics, as well as temporal affinities. Five different assemblages of supracrustal rocks, as well as different ages of plutonism, were identified and characterized. The oldest rocks are granodiorite gneiss dated at ca. 2520 Ma and interpreted to represent basement rocks for the Southern Indian domain. The Churchill River assemblage is composed of juvenile pillow basalt with intervening clastic sedimentary rocks, interpreted to be a relic of the Manikewan ocean or, alternatively, a back-arc basin of a juvenile oceanic arc. The Pukatawakan Bay assemblage, bracketed between ca. 1988 and 1890 Ma, consists mainly of massive to pillowed, juvenile metabasaltic rocks and associated basinal metasedimentary rocks. The Partridge Breast Lake assemblage is dominated by

bimodal continental-arc volcanic and volcanoclastic rocks associated with basinal metasedimentary rocks, and is intruded by the ca. 1860–1855 Ma Chipewyan-Wathaman batholith. The Strawberry Island assemblage is interpreted to have been deposited in a foreland or molasse-type basin environment during a period of about 11 m.y. The youngest sequence of supracrustal rocks identified in the study area, the Whyte Bay assemblage, is characterized by fluvial-alluvial orogenic sediments that unconformably overlie the Strawberry Island assemblage. The Whyte Bay assemblage has temporal links to the Sickle Group arkosic rocks in the Lynn Lake belt. A variety of granitoid rocks, dominantly monzogranite and granodiorite in composition and ca. 1896 to 1829 Ma in age, are found throughout the Southern Indian Lake area. Intermediate and mafic intrusions of similar ages are also present but less common. The youngest intrusions recorded in the vicinity of the map area are beryl-columbite pegmatites from the South Bay pegmatite group, with an interpreted crystallization age of ca. 1773 Ma.

The Southern Indian Lake area has seen little exploration activity in the last several decades, but recent work revealed a high potential for a variety of mineral deposits, including Homestake-type iron-formation Au, intrusion-related Au systems, volcanogenic massive sulphide, magmatic Ni–Cu–platinum-group elements (PGE), and diamonds. Follow-up work should be considered to properly evaluate the economical potential of this area of Manitoba.

Abstract	iii
Introduction.....	1
Previous work	1
Methods and scope	1
Regional geological setting	3
Geology of the Southern Indian Lake area	5
Deformation and metamorphism	5
Archean rocks	7
Granodiorite gneiss (unit 1).....	7
Rocks of uncertain age	7
Intermixed gneissic suite (units 2 and 3)	7
Paleoproterozoic rocks.....	8
Churchill River assemblage (unit 4)	8
Pukatawakan Bay assemblage (units 5–8).....	8
Greywacke paragneiss (unit 5)	9
Basalt and derived amphibolite, massive to pillowed, minor pillow-fragment breccias (unit 6)	9
Psammitic and pelitic greywacke, minor iron formation, graphitic and sulphidic layers (unit 7).....	11
Intermediate, mafic and ultramafic intrusive rocks (subunits 8a–c).....	12
Turtle Island complex (unit 9).....	12
Northern Indian Lake pluton (unit 10).....	12
Partridge Breast Lake assemblage (units 11–16).....	12
Feldspathic and aluminous migmatitic greywacke, minor conglomerate and calcsilicate (subunits 11a–d)	13
Massive and pillowed amygdaloidal basalt, locally with minor silicate- and sulphide-facies iron formation (unit 12) ..	13
Intermediate to felsic volcanic rocks, tuff and resedimented tuff (subunits 13a, b).....	13
Mafic to intermediate volcanoclastic and epiclastic rocks with minor flows (subunits 14a, b, c).....	15
Greywacke, mudstone and polymictic conglomerate (subunits 15a, b)	15
Intermediate, mafic and ultramafic intrusive rocks (unit 16).....	15
Chipewyan-Wathaman batholith (unit 17)	17
Granite, granodiorite and tonalite (unit 18)	17
Strawberry Island assemblage (unit 19)	18
Whyme Bay assemblage (unit 20)	19
Late intrusive rocks (unit 21)	19
Thorsteinson Lake pluton (unit 22).....	20
Biotite granite, pink monzogranite and other K-feldspar-rich granitoids (unit 23).....	21
Granitic pegmatite (unit 24)	22
Mackenzie dikes (unit 25).....	22
Lithogeochemistry and Sm-Nd isotopes.....	22
Sampling and analytical methods	22
Analytical results.....	24
Archean rocks (unit 1)	24
Churchill River assemblage (unit 4)	24
Pukatawakan Bay assemblage	29
Partridge Breast Lake assemblage	32
Mafic rocks.....	32
Felsic rocks	33

Granitoid rocks	34
U-Pb geochronology	37
Methodology	37
Sensitive high-resolution ion microprobe (SHRIMP)	37
Laser-ablation, multicollector, inductively coupled plasma–mass spectrometry (LA-MC-ICP-MS)	37
SHRIMP results.....	38
Garnet-sillimanite greywacke, Pukatawakan Bay assemblage (unit 5; sample 107-09-050A).....	38
Rhyolite, Partridge Breast Lake assemblage (subunit 13b; sample 107-09-047A)	38
Garnet greywacke gneiss, Partridge Breast Lake assemblage (subunit 11b; sample 107-09-295A).....	38
Monzogranite, south of the Missi Falls Control Structure (unit 18; sample CXA-02-D70b)	40
Northern Indian Lake pluton (subunit 10a; sample 107-09-041A).....	40
LA-MC-ICP-MS results	40
Orthogneiss, Northern Indian Lake (subunit 10a; sample 107-09-041B)	40
Polymictic conglomerate, Strawberry Island assemblage (subunit 19a; sample 107-09-164)	40
Thorsteinson monzogranite (unit 20; sample 113-13-THOR-01).....	41
Beryl-columbite pegmatite, South Bay pegmatite field.....	42
Summary of U-Pb data	42
Pukatawakan Bay assemblage (>1988 to 1890 Ma)	42
Partridge Breast Lake assemblage (>1883 to 1860 Ma)	42
Strawberry Island assemblage (>1860 to 1849 Ma)	42
Whyme Bay assemblage (>1832 to 1829 Ma)	42
Tectonic implications	43
Circa 2.5 Ga	43
Circa 1.98–1.89 Ga	43
Circa 1.89–1.87 Ga	44
Circa 1.87–1.83 Ga	44
Less than 1.83 Ga	45
Economic considerations.....	45
Volcanogenic massive sulphide.....	45
Magmatic Ni-Cu-platinum-group elements (PGE)	45
Gold mineralization.....	45
Diamonds.....	46
Other types of mineral deposits	46
Acknowledgments.....	46
References.....	47

TABLES

Table 1: Main supracrustal assemblages in the Southern Indian domain and possible tectonostratigraphic correlation with the Rottenstone domain in Saskatchewan	4
Table 2: Lithogeochemical data for representative samples of lithological units in the Southern Indian Lake area	25
Table 3: Samarium-neodymium isotopic data for rock samples from the Southern Indian Lake area	27

FIGURES

Figure 1: Simplified geology of the Southern Indian Lake area	2
Figure 2: Tectonic elements of the THO in northern Manitoba and Saskatchewan	3

Figure 3: Outcrop photos of structures in the Southern Indian Lake area	6
Figure 4: Outcrop photographs of orthogneiss	7
Figure 5: Outcrop photographs of rocks from the Churchill River assemblage	8
Figure 6: Outcrop photographs of greywacke from the Pukatawakan Bay assemblage	9
Figure 7: Outcrop photographs of volcanic rocks of the Pukatawakan Bay assemblage	10
Figure 8: Outcrop photographs of sedimentary rocks of the Pukatawakan Bay assemblage	11
Figure 9: Outcrop photographs of volcanic and volcanoclastic rocks of the Partridge Breast Lake assemblage	14
Figure 10: Outcrop photos of epiclastic rocks of the Partridge Breast Lake assemblage	16
Figure 11: Mafic intrusions of the Partridge Breast Lake assemblage	17
Figure 12: Outcrop photographs of felsic intrusive rocks	18
Figure 13: Outcrop photographs of the Strawberry Island assemblage	19
Figure 14: Outcrop photographs of clastic sedimentary rocks of the Whyte Bay assemblage	20
Figure 15: Outcrop photographs of late felsic intrusive units	21
Figure 16: Major-element and immobile trace-element discrimination diagrams for basalt from the Churchill River and Pukatawakan Bay assemblages	29
Figure 17: Chondrite-normalized extended-element diagrams and N-MORB normalized extended-element diagrams for Churchill River and Pukatawakan Bay assemblages	30
Figure 18: Geochemical discrimination diagrams for the volcanic rock samples from the Churchill River and Pukatawakan Bay assemblages	31
Figure 19: Major-element and immobile trace-element discrimination diagrams for volcanic rocks of the Partridge Breast Lake assemblage	33
Figure 20: Extended-element diagrams for rocks of the Partridge Breast Lake assemblage	34
Figure 21: Geochemical discrimination diagram for rocks of the Partridge Breast Lake assemblage	35
Figure 22: Geochemical discrimination diagrams for granitoid rocks	36
Figure 23: Range of values of ϵ_{Nd} for granitoid rocks from the Southern Indian Lake area plotted against their determined or inferred U-Pb age	37
Figure 24: Results from SHRIMP U-Pb geochronological analyses	39
Figure 25: Results from LA-MC-ICP-MS U-Pb geochronological analyses	41

MAPS

- Map GR2019-1-1: Bedrock geology of the Southern Indian Lake area (north), Manitoba (parts of NTS 64G7–10)
- Map GR2019-1-2: Bedrock geology of the Southern Indian Lake area (southwest), Manitoba (parts of NTS 64G1, 2, 7, 8)
- Map GR2019-1-3: Bedrock geology of the Southern Indian Lake area (southeast), Manitoba (parts of NTS 64G1, 8, 64H4, 5)
- Map GR2019-1-4: Bedrock geology of the Northern Indian Lake area, Manitoba (parts of NTS 64H3, 5–7)

DIGITAL DATA

Data Repository Item DRI2019001: Lithogeochemical, assay and U-Pb geochronological data for the Southern Indian domain, north-central Manitoba (parts of NTS 64G1, 2, 7–10, 64H3–6)¹

¹ MGS Data Repository Item DRI2019001 containing the data or other information sources used to compile this report is available online to download free of charge at <https://www.gov.mb.ca/iem/info/library/downloads/index.html>, or on request from minesinfo@gov.mb.ca, or by contacting the Resource Centre, Manitoba Growth, Enterprise and Trade, 360–1395 Ellice Avenue, Winnipeg, Manitoba, R3G 3P2, Canada.

Introduction

This report presents the results from regional bedrock geological mapping in parts of the Southern Indian domain of the Paleoproterozoic Trans-Hudson orogen (THO) in Manitoba. The study area encompasses Southern Indian, Partridge Breast, Pine and Northern Indian lakes, and parts of Gauer and Thorsteinson lakes. The Southern Indian domain is dominated by variably migmatitic metasedimentary rocks with screens of metavolcanic rocks, and variable amounts of metaplutonic rocks (e.g., Corrigan et al., 2007; Kremer et al., 2009b; Martins, 2015a, b). Metavolcanic and metasedimentary rocks in the area have been historically correlated with parts of the Wasekwan and Sickie groups in the Lynn Lake–Leaf Rapids domain (e.g., Cranstone, 1972; Frohlinger, 1972), which host several types of mineral deposits: volcanogenic massive sulphide (VMS), orogenic Au, magmatic Ni-Cu, and carbonatite with rare-earth-element (REE) mineralization.

Re-evaluating bedrock geology at Southern Indian Lake was a subproject of the Geological Survey of Canada's (GSC) collaborative Targeted Geoscience Initiative, Phase 3 (TGI-3). The Southern Indian Lake mapping project was designed to map and characterize the geology of the Southern Indian domain in greater detail and to provide an updated geoscientific understanding of the area, assess its mineral potential and test regional correlations with similar rocks elsewhere in the THO. This report details a newly revised tectonostratigraphic framework of the Southern Indian domain that is based on field characteristics, petrography, whole-rock geochemistry, tracer-isotope (Sm-Nd) analyses and high-precision U-Pb geochronology.

Previous work

The first geological investigations of the Southern Indian Lake area were conducted by the GSC in the early 20th century, initially by McInnes (1909, 1913) at a scale of 1:1 013 760 and then by Wright (1953) with mapping of the southern part of Southern Indian Lake at a scale of 1:253 440. Quinn (1960) carried out mapping of selected areas of Southern Indian Lake at a scale of 1:15 840, and Kretz (1967) focused on granitoid rocks at Northern Indian Lake. In the late 1960s, the Manitoba Geological Survey (MGS) initiated a large-scale mapping and prospecting program to examine the entire Southern Indian Lake area, including the Churchill River–Granville Lake area to the southwest. The program resulted in a series of reports with accompanying maps (e.g., Campbell, 1972; Cranstone, 1972; Frohlinger, 1972; Steeves and Lamb, 1972; Thomas, 1972). Subsequently, a regional correlation program took place in this area in the late 1970s (McRitchie, 1978). From the late 1960s to mid-1980s, exploration focused on base-metal mineralization was carried out by a number of companies (e.g., Sherritt Gordon Mines Ltd., Hudson Bay Exploration and Development Company Limited, Canadian Nickel Company Limited) and resulted in several airborne geophysical surveys and diamond drilling (e.g., Assessment Files 91649, 90174, 90176, 90178,

Manitoba Growth, Enterprise and Trade, Winnipeg) that led to the discovery of various showings and conductors. In the mid-1980s, all exploration activity ceased in the Southern Indian Lake area.

Lenton and Corkery (1981) conducted mapping of the Lower Churchill River area at a scale of 1:100 000, and Corkery followed up with 1:50 000 scale mapping from south of Partridge Breast Lake to west of Gauer Lake (Corkery, 1993; Corkery and Lenton, 1993) and the Pukatawakan Bay area (Corkery, 1995). In the early 2000s, the Southern Indian Lake area was included in the GSC's TGI-3 program, a collaborative effort designed to examine and update models of the lithotectonic evolution, and base- and precious-metal potential of the Paleoproterozoic THO, including the Kiseynew, Lynn Lake–Leaf Rapids and Southern Indian Lake domains in Manitoba and their equivalents in Saskatchewan (Corrigan et al., 1999, 2002, 2007; Corrigan and Rayner, 2002; Rayner and Corrigan, 2004). The main focus of the Flin Flon TGI-3 program, which included collaborators from the GSC, the MGS, the Saskatchewan Geological Survey, Laurentian University, the University of Manitoba and local industry geologists, was to better constrain the volcanic and hydrothermal systems that affect and control the setting and location of VMS deposits in the Flin Flon belt. A secondary goal of the Flin Flon TGI-3 program was to extend that knowledge to other poorly constrained, volcanic-dominated Paleoproterozoic terranes in the THO with known endowments of, or potential for, VMS deposits. Mapping by the MGS at Southern Indian Lake was initiated as a subcomponent of the TGI-3 program in 2008.

Methods and scope

The main objectives of the Southern Indian Lake project are to 1) update the existing geological maps in parts of the Southern Indian domain; 2) assess and document the mineral-resource potential of this area; and 3) provide a comprehensive geological interpretation of the area based on structural, litho-geochemical, Sm-Nd isotopic and geochronological data that can be used as a basis for regional comparison with volcanic and sedimentary terranes of similar age elsewhere in the THO.

The Southern Indian Lake project commenced in 2008 with 1:25 000 scale mapping of the Pukatawakan Bay area in west-central Southern Indian Lake (Kremer, 2008a, b) and continued in the summer of 2009 with 1:50 000 scale mapping between Southern Indian, Partridge Breast and Gauer lakes (Kremer et al., 2009a, b). After a hiatus, the project continued with 1:50 000 scale mapping of 1) the Northern Indian Lake area in 2014 (Kremer and Martins, 2014a, b); 2) the northern basin of Southern Indian Lake in 2015 (Martins, 2015a, b); and 3) the central part of Southern Indian Lake in 2016 (Martins, 2016a, b). Preliminary maps and reports of activities for the different map areas were released after each field season, and a revised, final geological compilation map at 1:50 000 scale, composed of four sheets, is included herein as Maps GR2019-1-1 to -4. Figure 1 presents the simplified geology of the Southern

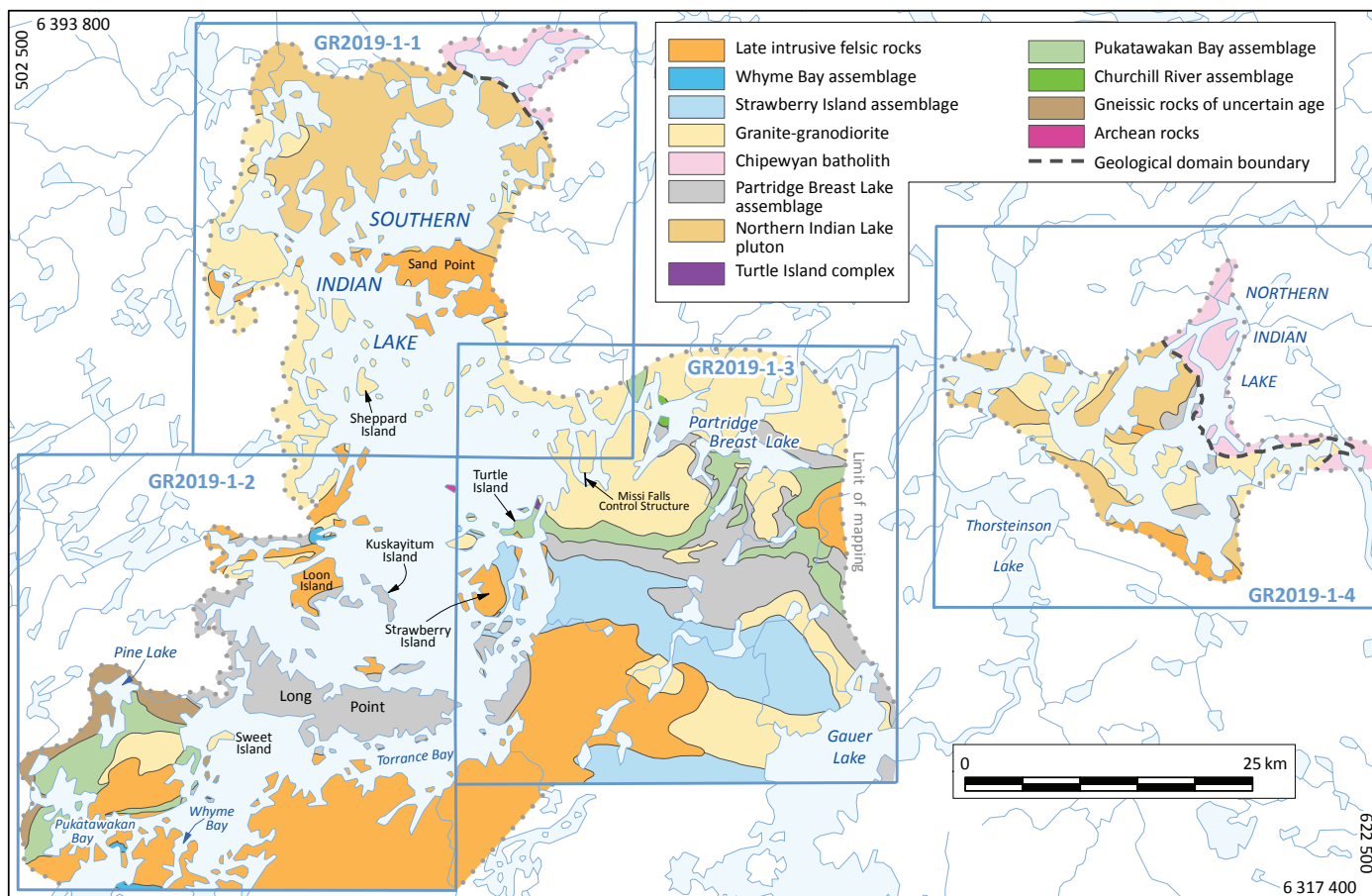


Figure 1: Simplified geology of the Southern Indian Lake area, showing the main supracrustal assemblages and major intrusions. Outlines are for Maps GR2019-1-1 to -4.

Indian Lake area and layout of the four map sheets that accompany this report.

Southern Indian Lake is accessible by all-weather road, via Provincial Road 391 from Thompson to Leaf Rapids, then via Provincial Road 493 to the nearest community on the southern part of the lake (O-Pipon-Na-Piwin; South Indian Lake), and from there by boat. For the Southern Indian Lake project, access was gained by fixed-wing float plane from Thompson, Manitoba. In 2008, small camps were set up on Pukatawakan Bay of Southern Indian Lake and on Pine and Partridge Breast lakes. In 2009, a camp was set up at Manitoba Hydro's Missi Falls Control Structure. In 2014, the field crew had a camp on Northern Indian Lake. In 2015, a camp was set up close to Sand Point on Southern Indian Lake and, in 2016, the camp was located just north of Long Point, also on Southern Indian Lake. Shoreline exposures were accessed and mapped by small inflatable boat from the various field camps; outcrop exposures inland were accessed by foot traverse using GPS and orthorectified SPOT satellite imagery (Airbus Defence and Space, 2016). In early July 2009, a helicopter was used to investigate areas not accessible via the above methods.

In areas of poor bedrock exposure, mapping was assisted by a high-resolution, residual total-field aeromagnetic survey conducted in the spring of 2008 by the GSC (Coyle and Kiss,

2008), and total-field magnetic intensity imagery (Natural Resources Canada, 1984). The detailed aeromagnetic survey provides an excellent complement to bedrock mapping by enabling more accurate interpretations in areas with limited or no outcrop.

All outcrops visited during the course of mapping were documented, described, measured and, where applicable, sampled and photographed. In the field, intrusive rocks were classified and named according to estimated modal mineralogy, following the classification of Streckeisen (1967). Subsequently, thin sections from the granitoid rocks were point-counted to obtain modal analyses. Representative samples were collected from all major lithological units and thin sections were cut to establish the petrographic character of units. Samples collected for whole-rock geochemical analyses ($n = 231$) and assay ($n = 68$) were submitted to Activation Laboratories Ltd. (Ancaster, Ontario) for analysis by inductively coupled plasma-mass spectrometry (ICP-MS) and inductively coupled plasma-emission spectrometry (ICP-ES). Selected samples ($n = 37$) were submitted to R.A. Creaser at the University of Alberta Radiogenic Isotope Facility for isotopic Sm-Nd analysis. Samples collected for U-Pb geochronology ($n = 22$) were analyzed using the sensitive high-resolution ion microprobe (SHRIMP) at the GSC (Ottawa, Ontario); and by isotope

dilution–thermal ionization mass spectrometry (ID-TIMS) and laser-ablation inductively coupled plasma–mass spectrometry (LA-ICP-MS) at the Radiogenic Isotope Facility of the University of Alberta (Edmonton, Alberta) and at the Department of Earth Sciences, University of New Brunswick (Fredericton, New Brunswick).

During the last decade, various authors released partial results from the geochronology studies (e.g., Rayner and Corrigan 2004; Kremer et al., 2009b; Rayner, 2013; Martins and McFarlane 2016a, b); therefore, this report includes only unpublished materials and makes reference to the previously published data. Full geochemical, isotopic and U-Pb geochronological unpublished data can be found in Data Repository Item DRI2019001², as well as in Tables 2 and 3 of this report.

Shoreline mapping at Southern Indian Lake and along the Lower Churchill River can be complicated by Manitoba Hydro's Churchill River Diversion, located in the central area of Southern Indian Lake where it drains into the Lower Churchill River. This control structure has been in operation since 1977, diverting water into the Burntwood and Nelson river systems. Water levels both upstream and downstream of the Missi Falls Control Structure are highly variable as a result of changes in outflow to the Churchill River at Missi Falls. Any planned work in the Southern Indian Lake or Lower Churchill River areas should bear this factor in mind.

Regional geological setting

The term 'Trans-Hudson orogen' (THO) was introduced by Hoffman (1981) and refers to the site of closure of the Manikewan Ocean (Stauffer, 1984). This represents a Paleoproterozoic zone of collision between the Superior craton and the western Churchill province. More recently, an overview by Corrigan et al. (2009) described the THO as an area of continuous structural and metamorphic overprint caused by ca. 1.83–1.80 Ga collision between the Superior craton, the Reindeer zone (the region between the western Churchill province and Superior craton; Stauffer, 1984), and the previously amalgamated Rae, Hearne and Slave cratons north of the Manikewan Ocean.

The Southern Indian domain and the Lynn Lake–Leaf Rapids, Flin Flon and Kiseynew domains form the northern flank of the THO in Manitoba (Figure 2). The Southern Indian domain is predominantly composed of variably migmatitic metasedimentary rocks, various granitoid units and less abundant belts dominated by metavolcanic rocks (Corrigan et al., 2007). The metasedimentary and metavolcanic rocks have been historically assigned to the Sickie and Wasekwan groups, respectively (Cranstone, 1972; Frohlinger, 1972). The Southern Indian domain is bounded to the south by the Lynn Lake–Leaf Rapids domain and, to the north and east, was intruded by the voluminous ca. 1.86–1.85 Ga Chipewyan-Wathaman batholith and the possibly related Baldock pluton (e.g., Lenton and Corkery,

² MGS Data Repository Item DRI2019001 containing the data or other information sources used to compile this report is available online to download free of charge at <https://www.gov.mb.ca/iem/info/library/downloads/index.html>, or on request from minesinfo@gov.mb.ca, or by contacting the Resource Centre, Manitoba Growth, Enterprise and Trade, 360–1395 Ellice Avenue, Winnipeg, Manitoba R3G 3P2, Canada.

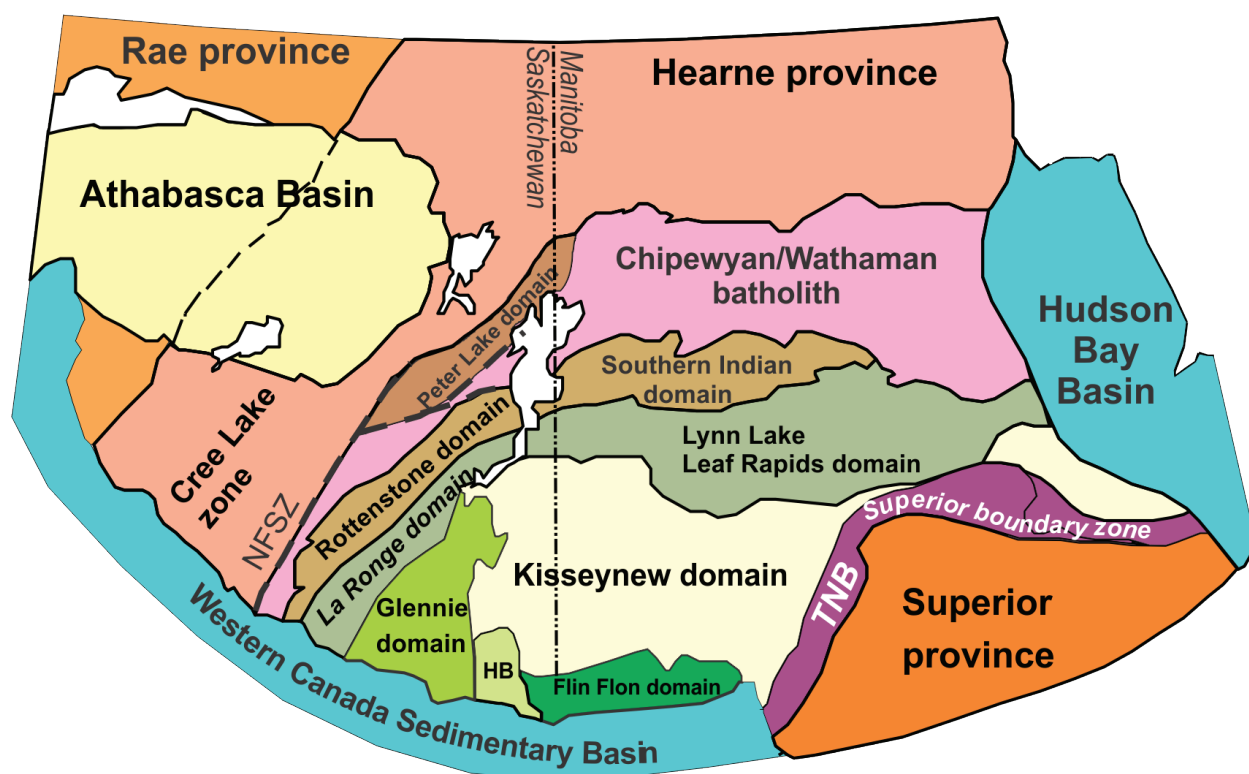


Figure 2: Tectonic elements of the Trans-Hudson orogen in northern Manitoba and Saskatchewan (after Hoffman, 1988). Abbreviations: HB, Hanson Lake block; NFSZ, Needle Falls shear zone; TNB, Thompson Nickel belt.

1981; Fumerton et al., 1984; Van Schmus and Schledewitz, 1986; Meyer et al., 1992), which stitch the Reindeer zone along the southern margin of the Hearne craton. The Baldock pluton (ca. 1855 Ma; Corrigan et al., 2002) intrudes supracrustal rocks and orthogneiss of the Southern Indian domain along its northern margin and supracrustal and plutonic rocks of the Rusty Lake belt on its southern flank. It appears to merge with the Chipewyan-Wathaman batholith east of Southern Indian Lake.

Geological mapping and lithogeochemical, Sm-Nd isotopic and geochronological results were used to subdivide the several units of the Southern Indian domain. The oldest rocks are orthogneiss with an interpreted crystallization age of ca. 2520 Ma (Kremer et al., 2009b); exposures are limited to a small group of islands in west-central Southern Indian Lake (south of Long Point). These late Neoarchean to early Paleoproterozoic rocks are interpreted to be the basement for the rocks making up the Southern Indian domain. Five supracrustal lithotectonic assemblages were identified and named after local geographic features (Table 1, Figure 1): the Churchill River, Pukatawakan Bay, Partridge Breast Lake, Strawberry Island and Whyme Bay assemblages.

The Churchill River assemblage is fault bounded and composed of pillow basalt with intervening clastic sedimentary rocks. This assemblage is petrographically similar to the Pukatawakan Bay assemblage but has distinct volcanic lithogeochemical signatures and detrital zircon populations (Kremer et

al., 2009a, b). The Pukatawakan Bay assemblage is composed of massive to pillowed, juvenile basaltic rocks and associated basinal sedimentary rocks (Kremer, 2008a, b; Kremer et al., 2009a, b) that occur mainly in Pukatawakan Bay and south of the Missi Falls Control Structure in Southern Indian Lake, and in Pine and Partridge Breast lakes. This assemblage was intruded by the 1889 ±11 Ma Turtle Island complex (Rayner and Corrigan, 2004), which provides a minimum age of deposition. The Partridge Breast Lake assemblage sits unconformably on top of the Pukatawakan Bay assemblage and is composed primarily of bimodal continental-arc volcanic and volcanoclastic rocks (Kremer, 2008a, b; Kremer et al., 2009a, b) exposed in Southern Indian, Partridge Breast and Gauer lakes. The Strawberry Island assemblage is composed exclusively of a quartzofeldspathic sandstone interlayered with a polymictic conglomerate; these sediments have predominant zircon ages around 1860 Ma and are cut by monzogranite dated at ca. 1849 Ma. The Whyme Bay assemblage, which crops out in Whyme Bay and on the western shoreline of Southern Indian Lake (north-west of Loon Island), is composed mainly of intervening arenite and conglomerate with predominant zircon ages around 1832 Ma (Kremer et al., 2009b). These sediments seem to have been deposited within a short time interval, since they are found as kilometre-scale rafts in ca. 1829 Ma plutonic rocks (Rayner and Corrigan, 2004).

Similar methodologies were used to divide the intrusive rocks into several units spread throughout the map area. The voluminous felsic intrusive rocks vary in age from ca. 1890 Ma

Table 1: Main supracrustal assemblages in the Southern Indian domain and possible tectonostratigraphic correlation with the Rottenstone domain in Saskatchewan.

Assemblage name	Age (Ma)	Equivalent units, Rottenstone domain (SK)	Key rock types and chemical affinity	Tectonic interpretation
Churchill River	>2500 or 1988 to 1889	Not known	Juvenile pillow basalt with intervening clastic sedimentary rocks	Relic of Manikewan ocean or back-arc basin of juvenile oceanic arc
Pukatawakan Bay	>1988 to 1890	Hickson Lake assemblage ¹ ; Clements Island belt ⁴	Massive to pillowed, juvenile basaltic rocks and associated basinal metasedimentary rocks; intruded by the ca. 1889 ±11 Ma Turtle Island complex	Juvenile oceanic arc; interpreted to be in fault contact with late Archean to early Paleoproterozoic orthogneiss
Partridge Breast Lake	>1883 to 1860	Crew Lake assemblage ¹ ; Milton Island assemblage ² ; Park Island assemblage ³	Bimodal continental-arc volcanic and volcanoclastic rocks (minor juvenile massive basaltic rocks) and associated basinal metasedimentary rocks; intruded by the Chipewyan batholith	Oceanic and continental arc, and associated fore-arc basin
Strawberry Island	>1860 to 1849	Kane Lake assemblage ^{3?}	Fluvial-alluvial orogenic sediments; intruded by a monzogranite body dated at 1849 Ma	Foreland or mollase basin environment
Whyme Bay	>1832 to 1829	Not known	Fluvial-alluvial orogenic sediments; unconformably overlie the Strawberry Island assemblage; shares temporal links to the Sickie Group arkose in the Lynn Lake belt	Fluvial-alluvial environment

¹ unpublished U-Pb geochronology data from K. MacLachlan

² Maxeiner et al. (2005)

³ MacLachlan (2005)

⁴ Corrigan et al. (2001)

to ca. 1773 Ma and, for the most part, are granitoid plutons that intrude the various supracrustal rocks present in the Southern Indian domain. Granitoid plutons include the foliated Northern Indian Lake pluton, dated at ca. 1890 Ma (this study; Martins and McFarlane, 2016a, b); the K-feldspar–megacrystic Chipewyan–Wathaman batholith, with a range in ages from 1860 to 1855 Ma (e.g., Fumerton et al., 1984; Van Schmus and Schledewitz, 1986; Meyer et al., 1992); a monzogranite unit in the vicinity of the Missi Falls Control Structure, dated at ca. 1846 Ma (Rayner and Corrigan, 2004) and 1849 Ma (this study); the younger monzogranite on Whyne Bay, dated at ca. 1829 Ma (Rayner and Corrigan, 2004); the Thorsteinson F-bearing monzogranite, dated at ca. 1829 Ma (this study); and the granitic pegmatite from the South Bay pegmatite field, dated at ca. 1773 Ma (this study). Intermediate or mafic intrusions are also present in the map area but are not as prevalent as the felsic intrusions. Intermediate to ultramafic rocks from the ca. 1890 Ma Turtle Island complex and the ca. 1829 Ma quartz diorite from the Pukatawakan Bay area are amongst the few intermediate to mafic intrusions that were dated (Rayner and Corrigan, 2004).

Geology of the Southern Indian Lake area

Paleoproterozoic supracrustal rocks in the Southern Indian Lake area have been historically assigned to the Wasekwan and Sickie groups (e.g., Cranstone, 1972; Frohlinger, 1972). However, more recent data (e.g., Corrigan et al., 2007; Kremer et al., 2009b; Martins, 2015b, 2016b) suggest that supracrustal successions in the area represent a collage of several assemblages with a variety of geochemical, geochronological, isotopic and tectonic affinities. In this report, a revised volcanic and sedimentary stratigraphy is presented, whereby supracrustal assemblages were assigned names based on their type localities in the Southern Indian Lake area. The nomenclature of the geological domains and terranes in the THO is disparate between Manitoba and Saskatchewan (Table 1). Although the general subdivision of domains is similar and domain boundaries are seamless across the provincial boundary (Figure 2), each jurisdiction utilizes a unique nomenclature. In this report, all efforts are made to abide by the nomenclature standard of Manitoba when referring to geological domains (i.e., Pukatawakan Bay assemblage in the Southern Indian domain). In some instances, however, specific examples from Saskatchewan are mentioned, in which case the local terminology is employed (i.e., Park Island assemblage in the Rottenstone domain).

All rocks from the Southern Indian Lake area have been metamorphosed to upper-amphibolite facies (locally a lower metamorphic grade is described by Lenton and Corkery, 1981); however, for the sake of brevity, the term ‘meta’ has been omitted from rock descriptions and the lithologies, where possible, are described in terms of their protoliths. The majority of supracrustal rocks described in this report have been recrystal-

lized, resulting in a relatively homogeneous, fine-grained, equigranular sugary texture.

Deformation and metamorphism

On the basis of crosscutting and overprinting relationships observed on outcrops, Kremer (2008a) identified four discrete generations of ductile deformation in rocks around Pukatawakan and Whyne bays of Southern Indian Lake, as well as on Pine Lake. These observations appear to be consistent throughout the Southern Indian domain and were also recorded elsewhere on Southern Indian, Partridge Breast, Gauer and Northern Indian lakes (e.g., Kremer and Martins, 2014a; Martins, 2016b).

Structures of the earliest generation of deformation (D_0) are restricted to the mixed gneiss sequence and are not manifested in any of the younger rocks. A well-developed gneissic foliation is crosscut by basaltic dikes interpreted to represent feeders to the Pukatawakan Bay assemblage (Figure 3a). At one location in Pukatawakan Bay, an early fold generation in paragneiss (F_0) is refolded by F_1 in the volcanic rocks of the Pukatawakan Bay assemblage.

Kremer (2008b) described supracrustal rocks of the study area as invariably containing a strongly developed, layer-parallel, S_1 transposition fabric. The S_1 foliation generally trends east, dips steeply and is defined by flattening of primary structures and parallel alignment of fine-grained hornblende and biotite. It is axial planar to rare, metre-scale F_1 isoclinal folds. These early structures in the supracrustal rocks are strongly reworked into a northeasterly orientation by subsequent deformation, attributed to D_2 (Figure 3b). The S_1 foliation is folded by tight to isoclinal F_2 folds with a variably developed S_2 axial-planar foliation that strikes northeast. The paucity of preserved younging indicators in the supracrustal rocks throughout the Southern Indian domain makes it difficult to confidently identify larger fold structures. Macroscopic F_2 folds, however, can be traced on the basis of reversals in the vergence between the S_1 and S_2 foliations near F_2 fold hinges (along F_2 fold limbs, the foliations are subparallel, forming a composite S_1 – S_2 fabric) and outcrop-scale parasitic F_2 fold asymmetry (s-, z- and m-folds are all present in the area, although z-asymmetric folds predominate). All linear structures associated with D_2 deformation (minor F_2 fold axes, hornblende mineral lineation, S_0 – S_2 intersection lineation) plunge moderately to steeply northeast. Numerous outcrop-scale chloritic shear zones with dextral kinematic indicators provide evidence for a strong dextral shear component associated with D_2 . Garnet, cordierite and sillimanite porphyroblasts in metasedimentary rocks overgrew the layer-parallel S_1 foliation and developed asymmetric pressure shadows consistent with dextral kinematics, suggesting that peak metamorphic conditions were reached during D_2 (Figure 3c).

Deformation structures in the supracrustal rocks throughout Southern Indian Lake all bear a penetrative, layer-parallel S_1 foliation that is axial planar to isoclinal F_1 folds. At Whyne

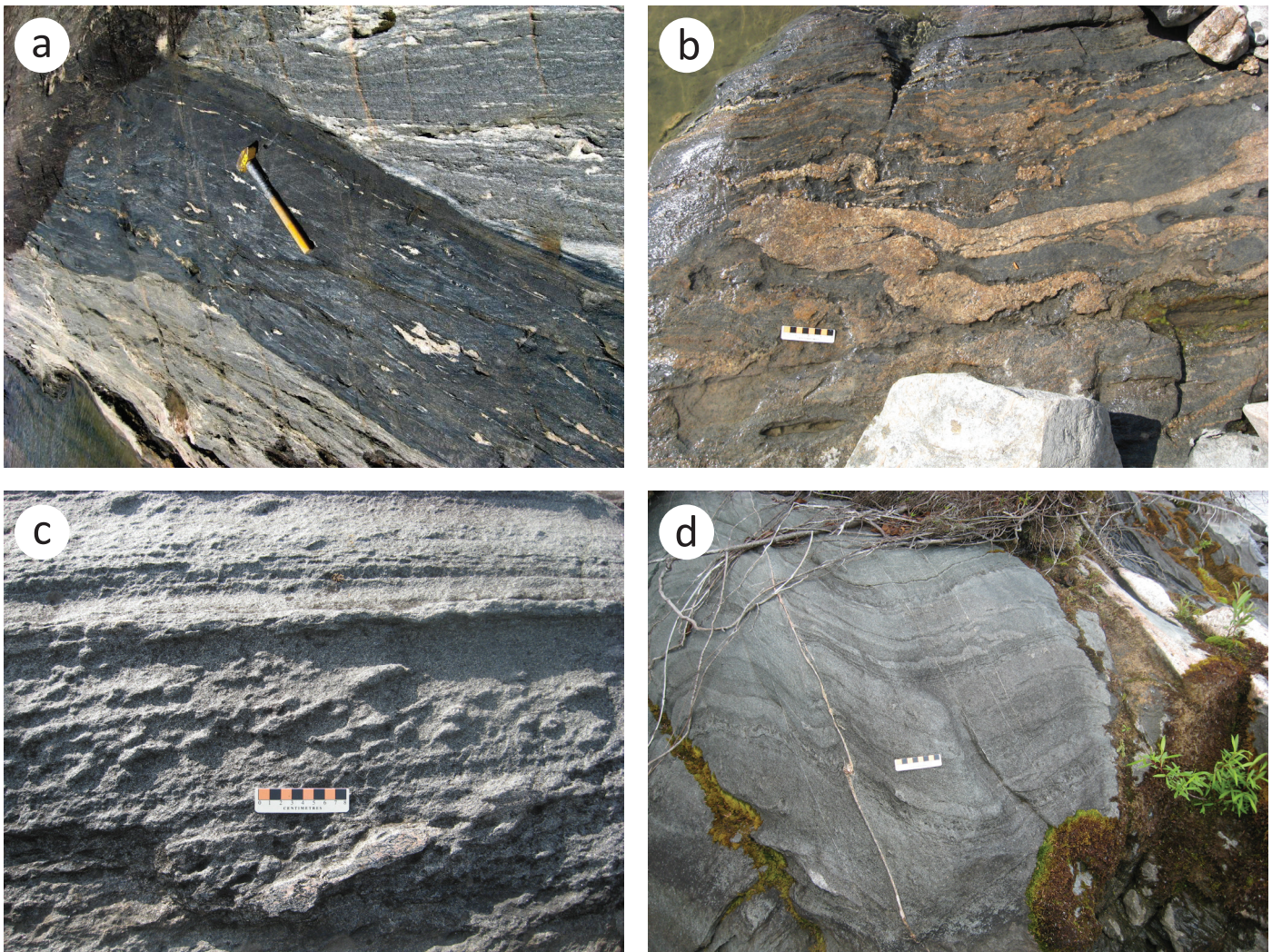


Figure 3: Outcrop photos of structures in the Southern Indian Lake area: **a)** basalt dike crosscutting gneissosity of late Neoproterozoic to early Paleoproterozoic rocks, south of Sweet Island; **b)** isoclinal F_1 fold refolded by northeast-trending F_2 fold in basaltic unit from the Pukatawakan Bay assemblage (unit 6); **c)** pinitized cordierite porphyroblasts in siltstone, west shore of Whyte Bay; cordierite shows dextral synkinematic asymmetry (oriented along S_2 oblique to bedding); **d)** upright F_2 fold with moderately developed axial-planar foliation in well-bedded greywacke-mudstone turbidites associated with basaltic rocks from the Partridge Breast Lake assemblage (unit 12).

Bay, S_1 fabrics trend east and are only mildly reworked by macroscopic, z-asymmetric F_2 folds (Kremer, 2008b). Similar trends of foliation and structure are also observed in other supracrustal rocks in the Southern Indian Lake area (Martins, 2015a, 2016a). The northeast-trending S_2 foliation is only weakly to moderately developed and is axial planar to outcrop-scale, upright F_2 folds (Figure 3d).

Broad, northwest-trending, gentle to open F_3 crossfolds that increase in frequency and spacing eastward are responsible for local reorientation of D_2 structures. Macroscopically, this is most readily apparent where the S_1 - S_2 composite foliation is rotated from its typical northeasterly orientation into a northerly direction through the narrows in Pine Lake (Kremer, 2008a, b). This axis can be traced to the southeast, where S_1 - S_2 follows the shoreline east of Pukatawakan Bay and sweeps northward toward Long Point. These F_3 crossfolds could be the result of displacement of pre-existing D_2 foliation (syn- D_2 porphyry dikes at ca. 1843 Ma; Kremer et al., 2009b) during

emplacement of the ca. 1829 Ma K-feldspar–megacrystic monzogranite (Rayner and Corrigan, 2004) that outcrops toward the southeast.

Metamorphic grades for the study area are of middle- to upper-amphibolite facies (e.g., Lenton and Corkery, 1981; Kremer, 2008b), with psammitic metasedimentary rocks (typically garnet-cordierite-sillimanite migmatitic gneiss) averaging 20–30% leucosome and locally reaching up to 80% leucosome. Locally, lower metamorphic grades were described by Lenton and Corkery (1981) for the Partridge Breast–Gauer Lakes area, where metasedimentary rocks show no development of leucosome. A gradual transition was tracked southward from garnet-cordierite-sillimanite gneiss with rare melt stringers into mobilizate-free andalusite-cordierite-muscovite schist and a core zone of chlorite-muscovite schist in the Gauer Lake area. Here, remnants of staurolite (mainly surrounded by plagioclase) are found in some rocks. The presence of andalusite indicates a lower total pressure during metamorphism (sillimanite

is the only aluminosilicate found outside of this restricted area at Gauer Lake). The transition in mineral assemblages from sillimanite–cordierite–K-feldspar through andalusite–cordierite–muscovite to chlorite–muscovite suggests decreasing temperatures from north to south within the Partridge Breast supracrustal rocks, indicating a gradual decrease from upper-amphibolite to upper-greenschist facies.

Archean rocks

Granodiorite gneiss (unit 1)

A granodiorite gneiss sample (107-08-448) of late Neoproterozoic to early Paleoproterozoic age was collected from a small isolated island just south of Sweet Island (Figure 1; Map GR2019-1-2). At this location, the gneissic sequence consists of biotite-rich bands separated by numerous veinlets of granodiorite mobilizate (Figure 4a). Gneissosity is truncated by fine-grained granitic rocks with irregular contacts that are generally subparallel to D_0 .

The identification of felsic rocks of late Neoproterozoic to early Paleoproterozoic age marks the first known occurrence of rocks older than ca. 1.9 Ga in the Southern Indian Lake area (Kremer et al., 2009b). The granodiorite gneiss crystallization age of 2520 Ma is similar to ages reported for parts of the Sask craton (Chiarenzelli et al., 1998; Rayner et al., 2005); however, older, Neo- to Mesoproterozoic crystallization ages (up to 3.2 Ga) reported for the exotic Sask craton have not been identified at Southern Indian Lake. Given the current dataset, the nature and relationship of these old orthogneisses remains uncertain.

Rocks of uncertain age

Intermixed gneissic suite (units 2 and 3)

In the Pukatawakan Bay area of Southern Indian Lake and at Pine Lake, several outcrops of orthogneiss and paragneiss

cannot be distinguished, based solely on outcrop observations, from the Archean rocks described above. McInnes (1913) and Quinn (1960) interpreted these rocks as magmatic in origin and subsequently Cranstone (1972) and Frohlinger (1972) mapped them as plagioclase and K-feldspar meta- and diatexite. Frohlinger (1972) also noticed a gradational nature between these rocks and “lesser migmatized” greywacke.

This intermixed gneissic suite (units 2 and 3), mapped in the Pukatawakan Bay area and at Pine Lake (Figure 1; Map GR2019-1-2), was interpreted by Kremer (2008a, b) as basement to the Pukatawakan Bay assemblage based on crosscutting relationships between intermixed gneiss, diabase and gabbroic dikes. Furthermore, mafic rocks at Pine Lake were interpreted to represent feeders to the Pukatawakan Bay assemblage, although contact zones were described by Kremer (2008b) as strongly reworked, sheared and intruded by abundant pegmatitic dikes, making the correlation of the mafic rocks and the intermixed gneissic suite difficult. Based on available data and limited outcrop exposure, the current authors favour the interpretation of the gneissic suite representing basement rocks to the Pukatawakan Bay assemblage. Similar relationships were suggested by Frohlinger (1972) on the basis of rare xenoliths of folded paragneiss in volcanic rocks at Pukatawakan Bay. However, these relationships were not seen during this study.

Kremer (2008b) described paragneiss (unit 2) in detail as having strong compositional banding reflective of primary layering, and variations in texture, grain size and mineralogy. Fine- to medium-grained, quartzofeldspathic garnet-biotite gneiss was observed west-southwest of Long Point; fine-grained, locally sillimanite-bearing banded gneiss was mapped on the western shore of Pine Lake; and medium-grained, crudely layered quartz arenite gneiss is prevalent along the northeastern shore of Pine Lake. Locally, xenoliths of preserved paragneiss are bounded by and, in some instances, gradational into larger bodies of granodioritic gneiss (unit 3) that contain 10–30%

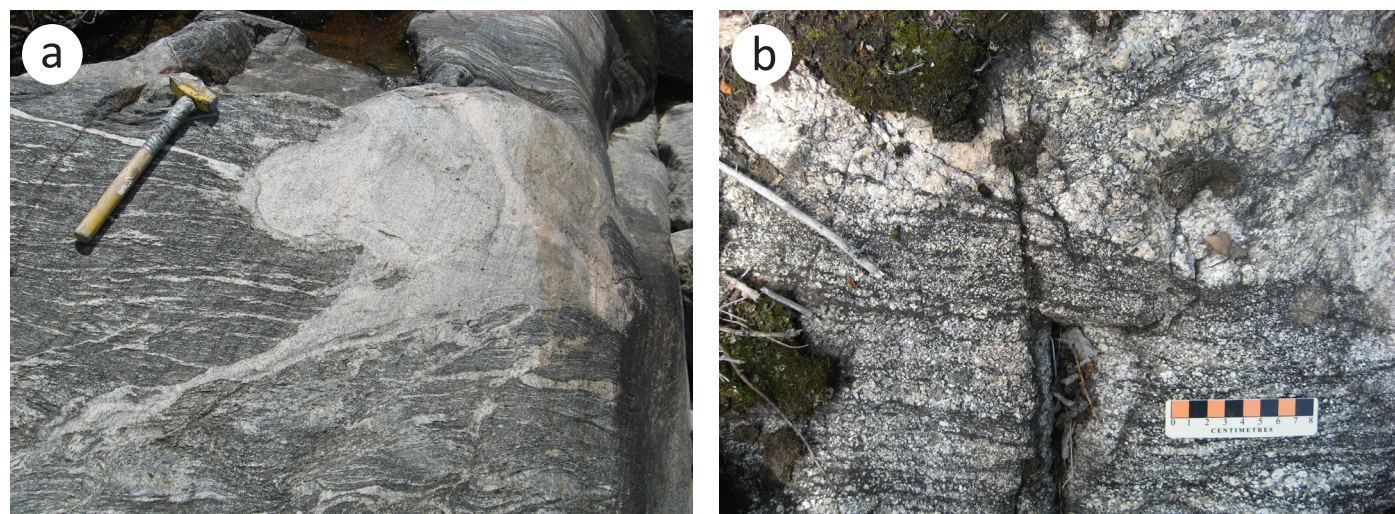


Figure 4: Outcrop photographs of orthogneiss: **a)** Archean gneissic sequence with biotite-rich bands separated by numerous veinlets of leucosome that pooled into a large pocket, island east of Pukatawakan Bay; **b)** orthogneiss of unknown age cut by pegmatite dike, Pine Lake.

wispy, discontinuous mafic schlieren, interpreted as restite in intensely migmatized sedimentary rocks.

Orthogneiss (unit 3) ranges from tonalitic to granodioritic in composition and locally contains xenoliths of paragneiss (Kremer, 2008b). The orthogneiss has heterogeneous textures that vary from medium grained, massive and weakly deformed to strongly banded across and/or along strike. In some instances, where flooded by younger intrusive phases, gneissic foliation is overgrown by randomly oriented, euhedral, metasomatic K-feldspar crystals up to 4 cm in size. Both ortho- and paragneiss, particularly at Pine Lake, are intruded by abundant granodioritic to tonalitic material, part of which may represent in situ mobilized. Pegmatites commonly cut the orthogneiss (Figure 4b).

Paleoproterozoic rocks

Churchill River assemblage (unit 4)

This assemblage is composed of a succession of pillow basalt with intervening clastic sedimentary rocks. It occurs as a narrow, fault-bounded strip along the Churchill River where it enters Partridge Breast Lake (Figure 1; Map GR2019-1-3) and was identified at this location only. Pillow basalt weathers medium to dark grey and is nonmagnetic. Pillows range in size from 0.2 to 1 m, are elongate to bun shaped, and are aphyric with rare amygdulites. Selvages are 1–2 cm thick and nonrecessive. Approximately 5–10% recessive, carbonate-rich, interpillow material is present in all exposures (Figure 5a). Pillows are medium grained due to recrystallization and grain coarsening during metamorphism, imparting a spotted appearance to the rock. The clastic sedimentary rocks interlayered with the pillowed basalt are greywacke that weathers light grey, is nonmagnetic and contains 10–20% garnet and cordierite porphyroclasts up to 2 cm in size. Foliation of the greywacke is defined by anastomosing biotite stringers that wrap around the porphyroblasts and bound domains of recrystallized

quartz and feldspar (Figure 5b). Rare beds of clast-supported conglomerate and horizons of thinly bedded sandstone and mudstone are also present (described as “arkosic sandstone” in Kremer et al., 2009b). Both the pillowed basalt and the sediments indicate younging toward the west. The entire assemblage is crosscut by pegmatite dikes with many inclusions of the rocks from the Churchill River assemblage.

Although only exposed in a few outcrops, the Churchill River assemblage can be clearly differentiated from the petrographically similar Pukatawakan Bay assemblage by very distinct lithogeochemical and Sm-Nd isotopic signatures, and detrital zircon populations (see ‘Lithogeochemistry and Sm-Nd isotopes’ section).

Pukatawakan Bay assemblage (units 5–8)

The supracrustal rocks cropping out in the Pukatawakan Bay area of Southern Indian Lake were previously mapped by Frohlinger (1972) and Cranstone (1972), and interpreted to be part of the Sickle group. Later, Corrigan et al. (2002) introduced the name ‘Pukatawakan belt’ and Kremer (2008b) described these rocks as part of the ‘Pukatawakan Bay assemblage’. This assemblage was initially thought to be restricted to the Pukatawakan Bay and Pine Lake areas (Figure 1; Map GR2019-1-2), but further studies have indicated that it also crops out around Turtle Island (southwest of the Missi Falls Control Structure; Figure 1) and continues east toward Partridge Breast Lake (Map GR2019-1-3). The Pukatawakan Bay assemblage consists of massive to pillowed, variably strained and altered basalt with subsidiary volcanoclastic facies. Mafic volcanic rocks are interlayered at various scales with variably migmatitic, psammitic to pelitic sedimentary rocks, including occasional beds of exhalative, semimassive sulphide and iron formation. In the Pukatawakan Bay area and the southern portion of the Pine Lake area, volcanic rocks are the dominant lithofacies; around the Missi Falls Control Structure and at Partridge Breast Lake,

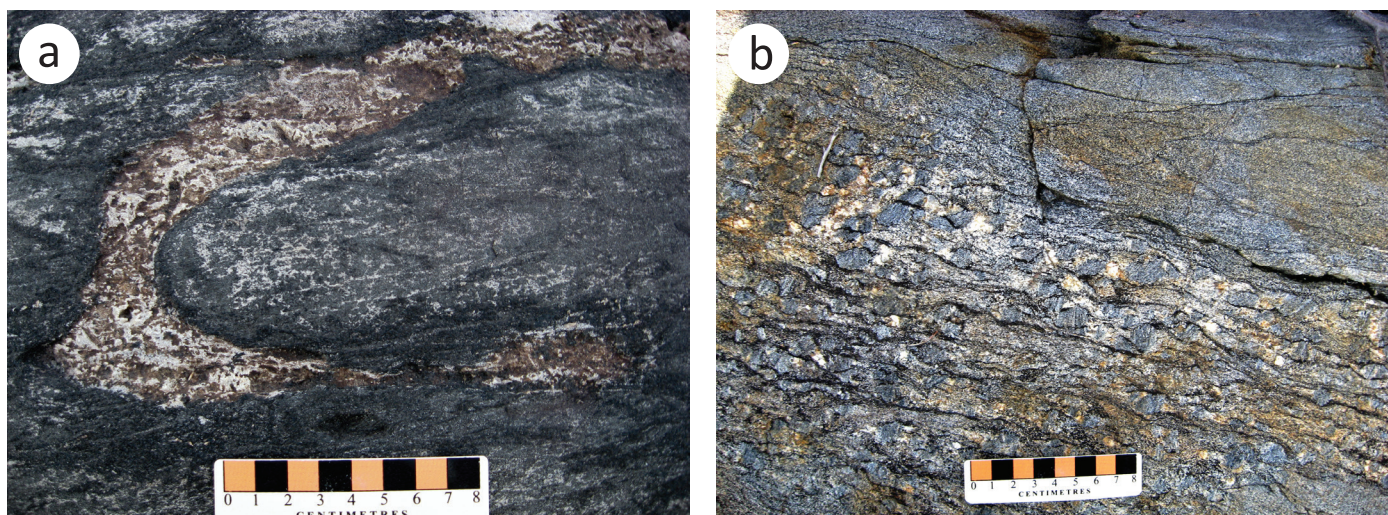


Figure 5: Outcrop photographs of rocks from the Churchill River assemblage: **a)** pillowed basalt with recessive carbonate-rich interpillow material; **b)** foliated greywacke showing anastomosing biotite stringers that wrap around cordierite porphyroblasts.

psammitic to pelitic rocks dominate. All rocks of this assemblage are intruded by large plutons that range in composition from gabbroic to granitic.

Two samples of greywacke yielded similar detrital zircon spectra, with the dominant population in both samples ranging between ca. 2520 Ma and 2.3 Ga, and the youngest detrital zircons at 1986 ± 14 Ma and 1988 ± 11 Ma, the latter providing the best constraint on the maximum age of deposition for the Pukatawakan Bay assemblage (see 'U-Pb geochronology' section). Both samples contain a few Mesoarchean detrital zircons up to ca. 3.45 Ga. The dominant ca. 2520 Ma to 2.3 Ga population in the greywacke gneiss suggests that rocks of this age (such as unit 1, with a crystallization age of 2520 Ma; Kremer et al., 2009b), although limited in current exposure, were an important sediment source shedding into the basin. The Pukatawakan Bay assemblage is crosscut by the Turtle Island intrusive complex, which has a crystallization age of 1889 ± 11 Ma (Rayner and Corrigan, 2004) that provides a minimum age of deposition for the assemblage.

Greywacke paragneiss (unit 5)

Greywacke paragneiss, well exposed along the south shoreline of Partridge Breast Lake, weathers dark grey and is well bedded, with alternating psammitic and pelitic layers varying in thickness from 5 to 25 cm. Psammitic layers are composed of fine-grained quartz and plagioclase, with biotite, local muscovite knots and rare garnet. Pelitic layers are medium to coarse grained, with staurolite and quartz-sillimanite knots (Figure 6a). Bedding is transposed by isoclinal F_3 folds, with axial planes parallel to F_2 foliation. Weakly to well-developed crenulation cleavage is observed locally (Figure 6b). Greywacke paragneiss is petrographically similar to the "migmatitic garnet paragneiss" described along the margins of Long Point at Southern Indian Lake by Kremer et al. (2009a), but U-Pb geo-

chronology results reveal that the unit 5 greywacke paragneiss has a maximum depositional age of 1950 ± 10 Ma (see 'U-Pb geochronology' section) and is interpreted here as part of the Pukatawakan Bay assemblage, which differs from field interpretations by previous workers (Corkery, 1993, 1995; Corkery and Lenton, 1990; Kremer et al., 2009a, b).

Basalt and derived amphibolite, massive to pillowed, minor pillow-fragment breccias (unit 6)

At Pukatawakan Bay, basalt is fault bounded to the east against granodiorite gneiss (unit 3) and to the north by variably pelitic to quartzofeldspathic migmatitic paragneiss (unit 2), and is intruded to the south by K-feldspar-phyric monzogranite (unit 21a; Map GR2019-1-2). South of the Missi Falls Control Structure, basalt is exposed on the nose of the macroscopic fold closure east of Long Point (Coyle and Kiss, 2008) and on the southwestern shore of Turtle Island (Map GR2019-1-3). Basalt weathers medium to dark green-grey, has dark grey fresh surfaces, and consists of hornblende, plagioclase, biotite (after hornblende) and minor quartz. Both pillowed and massive flows are recognizable in outcrop; however, the relatively high strain and lack of continuous exposure of the sequence in most locations preclude any detailed internal stratigraphic subdivisions at the map scale.

Descriptions by Kremer (2008b) of the outcrops in the Pukatawakan Bay area are similar to outcrops observed south of the Missi Falls Control Structure. Kremer (2008b) described pillowed flows as aphyric and nonamygdaloidal, although rare quartz- and carbonate-filled amygdules were observed in a few locations. Pillows are densely packed, with generally less than 5% interpillow material. Selvages are thin, generally <1 cm, and occasionally contain euhedral garnets averaging 0.5 cm in size. Characteristic exposures contain moderately to strongly flattened pillow structures, with aspect ratios averaging 10:1 but reaching >20:1 in some locations. On a large outcrop north of

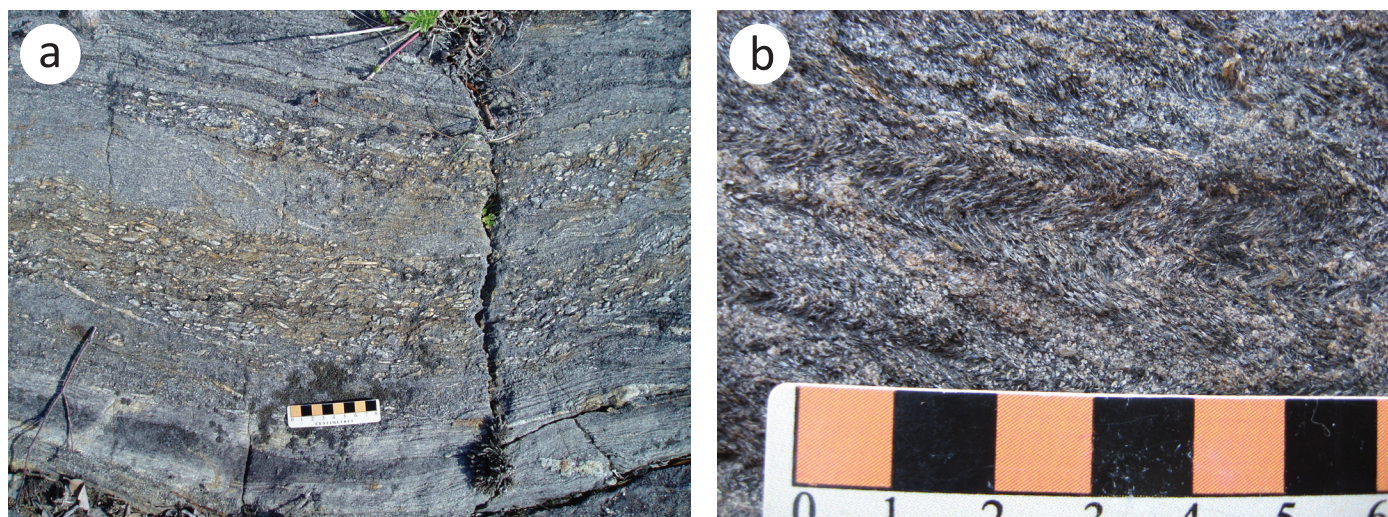


Figure 6: Outcrop photographs of greywacke paragneiss from the Pukatawakan Bay assemblage: **a)** alternating layers of fine-grained mudstone and medium- to coarse-grained pelite, the latter containing sillimanite and staurolite, Partridge Breast Lake; **b)** crenulation cleavage in the feldspathic greywacke, Partridge Breast Lake (scale card in centimetres).

Whyme Bay, a very well preserved succession of pillow basalt is exposed. At this location, successive pillowed flows up to 5 m thick are separated by layers of pillow-fragment breccia. Pillows are 0.2 to 2 m in size, densely packed and irregular to bun shaped (Figure 7a). Pillow cusps indicate tops to the north, making this one of the few locations where concrete younging criteria were identified in the basalts of the Pukatawakan Bay assemblage. Intervals of pillow-fragment breccia are generally <2 m thick. They are matrix supported, with pillow fragments ranging in size from 5 to 50 cm. The matrix is composed of a red-brown–weathering, fine- to medium-grained ferruginous material (Figure 7b). Pale green calcsilicate alteration, consisting of varying amounts of epidote, actinolite, diopside and tremolite, is present in most pillow basalt and ranges from patchy to irregular in character.

Massive basalt is dark grey on both weathered and fresh surfaces, and is aphyric and nonamygdaloidal (Kremer, 2008b). Contacts between adjacent massive flows were not observed in outcrop, and individual flow thicknesses could not be determined. Massive basalt contains light grey-green zones of calcsilicate alteration in most exposures (Figure 7c). Where strain is low, this alteration imparts a mottled texture to the rock; in areas of higher strain, the alteration is transposed parallel to the dominant deformation fabric, imparting a structural

and metamorphic layering on the rock (Figure 7c). Cranstone (1972) suggested that many of the layered calcsilicate rocks observed in outcrop represent primary sedimentary bedding but noted that “pillow-like structures occur locally within the unit”, implying an igneous origin in some instances. Although a sedimentary origin cannot be ruled out, the present interpretation favours derivation of the layering primarily from intense transposition of altered massive and pillowed volcanic facies. South of the Missi Falls Control Structure, rare intervals of thinly bedded mafic tuff to lapilli tuff, with beds ranging from 2 to 20 cm, occur interlayered within successions of massive basalt. In many instances, the basalt is completely recrystallized to homogeneous, fine- to medium-grained orthoamphibolite in which any primary features are difficult or impossible to discern.

An andesite to dacite, monolithic to slightly heterolithic volcaniclastic sequence was identified at only one outcrop on Pine Lake (107-08-559). It ranges from clast-supported tuff breccia to bedded scoriaceous breccia. The matrix is composed largely of biotite and locally is highly ferruginous. Most of the clasts are siliceous and locally contain garnet. This volcaniclastic sequence is cut by a fine-grained andesite to dacitic dike that bears similarities to clasts in the breccia, perhaps making this a shallow-level intrusion.



Figure 7: Outcrop photographs of volcanic rocks of the Pukatawakan Bay assemblage: **a)** well-preserved pillow basalt with primary structures showing younging to the north (top of photo), north of Whyme Bay; **b)** matrix-supported pillow-fragment breccia, same outcrop as previous photo; **c)** highly strained massive basalt with calcsilicate alteration, north shore of Turtle Island.

Psammitic and pelitic greywacke, minor iron formation, graphitic and sulphidic layers (unit 7)

Psammitic and pelitic greywacke of the Pukatawakan Bay assemblage are marked by a significant high on the high-resolution residual total-field aeromagnetic map over Partridge Breast Lake and the east shore of Southern Indian Lake at Turtle Island (Figure 1; Map GR2019-1-3; Coyle and Kiss, 2008). Regional trends on the aeromagnetic map suggest that this unit extends east and southeast toward Gauer and Thorsteinson lakes and around the Thorsteinson Lake pluton, where it thins and tapers out. In the Pukatawakan Bay area, rare outcrops of fine- to medium-grained, pelitic to semipelitic greywacke occur interlayered with basalt, whereas psammitic to pelitic greywacke is interlayered with massive to pillowed basalt at various scales in the Turtle Island area, south of the Missi Falls Control Structure and at Partridge Breast Lake.

Massive to crudely bedded pelitic greywacke weathers medium grey to spotted, is fine to medium grained and is moderately to well bedded. It is composed predominantly of foliated biotite (>70%, 1–2 mm), euhedral to subhedral plagioclase (25–30%, 1–2 mm) and minor quartz (<5%) with a recrystallized texture. Elongate to wispy porphyroblasts of

sillimanite and, to a lesser extent, garnet are common. Where present, sillimanite is consistently oriented at an angle to layering (S_0) and subparallel to main foliation (S_2), suggesting that peak metamorphic conditions postdate regional D_2 deformation (Figure 8a). Narrow bands of graphitic to sulphidic shale (silicate-facies iron formation) occur along the northwestern shore of Turtle Island. These layers are characterized by light orange–weathering calcrete that adheres to the surface of the outcrops and consist of thin beds of fine- to medium-grained, semimassive to massive sulphide interlayered with graphite-rich horizons (Figure 8b).

Psammitic greywacke is distinguished from the massive to crudely bedded pelitic greywacke by a slightly coarser grain size (2–4 mm), a lesser amount of biotite, an increased amount of plagioclase and quartz, and an absence of sillimanite porphyroblasts (Figure 8c). Narrow, boudinaged to irregularly mobilized granitic to quartz monzonitic injection veins are present but rare. Local layers of oligomictic and polymictic clast-supported conglomerate, associated with psammitic and pelitic greywacke, were mapped by Corkery and Lenton (1993) and Kremer et al. (2009a) but were not separated into an individual rock unit in this report and on the accompanying maps.



Figure 8: Outcrop photographs of sedimentary rocks of the Pukatawakan Bay assemblage: **a)** elongate sillimanite porphyroblasts oblique to layering in greywacke, northwestern Turtle Island; **b)** silicate-facies iron formation, south of the Missi Falls Control Structure; **c)** bedded and folded psammitic layer with centimetre-scale Z-folds representing F_2 foliation, western Pukatawakan Bay.

Intermediate, mafic and ultramafic intrusive rocks (subunits 8a–c)

Dikes and sills of gabbro, quartz diorite and rare ultramafic rocks intrude volcanic rocks of the Pukatawakan Bay assemblage. They are generally too narrow to be depicted at the map scale, with the exception of a few wider occurrences in the Pukatawakan Bay area. Where well preserved, gabbro (subunit 8a) is fine to medium grained with equigranular to subophitic textures consisting of equal amounts of plagioclase (3–10 mm) and hornblende (3–8 mm). Gabbro locally grades to medium-grained quartz diorite containing 5–10% anhedral quartz. Exposures of gabbro, similar to those of volcanic rocks of the Pukatawakan Bay assemblage, are typically strongly recrystallized to fine grained, with sugary textured plagioclase, biotite and hornblende. Where clear contact relationships exist in outcrop, recrystallized gabbro can be distinguished from the volcanic rocks; however, in the absence of contact relationships, it can be difficult to make a distinction. Quartz diorite (part of subunit 8a) was only identified in a few outcrops in the Pukatawakan Bay area (Kremer, 2008a). The gabbroic intrusion at Pine Lake (subunit 8b), described by Kremer (2008b), forms a distinct, round high on the high-resolution residual total-field aeromagnetic map (Coyle and Kiss, 2008) and is different from the gabbro in the Pukatawakan Bay area. The intrusion at Pine Lake, however, shows evidence of igneous or metamorphic layering or multiple injections (Kremer, 2008b), and variations in texture and mineralogy. The rim of the intrusion consists of fine- to medium-grained, strongly magnetic, pyroxene-hornblende gabbro, and the core is composed of pyroxene-bearing leucogabbro with 2–5% phenocrysts of anorthositic feldspar. Rare serpentized, folded peridotite dikes (subunit 8c) occur on a small island in the Pukatawakan Bay area mapped by Kremer (2008a, b). These dikes are fine to medium grained and contain stringers of sulphides. Their mineralogy is serpentine (probably after olivine), anthophyllite (probably after orthopyroxene), spinel, magnetite, chlorite and phlogopite. Spinel could have formed at peak metamorphism and retrogression could be responsible for the magnetite aureoles.

Whole-rock lithogeochemical compositions of intermediate, mafic and ultramafic intrusive samples are similar to those of the associated volcanic rocks of the Pukatawakan Bay assemblage, suggesting a possible cogenesis between the two (see ‘Lithogeochemistry and Sm-Nd isotope geochemistry’ section).

Turtle Island complex (unit 9)

The Turtle Island complex is a layered igneous intrusion with intermediate to ultramafic compositions and dated at ca. 1889 ±11 Ma (Rayner and Corrigan, 2004). Early work by Cranstone (1972) described this intrusion as a hornblende ranging from medium grained to pegmatitic and composed largely of amphibole in a fine-grained groundmass of anorthite and quartz. Corrigan et al. (2002) described the Turtle Island

complex as a mixed intrusion ranging in composition from pyroxenite–hornblende, gabbro, leucogabbro, diorite and quartz diorite to tonalite. Some of the best outcrops, located on the north shores of Turtle Island (Figure 1; Map GR2019-1-3), show well-preserved igneous layering, crossbedding, scour structures, dropstones, cognate xenoliths and ultramafic veinlets cutting earlier fabrics. These kinds of textures represent evidence for multiple injection in a dynamic magma chamber.

Northern Indian Lake pluton (unit 10)

The granitoid rocks assigned to subunit 10a are of granodioritic composition and the majority of outcrops are found in Northern Indian Lake (Map GR2019-1-4). In the north basin of Southern Indian Lake (Map GR2019-1-1), extensive areas of this unit are also interpreted to be present, based on field observations of the limited rock exposure and aeromagnetic data (Natural Resources Canada, 1984). Detailed characterization of this large granodioritic body dated at ca. 1890 Ma (subunit 10a; Martins and McFarlane, 2016a, b), including outcrop descriptions, petrography and whole-rock geochemistry, can be found in Kremer and Martins (2014a), and Martins and McFarlane (2016a). A few outcrops of quartz monzonite and quartz diorite with biotite and hornblende are considered subunit 10b; Kremer and Martins (2014a) described this subunit as medium to very coarse grained, melanocratic and porphyritic (with plagioclase or K-feldspar phenocrysts). The groundmass is composed mainly of biotite and hornblende (30–40%), quartz (10%) and trace amounts of sulphides.

Partridge Breast Lake assemblage (units 11–16)

The Partridge Breast Lake assemblage crops out in the area extending from south of Partridge Breast Lake toward Gauer Lake (Figure 1; Map GR2019-1-3), as well as along Long Point in Southern Indian Lake, where extensive outcrops of feldspathic and aluminous greywacke are dominant (Figure 1; Map GR2019-1-2). Rocks assigned to the Partridge Breast Lake assemblage are also locally preserved in kilometre-scale screens in felsic plutonic rocks at Northern Indian Lake (Kremer and Martins, 2014a, b) and scattered throughout the northern and central parts of Southern Indian Lake (Martins, 2015a, b; 2016a, b). Rocks belonging to the Partridge Breast Lake assemblage were previously described by Corrigan et al. (2002), Kremer (2008a, b) and Kremer et al. (2009a, b) as predominantly mafic to felsic volcaniclastic and reworked volcaniclastic rocks. Mafic to felsic flows, although present, form a minor portion of the exposed succession. Feldspathic and quartz-rich greywacke and mudstone occur throughout the sequence. The age of volcanism that formed the Partridge Breast Lake assemblage is poorly defined. A maximum age of deposition (ca. 1890–1880 Ma) is best constrained by the youngest detrital zircons recovered from three samples of sedimentary and resedimented volcaniclastic rocks. A minimum age is constrained by the intrusion of the ca. 1860 Ma Chipewyan-Wathaman batholith.

A 2520–2300 Ma zircon population is also present but is not dominant, like in the Pukatawakan Bay assemblage rocks.

Feldspathic and aluminous migmatitic greywacke, minor conglomerate and calcsilicate (subunits 11a–d)

This package of sedimentary rocks, described in detail by Martins (2016b), underlies the central area of Southern Indian Lake, especially along the north shore of Long Point (Figure 1; Map GR2019-1-2), where feldspathic and aluminous greywackes are the most abundant rock types. Minor conglomerate and calcsilicate layers are commonly found on smaller islands north of Long Point. Subunit 11a (feldspathic greywacke) is foliated and nonmagnetic, with 10–20% leucosome. This subunit weathers dark grey, is medium grained and massive to crudely bedded, and locally contains garnet. The aluminous greywacke (subunit 11b) is medium grey and fine grained, and contains garnet and sillimanite that likely formed during peak, upper-amphibolite-facies metamorphism. This unit corresponds to the “migmatite garnet greywacke paragneiss” mapped by Kremer et al. (2009a). In both the feldspathic and the aluminous greywackes, up to 20% quartzofeldspathic mobilize occurs as stringers, veins and dikes that are generally oriented subparallel to the main transposition fabric in the sedimentary rocks. Also in both greywackes, the main foliation (S_1) is folded by steeply dipping isoclinal F_2 folds of predominantly z-asymmetry, with a northeast-striking S_2 axial-planar foliation. Numerous outcrop-scale shear zones are observed in both feldspathic and aluminous greywackes, with kinematic indicators providing evidence for a strong dextral shear component associated with D_2 .

Poorly exposed underwater outcrops of polymictic, clast-supported conglomerate (subunit 11c) occur on the east shore of Canada Island (Map GR2019-1-1). This conglomeratic unit is moderately deformed, appears to be moderately to well sorted, and contains subrounded felsic lithic clasts varying from 8 to 20 cm in size. Locally interbedded with this conglomerate is a rusty layer containing abundant pyrite and chalcopyrite, and interpreted as sulphide-facies iron formation. Associated with the conglomeratic unit are calcsilicate rocks (subunit 11d) with pervasive carbonate and epidote alteration. Rare outcrops of these rocks were found only on the south shore of Canada Island. They are fine to medium grained and show compositional layering, with pink layers composed of K-feldspar, quartz, hornblende and titanite; purple-green layers composed of garnet, epidote, amphibole, quartz, calcite, biotite, magnetite and titanite; and green layers composed of quartz, epidote, titanite and calcite.

Previous workers (e.g., Corkery 1993; Corkery and Lenton, 1993; Corrigan et al, 2002; Kremer et al., 2009a, b) interpreted the rocks outcropping along the north shore of Long Point as equivalent to petrographically similar paragneiss on the southern shore of Partridge Breast Lake. However, geochronology studies indicate that the latter unit is part of the older Pukatawakan Bay assemblage (unit 5 of the present study).

Massive and pillowed amygdaloidal basalt, locally with minor silicate- and sulphide-facies iron formation (unit 12)

This unit was identified at Whyme Bay, along the north shore of Long Point (Figure 1; Map GR2019-1-2) and south of Strawberry Island (Figure 1; Map GR2019-1-3). Initial work by Kremer (2008a, b) classified this unit as part of a separate assemblage named the ‘Whyme Bay assemblage’. Subsequent lithogeochemical and geochronological studies indicated that the basalt from this unit has affinities with the basaltic rocks from the Partridge Breast Lake assemblage and is therefore considered as such in this report.

At Whyme Bay, the basalt occurs as large screens within the ca. 1829 Ma monzogranite batholith (Rayner and Corrigan, 2004). The basaltic unit includes heterolithic volcanic conglomerate interlayered with pillowed basalt to andesite flows and well-bedded greywacke and mudstone turbidites. The conglomerate is massive, matrix supported and magnetic. Clasts are 1–30 cm in size, subrounded to subangular and predominantly mafic (basalt and andesite) in composition, but quartz- and/or feldspar-phyric felsic clasts dominate in some outcrops. The matrix is fine grained and contains plagioclase (40%, 2–5 mm), biotite (30%, 2–5 mm), hornblende (10–15%, 3–8 mm) and quartz (5–10%, 2–5 mm). Crude layering was observed in a couple of outcrops. Pillowed basalt to andesite weathers medium blue-grey. Pillows are relatively uniform in size, averaging around 1 m, locally contain up to 10% euhedral plagioclase phenocrysts up to 0.8 cm, and have 5–10% quartz- and chlorite-filled amygdules concentrated around pillow margins. Pillow selvages are approximately 1 cm thick and are nonrecessive; up to 10% interpillow hyaloclastite occurs in some exposures. Occasional outcrops of massive, plagioclase-phyric andesite occur in Whyme Bay, containing up to 50% euhedral lath-shaped plagioclase up to 1.5 cm and 5–10% quartz- and chlorite-filled amygdules (Figure 9a). Contact relationships have not been observed, so it remains unclear if the andesite outcrops represent massive flows or shallow synvolcanic dikes and sills.

Along the north shore of Long Point and south of Strawberry Island, basalt is associated with feldspathic and aluminous greywackes (subunits 11a and b). The basalt is described as predominantly massive (pillowed basalt was identified at one location only) and typically fine grained, dark grey and foliated, such that primary features are difficult to discern due to light grey-green zones of calcsilicate (epidote) alteration (Martins, 2016a, b). Locally, on the north shore of Long Point, an intrusion breccia of massive basaltic flows (Figure 9b) was found interbedded with the feldspathic and aluminous greywackes of subunits 11a and b.

Intermediate to felsic volcanic rocks, tuff and resedimented tuff (subunits 13a, b)

Subunit 13a consists of a narrow sequence of well-bedded volcanic sandstone that occurs along the Churchill River (Map

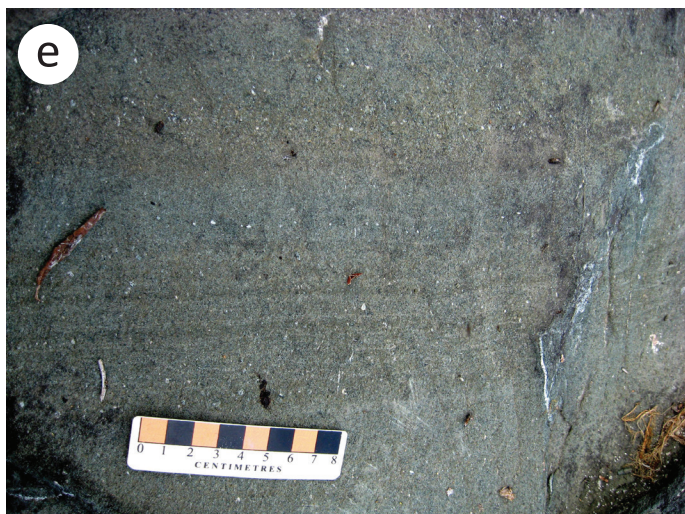
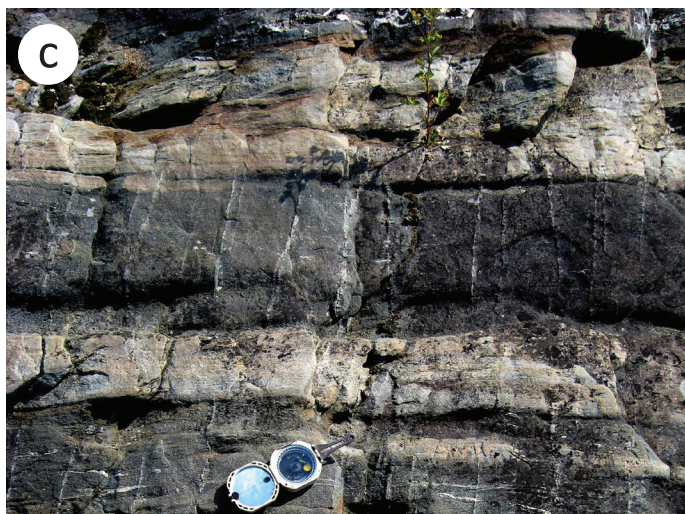


Figure 9: Outcrop photographs of volcanic and volcanoclastic rocks of the Partridge Breast Lake assemblage: **a)** massive basalt with quartz-feldspar-chlorite-filled amygdules, Whyme Bay (sample 107-08-265); **b)** broken pieces of altered volcanic rocks in a granodioritic matrix, north shore of Long Point; **c)** bedded mafic and felsic volcanic sandstone, Churchill River north of Partridge Breast Lake; **d)** matrix-supported fragmental felsic volcanic, south of Partridge Breast Lake; **e)** normally graded mafic tuff, northeast shore of Gauer Lake.

GR2019-1-3). The succession consists of alternating felsic and mafic beds, with bed thickness ranging from 5 to 30 cm. Felsic beds weather light beige to buff and consist of medium-grained (0.3–0.8 cm) subrounded to rounded quartz (30–50%), euhedral to subhedral plagioclase and broken plagioclase fragments (30–40%), and fine-grained sericite and minor muscovite (10%). Mafic beds weather medium to dark grey and

consist of varying amounts of hornblende, biotite and plagioclase, and local garnet (Figure 9c).

Felsic volcanic and volcanoclastic rocks of subunit 13b are limited to the area between Partridge Breast and Gauer lakes, where they form discontinuous, poorly exposed lenses on a few ridges and on the shores of small lakes (Map GR2019-1-3). Outcrops weather buff to light grey and consist of either

massive or fragmental rhyolitic to dacitic rocks. Massive rhyolite is sparsely porphyritic, with 5–10% euhedral plagioclase (2–5 mm) and subrounded pale-blue quartz phenocrysts (1–2 mm). No internal structures (i.e., flow banding, flow lobes) could be identified in any of the outcrops. Fragmental rhyolite is matrix supported, with 10% subangular to subrounded quartz and quartz-feldspar-phyric clasts in a fine-grained, sugary-textured, equigranular matrix containing minor biotite and magnetite. Rare exposures of fine-grained, plagioclase-crystal-rich felsic tuff are locally associated with massive to fragmental felsic volcanic rocks. Crystal tuff is massive, and contains approximately 60% euhedral to subhedral plagioclase crystals and crystal fragments (2–4 mm) in a fine to very fine grained siliceous groundmass (Figure 9d).

A sample from subunit 13b, composed of fragmental quartz- and feldspar-phyric rhyolite revealed a detrital zircon distribution dated at 2.8–2.3 Ga (see ‘U-Pb geochronology’ section). This result does not allow clear correlation with other supracrustal rocks of the Southern Indian domain. However, subunit 13b has been considered part of the Partridge Breast Lake assemblage because felsic volcanoclastic units are rarely associated with the Pukatawakan Bay assemblage (identified at only one location at Pine Lake).

Mafic to intermediate volcanoclastic and epiclastic rocks with minor flows (subunits 14a, b, c)

Mafic volcanoclastic and epiclastic rocks of the Partridge Breast Lake assemblage occur south of Partridge Breast Lake and are best exposed and preserved on the northeast shore of Gauer Lake (Figure 1; Map GR2019-1-3). Subunit 14a, mapped by Corkery and Lenton (1993), consists of andesitic tuff and resedimented tuff flows. Subunit 14b consists of massive to crudely layered, mafic volcanic conglomerate with minor heterolithic volcanic conglomerate. Mafic crystal and lapilli tuff, and rare flows occur in a few outcrops but cannot be traced continuously across the map area. On Gauer Lake, massive to well-bedded, mafic crystal to lapilli tuff is exposed in several large outcrops (Figure 9e). Beds range from 10 cm to several metres in thickness and normal grading is observed in several locations. Mafic tuff is interlayered at various scales with matrix- to clast-supported heterolithic volcanic conglomerate. Clasts range from pebble to cobble size (0.5–15 cm) and are rounded to subrounded. The majority of clasts are mafic in composition (basalt, andesite), whereas approximately 20% of the clasts are felsic. South of Partridge Breast Lake, conglomerate is massive in individual outcrops; however, the dominant clast type varies from exposure to exposure, suggesting that very thick layering may be present in the unit. The matrix is dark grey and consists of 60–80% pale to dark green, euhedral to subhedral feldspar (1–2 mm in size); 20–40% euhedral to subhedral hornblende; and rare (up to 3%), pale blue to grey, rounded quartz grains. Characteristic outcrops for subunit 14c (Map GR2019-1-4) are strongly foliated felsic volcanoclastic rocks interbedded with amphibolite, interpreted to be a

massive volcanic flow, although pillows were tentatively identified in one outcrop. The felsic volcanoclastic is bedded and locally graded, with coarse clasts (<2 cm) at the base grading to fine- to medium-grained clasts near the top. Clasts are variable, with amphibolitic affinity or felsic material; rare rounded quartz eyes and garnet were also observed. The volcanoclastic rocks have abundant biotite alteration and quartz veining. Locally, this unit is siliceous, with stringers of pyrrhotite. Strongly recrystallized, almost sugary texture was observed in some outcrops.

Greywacke, mudstone and polymictic conglomerate (subunits 15a, b)

Successions of crudely to well-bedded greywacke and mudstone (subunit 15a), up to several hundred metres thick, occur within the volcanic and volcanoclastic rocks south of Partridge Breast Lake (Map GR2019-1-3). Greywacke beds weather light to medium grey, are fine grained and are composed of plagioclase (40%, 2–5 mm), biotite (30%, 1–4 mm) and quartz (15–30%, 2–5 mm), with minor hornblende locally and accessory magnetite. Garnet and cordierite porphyroblasts are common in greywacke beds, locally forming up to 15% of individual beds. Greywacke is interbedded with mudstone layers ranging from a few to tens of centimetres thick. Mudstone beds weather medium to dark grey, are very fine grained and are composed dominantly of biotite and muscovite, with locally discernible plagioclase (1–2 mm). All mudstone beds are porphyroblastic and contain up to 50% combined garnet, cordierite and sillimanite (Figure 10a). Greywacke-mudstone successions south of Partridge Breast Lake are commonly isoclinally folded at outcrop scale (Figure 10b).

Altered and recrystallized porphyroblasts are locally oriented at an angle to bedding and, in many instances, have asymmetries indicative of synkinematic growth during dextral shearing (Figure 3c). Occasional outcrops of polymictic conglomerate (subunit 15b) are located in association with greywacke of the Partridge Breast Lake assemblage (e.g., west shore of Partridge Breast Lake; Figure 1; Map GR2019-1-3). Conglomerate is clast supported, with clasts of mafic to felsic volcanic rocks and lesser amounts of mafic intrusive rocks (gabbro) in a fine- to medium-grained, biotite-rich matrix (Figure 10c). Clasts range from 2 to 30 cm and are highly flattened.

Intermediate, mafic and ultramafic intrusive rocks (unit 16)

Dikes and sills, ranging from ultramafic to intermediate in composition, are intrusive into all units of the Partridge Breast Lake assemblage. Whole-rock lithochemistry of samples from these intrusions is similar to that of the associated volcanic rocks of the Partridge Breast Lake assemblage, suggesting a possible cogenesis (see ‘Lithochemistry’ section).

Quartz diorite (subunit 16a) at Partridge Breast Lake is usually nonmagnetic, coarse grained, equigranular, moderately to



Figure 10: Outcrop photos of epiclastic rocks of the Partridge Breast Lake assemblage: **a)** sillimanite and andalusite porphyroblasts in mudstone, Partridge Breast Lake; **b)** isoclinal fold in interbedded greywacke and mudstone, Partridge Breast Lake; **c)** polymictic conglomerate with highly flattened clasts, Partridge Breast Lake.

strongly foliated and intruded by fine-grained gabbro. It consists of quartz (10–15%), feldspar, biotite and hornblende. Outcrops of this subunit at Long Point (Map GR2019-1-2) and in the north basin of Southern Indian Lake (Map GR2019-1-1) were described by Martins (2016b) and Martins (2015a, b), respectively. At Southern Indian Lake, the quartz diorite is mottled black and white to dark grey on fresh surfaces, massive to weakly foliated, medium- to very coarse grained and weakly magnetic. It is mainly homogeneous but locally contains cognate xenoliths and xenoliths of amphibolite (interpreted as altered volcanic rocks). The rock is composed of plagioclase (40–50%), biotite and hornblende (30–35%), and quartz (10–15%). Garnet is present locally (up to 20% of mode). The presence of garnet appears to be always associated with gossanous occurrences and, at these locations, the rock is reddish brown; these gossans are interpreted to be the product of hydrothermal alteration.

Diorite (subunit 16b) was mapped and described by previous workers (Corkery and Lenton, 1993; Corkery 1993, 1995; Kremer, 2009a). Gabbro (subunit 16c; Maps GR2019-1-1, -2, -3) is moderately to well foliated and weakly to strongly magnetic, and varies from fine to medium grained and locally coarse grained, with equigranular or poikilitic textures consisting of

similar amounts of plagioclase and hornblende. Locally, igneous layering is observed between pyroxene-phyric gabbro to oikocrystic gabbro and leucogabbro (Figure 11a). Layers have sharp to slightly diffuse contacts and are less than 10 cm in width. Offset of layering by dextral shear zones was observed, and shear zones can locally have quartz veining and alteration. On Kuskayitum Island, quartz gabbro has cognate xenoliths (Figure 11b); locally, several xenoliths of epidote-altered volcanic rocks were found associated with massive magnetite aggregates varying in size up to 20 cm. The mineralogy of the most homogeneous phase of the quartz gabbro comprises biotite (15–20%), pyroxene (20–30%), quartz (5–10%), titanite (3–5%) and magnetite (2–3%), with the remainder being plagioclase feldspar. Quartz gabbro also outcrops on the north shore of Loon Island. There, a distinct texture consisting of aggregates of subhedral to euhedral crystals of plagioclase, magnetite, pyroxene and quartz was observed. At the same location, potassic and chloritic alteration associated with euhedral crystals of titanite, magnetite and pyrite forms pockets within the quartz gabbro.

Subunit 16d (pyroxenite) was mapped on a few small lakes south of Partridge Breast Lake (Figure 1; Map GR2019-1-3; Corkery 1993, 1995; Corkery and Lenton, 1993; Kremer et

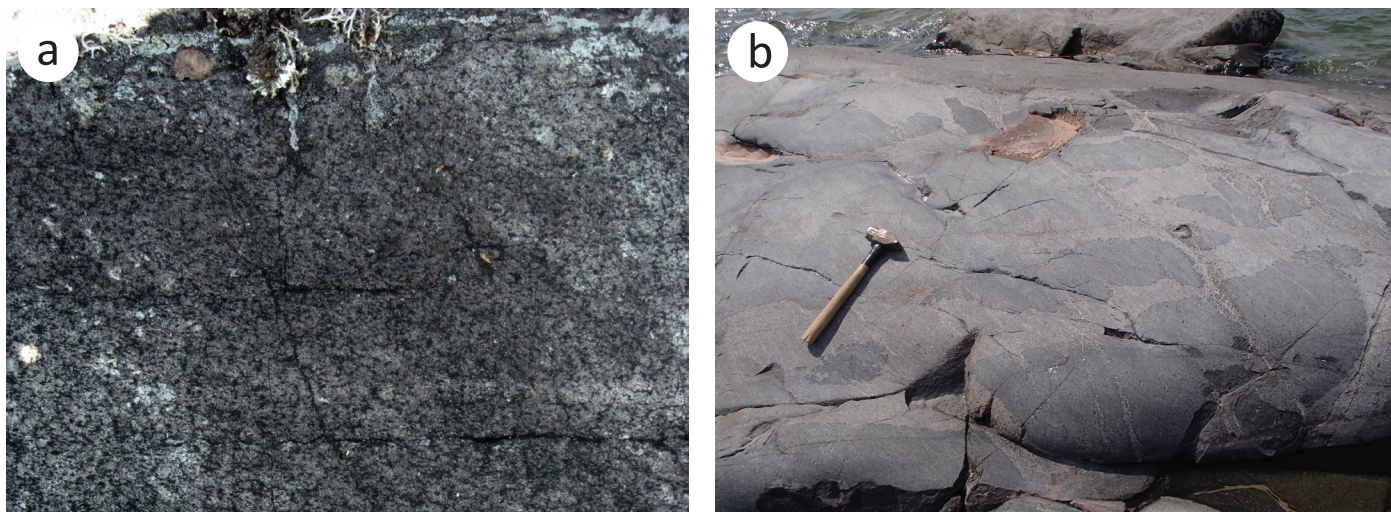


Figure 11: Mafic intrusions of the Partridge Breast Lake assemblage: **a)** igneous layering in pyroxene-phyric gabbro, south of Partridge Breast Lake; **b)** cognate xenoliths in quartz gabbro, Kuskayitum Island.

al., 2009a). A pyroxenite dike was also described on a small island west of the Missi Falls Control Structure (Figure 1; Maps GR2019-1-1 -3; Martins, 2015b), where the contact of the dike is sharp and a 2–3 cm wide chilled margin was observed. The dark green, medium- to coarse-grained pyroxenite is composed mainly of orthopyroxene, biotite and hornblende, and accessory plagioclase.

Chipewyan-Wathaman batholith (unit 17)

The Chipewyan-Wathaman batholith is a massive granitic body interpreted as part of a continental-margin magmatic arc (Lewry et al., 1981; Meyer, 1987; Hoffman, 1988) that extends more than 800 km across northern Saskatchewan and Manitoba (e.g., Lewry et al., 1981; Fumerton et al., 1984). This batholith has a reported crystallization age of 1852–1865 Ma (e.g., Ray and Wanless, 1980; Meyer, 1987). It has been described as petrographically and compositionally uniform, with characteristic K-feldspar megacrysts, and varying in composition from granite through quartz monzonite to granodiorite (e.g., Lewry et al., 1981; van Schmus et al., 1986).

In the study area, the dominant phase of the Chipewyan-Wathaman batholith is K-feldspar–megacrystic granodiorite. A few different phases of granitoid rocks were identified and interpreted as part of the same batholith but are not differentiated at the map scale. The main phase of this batholith is well exposed at Northern Indian Lake (Map GR2019-1-4), where it is characterized by a medium-grained groundmass and K-feldspar megacrysts up to 4 cm (Figure 12a). At the mapped outcrops, this unit is weakly to moderately magnetic, weakly foliated and homogeneous. Locally, the K-feldspar megacrysts have a preferred orientation subparallel to the biotite and hornblende crystals that is interpreted as primary flow foliation. In the majority of visited outcrops, however, no structure is evident. The Chipewyan-Wathaman batholith contains rare xenoliths of amphibolite and of sedimentary rock interpreted

to be from supracrustal rocks of the Southern Indian domain, possibly the Partridge Breast Lake assemblage but older supracrustal rocks could also be present.

The estimated average composition for the main phase of the Chipewyan-Wathaman batholith mapped in the study area is quartz (30–40%), plagioclase feldspar (40–50%), biotite (5–10%), pyrite and rare chalcopyrite (<1%), magnetite (<1%) and trace amounts of apatite. Petrographic observations indicate that locally, both plagioclase and K-feldspar weather to very fine grained white mica. Myrmekite and perthite are commonly observed amongst the feldspars. Mafic minerals occur isolated but can also form clusters of hornblende, biotite, zircon, ilmenite and titanite. Zircon occurs isolated throughout the thin section, in clusters as described above or as inclusions in biotite. Titanite crystals occur isolated, in clusters as described above or as overgrowths surrounding ilmenite.

Granite, granodiorite and tonalite (unit 18)

This unit encompasses a number of felsic intrusive rocks, with composition varying from granite to tonalite, that outcrop throughout the map area. Based on outcrop observations and U-Pb geochronological studies (see ‘U-Pb geochronology’ section), these rocks are interpreted to be ca. 1849 Ma, possibly related to Chipewyan-Wathaman magmatism. Extensive outcrops of subunit 18a can be found at Northern Indian Lake (Figure 1; Map GR2019-1-4) and in the north basin of Southern Indian Lake (Map GR2019-1-1). Characteristic outcrops of subunit 18a are granodiorite in composition, beige to light pink, medium to coarse grained, weakly to moderately foliated, weakly to moderately magnetic, and locally rusty due to weathering of disseminated sulphides. This subunit presents some variation in terms of its texture but, overall, the abundance and variation in major mineral modes is similar. The major mineral components have the following variable proportions: plagioclase (30–40%), quartz (25–40%), K-feldspar (10–15%),



Figure 12: Outcrop photographs of felsic intrusive rocks: **a)** Chipewyan-Wathaman batholith at Northern Indian Lake, showing characteristic K-feldspar megacrysts; **b)** granodiorite with mafic xenoliths, Partridge Breast Lake area; **c)** gneissic granodiorite near the Missi Falls Control Structure.

biotite-hornblende (up to 15%) and magnetite (<1–2%), with trace amounts of garnet, disseminated chalcopyrite, pyrite and minor pyrrhotite. In a few outcrops at Partridge Breast Lake, the granodiorite has abundant mafic xenoliths (Map GR2019-1-3; Figure 12b) and locally contains magnetite and garnet.

The foliated granodiorite and tonalite (subunit 18b) extends from the area of the Missi Falls Control Structure to the northeast of Partridge Breast Lake. This subunit is texturally differentiated by its strong foliation; it is beige when fresh and white when weathered, medium to coarse grained and nonmagnetic (Figure 12c). Locally, a less foliated plagioclase- and quartz-phyric texture was described (Martins, 2015a, b). This texture is characterized by plagioclase phenocrysts up to 1 cm in a medium-grained groundmass. Xenoliths of an older granitic intrusion (interpreted to be from the Northern Indian Lake pluton) occur throughout the plagioclase-phyric granodiorite, along with feldspathic and aluminous greywackes interpreted to be part of the Partridge Breast Lake assemblage. Detailed petrographic examination reveals the major mineral components as plagioclase (30–40%), quartz (30–35%), biotite and hornblende (5–8%), K-feldspar (<5%) and trace sulphides (pyrite and chalcopyrite).

Subunit 18c is a megacrystic granite that was found east of Sheppard Island (Figure 1; Map GR2019-1-1). It is pink, coarse

to very coarse grained, weakly magnetic and massive. This subunit is characterized by K-feldspar crystals up to 8 cm in a medium-grained groundmass of quartz, K-feldspar and plagioclase. The bulk-mineral assemblage of this unit comprises K-feldspar (40–50%), quartz (25–35%), plagioclase (10–30%) and biotite (<5%).

Subunit 18d was mapped in the Pukatawakan Bay area (Figure 1; Map GR2019-1-2) and described in detail by Kremer (2008a, b). It consists of swarms of synkinematic feldspar porphyry dikes that intruded along S_2 foliation planes. The dikes are described as having large textural variability, ranging from fine grained and homogeneous to pegmatitic (Kremer, 2008b). A dike interpreted as a structure emplaced during D_2 deformation and associated with up to 5% disseminated and stringer sulphide mineralization yielded a weighted mean $^{207}\text{Pb}/^{206}\text{Pb}$ age of 1843 ± 3 Ma (Kremer et al., 2009b). This result is interpreted as representing the crystallization age of the felsic porphyry dike.

Strawberry Island assemblage (unit 19)

The Strawberry Island assemblage outcrops along the northeast shore of Strawberry Island and south of the Missi Falls Control Structure from the east shore of Southern Indian Lake

(Figure 1; Map GR2019-1-3) to Gauer Lake. This assemblage is composed of isoclinally folded, massive to well-bedded, feldspathic to quartz sandstone intercalated with polymictic conglomerate. The sandstone (subunit 19a) varies from massive to well bedded and from fine to medium grained, and is usually magnetic and interbedded with narrow (<1 m) conglomeratic beds (Figure 13a). Amounts of feldspar and quartz vary (locally up to 80% quartz is observed). The unit is locally migmatitic, although primary features (such as bedding and crossbedding) are still preserved in a few outcrops. Typical outcrops of the polymictic conglomerate (subunit 19b) show low strain with weak flattening foliation, but locally the clasts are strongly recrystallized, strongly flattened, and folded (s-asymmetry). The polymictic conglomerate is clast supported, with sub- to well-rounded, poorly sorted clasts of granite, basalt (with epidote alteration), gabbro and a feldspar-phyric volcanic rock in a fine- to medium-grained, biotite-rich matrix (Figure 13b). Clast size varies from <2 cm to >30 cm. Where observed, crossbedding and scour structures indicate younging to the south.

This assemblage's maximum age of deposition was constrained at 1860 Ma and the minimum age of sedimentation is interpreted to be 1849 Ma, based on the age of a crosscutting monzogranite intrusion (see 'U-Pb geochronology' section).

Whyme Bay assemblage (unit 20)

The Whyme Bay assemblage was identified on a ridge between Whyme Bay and Pukatawakan Bay as kilometre-scale screens in K-feldspar-phyric monzogranite, and north of Loon Island (Figure 1; Map GR2019-1-2). These clastic sedimentary rocks display a prominent high on the high-resolution residual total-field aeromagnetic map (Coyle and Kiss, 2008) in the Whyme Bay area, but their extent in outcrop is limited. This assemblage was described by Kremer (2008b) in the Whyme Bay area and by Martins (2015b, 2016b) north of Loon Island. It consists of a sequence of magnetite-bearing fluvial-alluvial clastic sedimentary rocks with alternating mafic layers (biotite,

amphibole and sometimes mostly magnetite) and felsic layers (mostly feldspar and quartz). The dominant sedimentary facies is well-bedded to massive, fine- to medium-grained arenitic sandstone (subunit 20a; Figure 14a) with well-preserved primary features such as normal graded bedding and crossbedding. Lesser amounts of crudely bedded quartzite are found in some outcrops. A large exposure of polymictic, clast-supported conglomerate, located on a ridge between Whyme Bay and Pukatawakan Bay, may represent the basal unit of the clastic sedimentary sequence (subunit 20b). The conglomerate contains clasts of fine- to coarse-grained granite, mafic volcanic and intrusive rocks, and sedimentary rocks similar to those in the Partridge Breast Lake assemblage identified at Whyme Bay, as well as rare cobbles of felsic volcanic rocks and massive quartz (Figure 14b).

A sample of the fluvial-alluvial clastic sedimentary rocks taken at Whyme Bay yielded zircon ages within the range 1897–1753 Ma (Kremer et al., 2009b). Except for two older grains at 2320–2310 Ma, sixty-six of these analyses form a single statistical population centred at ca. 1832 Ma (Kremer et al., 2009b). A crystallization age of 1829 ± 1 Ma for the intrusive monzogranite (subunit 21a; Rayner and Corrigan 2004) provides an independent, precise constraint on the minimum age of sedimentation for the Whyme Bay assemblage. This tight time bracket between the dominant detrital mode and the crosscutting monzogranite indicates rapid burial, lithification and folding of the Whyme Bay assemblage (Kremer et al., 2009b).

Late intrusive rocks (unit 21)

Subunit 21a comprises granitoid rocks, dated at ca. 1829 Ma (Rayner and Corrigan, 2004), that outcrop in the southeast corner of Southern Indian Lake and extend into Whyme Bay (Figure 1; Map GR2019-1-2), forming a large plutonic body that is easily recognized on the high-resolution residual total-field aeromagnetic map (Coyle and Kiss, 2008).

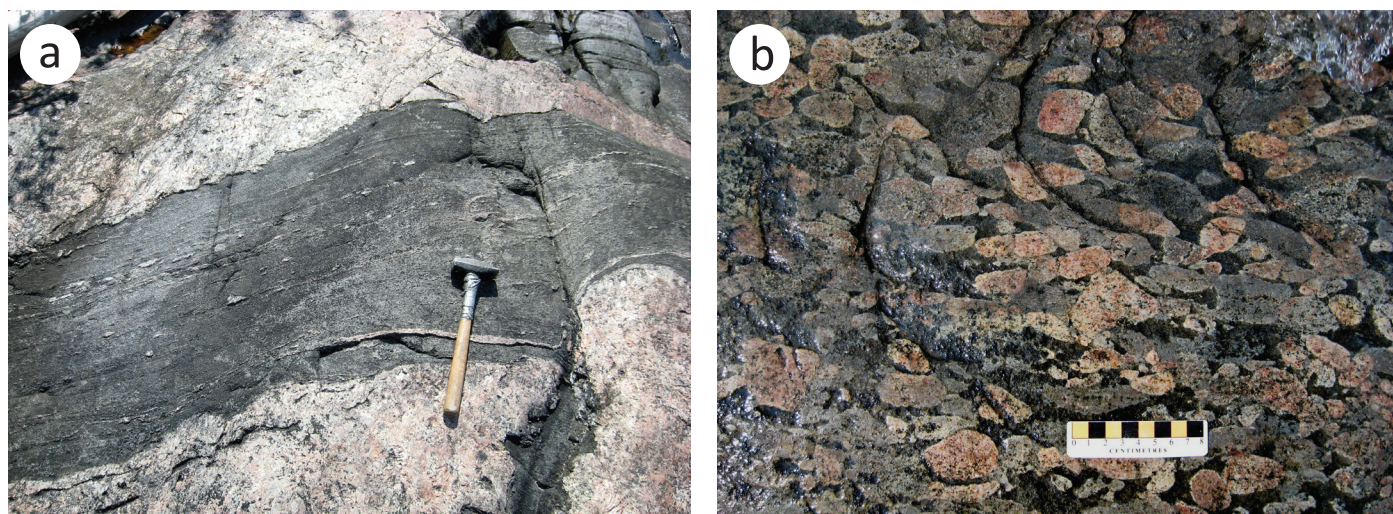


Figure 13: Outcrop photographs of the Strawberry Island assemblage: **a)** well-bedded grey sandstone, west shore of Strawberry Island; **b)** polymictic conglomerate with abundant rounded granitic clasts, east shore of Southern Indian Lake.



Figure 14: Outcrop photographs of clastic sedimentary rocks of the Whye Bay assemblage: **a)** thinly bedded arenite, east of Whye Bay; **b)** clast-supported polymictic conglomerate cut by K-feldspar megacrystic monzogranite, west of Whye Bay.

Taking into account outcrop descriptions and unit relationships, this subunit also encompasses texturally similar granitoid bodies that occur in other parts of the Southern Indian Lake area and have been described by several authors (e.g., Corrigan et al., 2002; Kremer, 2008b; Kremer et al., 2009b; Martins, 2015b, 2016b).

Granitoids typically are pink when fresh, weakly to moderately magnetic and variably deformed (locally tectonized on Loon Island; Martins, 2016b), and contain rare xenoliths of metasedimentary rocks interpreted to be from the Whye Bay and Partridge Breast Lake assemblages (historically linked to the Sickie Group; Frohlinger, 1972; Cranstone, 1972). Subunit 21a is monzogranite in composition with characteristic megacrystic K-feldspar texture present in the majority of the pluton, similar to the texture of the Chipewyan-Wathaman and Baldock batholiths. Point counts on four representative thin sections of the K-feldspar–megacrystic monzogranite ($n = 2592$) yielded a modal analysis of 33.1% K-feldspar, 24.9% plagioclase, 24.8% quartz, 7.4% biotite, 7.0% hornblende, 1.3% titanite, 1.1% ilmenite, 0.3% zircon and <0.1% allanite. Potassium-feldspar and plagioclase are locally found altered to fine, secondary white mica. Perthite and myrmekite are both observed throughout the thin section. Hornblende occurs associated with biotite, titanite, ilmenite, zircon, allanite and rare magnetite. Biotite exhibits pleochroic haloes as a consequence of radiation damage from zircon. Zircon occurs either isolated or as inclusions in hornblende and biotite. Titanite occurs rarely as an isolated crystal, and more commonly forms reaction rims around ilmenite (as is characteristic for S-type granite; Whalen and Chappell, 1988). In a series of outcrops along the east shore of Pukatawakan Bay, potassic alteration is common in magnetite-bearing granodiorite. The alteration is limited to narrow (<5 cm) anastomosing zones that crosscut the S_2 foliation at a shallow angle (Kremer, 2008a).

Subunit 21b comprises mafic to intermediate intrusions of gabbro, diorite and quartz diorite that occur in Pukatawakan Bay in close spatial association with the K-feldspar–megacrystic monzogranite (Kremer, 2008a) and also dated at ca. 1829 Ma (Rayner and Corrigan, 2004). These rocks usually do not present any evidence of deformation, or are weakly foliated, homogeneous, medium grained and equigranular with rare oikocrysts and plagioclase phenocrysts. Locally, metasomatic K-feldspar occurs in gabbro and quartz diorite near the contacts with the K-feldspar–megacrystic monzogranite. Typically, this subunit is crosscut by K-feldspar–dominant granitic pegmatites.

Thorsteinson Lake pluton (unit 22)

The Thorsteinson Lake pluton plots in the monzogranite field of the Streckeisen (1967) diagram. This large intrusion, located between the Chipewyan-Wathaman and Baldock batholiths at Thorsteinson Lake and extending to the west, causes a positive anomaly on the high-resolution residual total-field aeromagnetic map (Coyle and Kiss, 2008). Previous workers described this granitic body as a biotite–hornblende–bearing granite containing fluorite and interpreted as an anorogenic-type granite thought to represent a late-stage consolidation of the Proterozoic craton (Halden et al., 1990). Age determination by Rb–Sr geochronology indicates an age of 1740 Ma with an initial Sr isotopic ratio of 0.7013 (Clark, 1981). Later work by Halden et al. (1990) using Rb–Sr whole-rock geochemistry yielded an age of 1713 ± 19 Ma for this granitic body. The present study reveals a significantly older crystallization age of 1829 ± 5.5 Ma (see ‘U–Pb geochronology’ section), very similar to the age of other large granitic bodies in the area.

Outcrops of the Thorsteinson Lake monzogranite observed during this study are located in the southwesternmost corner of Thorsteinson Lake (outside the current map area). Locally,

this pluton is intruded by granitic pegmatite. The Thorsteinson Lake monzogranite is beige to pink, medium to coarse grained and locally weakly to moderately magnetic, and shows very few deformation fabrics (Martins and Kremer, 2013). Point counts ($n = 1908$) on four thin sections yielded a modal analysis of 36.2% quartz; 35.4% K-feldspar; 24.4% plagioclase; 2.2% biotite; 0.7% hornblende; 0.6% fluorite; 0.3% each of titanite, ilmenite, magnetite and other unidentified opaque minerals; 0.2% zircon; and 0.1% each of apatite and allanite. Petrographic studies revealed that fluorite occurs throughout the thin section and has a maximum size of 2 mm. It occurs as isolated grains and in association with ilmenite, magnetite, biotite and hornblende. Titanite has associations similar to those of fluorite and is locally found replacing ilmenite. Titanite and ilmenite locally replace biotite and hornblende. Zircon, measuring up to 1 mm, was found associated with biotite and hornblende; both metamict and crystalline zircon grains are evident.

Biotite granite, pink monzogranite and other K-feldspar–rich granitoids (unit 23)

Outcrops of biotite granite, pink monzogranite and minor K-feldspar–rich granitoids occur around Sand Point, in the west-central part of Southern Indian Lake (Figure 1;

Map GR2019-1-1) and the southern part of Northern Indian Lake (Map GR2019-1-4). Biotite granite (subunit 23a), which is the most abundant rock type of unit 23, is typically greyish pink when fresh and beige when weathered, nonmagnetic to weakly magnetic, medium grained, massive, equigranular and homogeneous. A few outcrops contain xenoliths of supracrustal rocks from the Southern Indian domain, possibly the Partridge Breast Lake assemblage. The granite's typical mineral composition is quartz (30–40%), K-feldspar (<40%), biotite (2–5%), minor plagioclase and trace magnetite.

In a few outcrops of the K-feldspar megacrystic monzogranite (subunit 21a), a late medium-grained pink monzogranite (subunit 23b; with composition close to the syenogranite subfield) is also present. This subunit also outcrops on Kuskayitum Island, where it intrudes gabbro, and in the northern basin of Southern Indian Lake (Figure 15a). Point counts ($n = 663$) on pink monzogranite yielded a modal analysis of 38.0% K-feldspar, 36.4% quartz, 22.8% plagioclase and 1.5% biotite.

On the south shore of Northern Indian Lake, a porphyritic K-feldspar–rich granite (subunit 23c) occurs close to the boundary of the Chipewyan domain to the northeast. The granite is pink when fresh, medium to coarse grained, massive to moderately foliated and homogeneous. It typically contains 20–30%

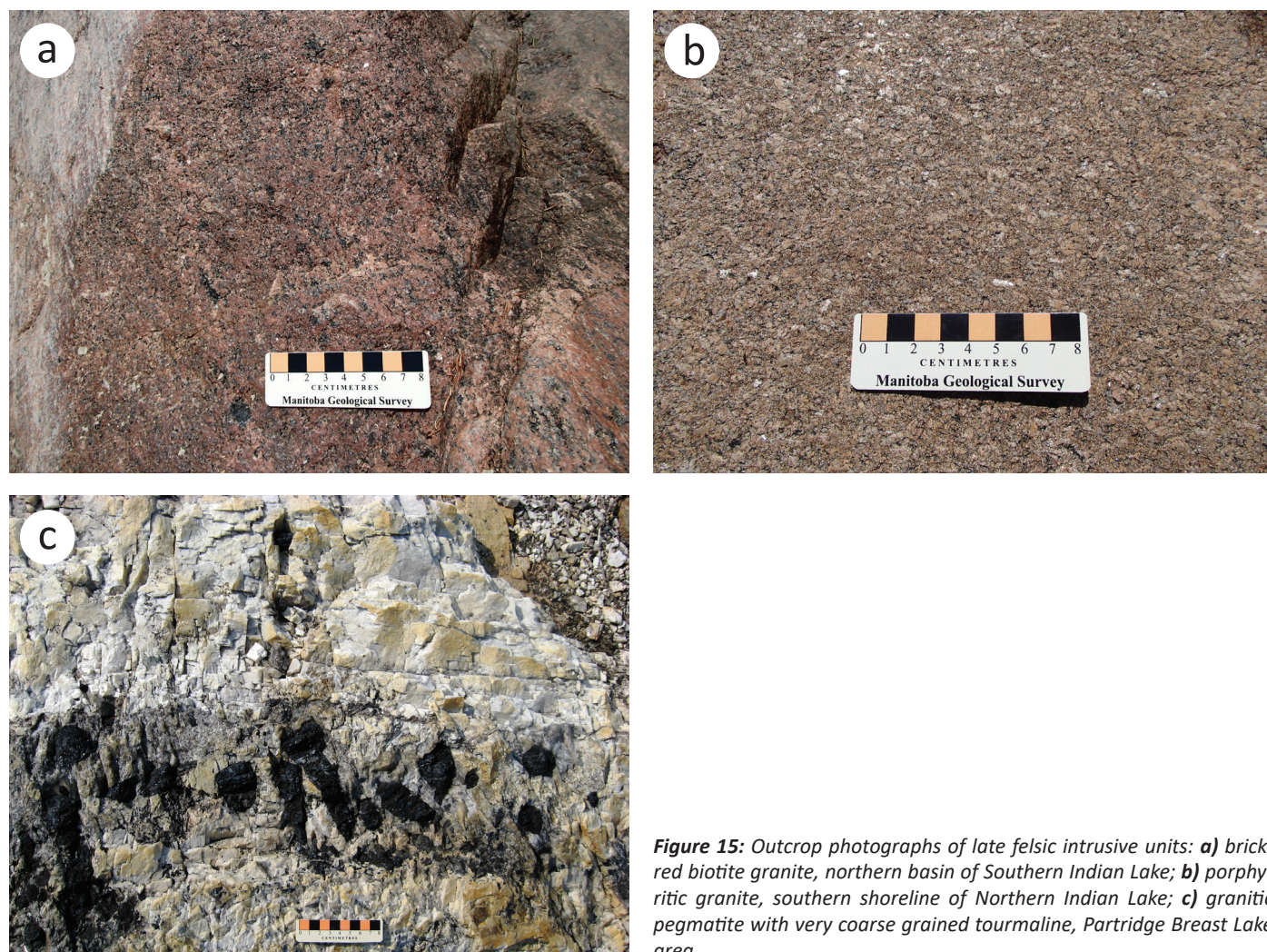


Figure 15: Outcrop photographs of late felsic intrusive units: **a)** brick-red biotite granite, northern basin of Southern Indian Lake; **b)** porphyritic granite, southern shoreline of Northern Indian Lake; **c)** granitic pegmatite with very coarse grained tourmaline, Partridge Breast Lake area.

K-feldspar phenocrysts that vary in size from 0.3 to 1 cm (Figure 15b), 30–40% quartz, 5–10% biotite and trace amounts of magnetite and plagioclase. It is possible that this granitic unit is related with the Thorsteinson monzogranite, but this is difficult to confirm based on current information.

Granitic pegmatite (unit 24)

Late pegmatite dikes are abundant in the Southern Indian Lake area and cut the various map units. The more abundant pegmatite bodies are either albite dominant or K-feldspar dominant (subunit 24a). Usually, the pegmatite bodies dip steeply and have variable strikes (mainly oriented north-northeast, south-southeast and southwest). Most of the pegmatite dikes are less than 2 m wide (some can be up to 10 m), unzoned or very crudely zoned and composed mostly of K-feldspar, albite, quartz, biotite and muscovite. Common accessory minerals are garnet, apatite and tourmaline (Figure 15c). Characteristic textures of granitic pegmatite, such as graphic texture, comb texture and rhythmic banding (also known as line rock), were observed in most of the pegmatite bodies.

Albite-dominant pegmatite is white and composed mostly of albite, quartz and K-feldspar, along with common accessory biotite, garnet and apatite. Green apatite is typically associated with white pegmatite and occurs either isolated within the pegmatite or closely associated with concentrations of biotite. Potassium-feldspar-dominant pegmatite is pink and composed mostly of K-feldspar, quartz, albite and biotite. Garnet, tourmaline and magnetite (crystals up to 1.5 cm) are common accessory phases.

A leucocratic variety of alkali-feldspar granitic pegmatite (also known as alaskite; subunit 24b; Map GR2019-1-2) occurs as an isolated body in the northwestern corner of Pukatawakan Bay, as described by Kremer (2008b).

Association of Au and base metals with pegmatite bodies was observed in the central part of Southern Indian Lake (see 'Economic considerations' for details). A detailed description of pegmatite dikes outcropping in the Southern Indian and Partridge Breast lakes area can be found in Martins and Kremer (2013), and accompanying whole-rock geochemical analyses are provided in Martins (2014). A detailed description of the pegmatites from the South Bay pegmatite field can be found in Martins (2016c).

Mackenzie dikes (unit 25)

Kremer (2008) described late diabase dikes at Pukatawakan Bay and Pine Lake as narrow (<5 m), northwest trending, homogeneous, massive, fine to medium grained, equigranular and strongly magnetic. Locally, a spinifex texture of plagioclase laths was observed. These dikes were interpreted as part of the Mackenzie dike swarm (1267 Ma; LeCheminant and Heaman, 1989), based on orientation and field observations. Other northwest-trending features from high-resolution, residual total-field aeromagnetic maps (Coyle and Kiss, 2008)

were also interpreted as part of the northwest-trending Mackenzie swarm, based on orientation.

Lithogeochemistry and Sm-Nd isotopes

In order to geochemically characterize the rocks mapped during this study, a comprehensive suite of samples (including several samples from each lithostratigraphic assemblage) was collected during the course of mapping. The purpose of the lithogeochemical sampling was to fully characterize the major- and trace-element chemistry of volcanic, sedimentary and granitoid rocks, and to test field observations. The purpose of applying Sm-Nd isotopic analysis was to try to characterize possible relationships and sources of rocks mapped during this study. The lithostratigraphic subdivision in the preceding text is based largely on variations in the geochemical and Sm-Nd isotopic data presented below.

Samples were collected for analysis during the following field seasons: 1980 and 1993 by M.T. Corkery (formerly MGS) from the Partridge Breast Lake area; 1999–2001 by D. Corrigan (GSC); 2008 by P.D. Kremer (formerly MGS) and N. Rayner (GSC) from Pukatawakan and Whyme bays, and Partridge Breast Lake; 2009 by P.D. Kremer from Partridge Breast and Gauer lakes; 2014 by P.D. Kremer and T. Martins from Northern Indian Lake; 2015 and 2016 by T. Martins from the northern basin and central part of Southern Indian Lake, respectively. A complete set of results from the lithogeochemical and Sm-Nd isotope analyses, as well as Universal Transverse Mercator (UTM) coordinates (all in Zone 14, NAD 83), are provided in Data Repository Item DRI2019001, which complements this report.

Sampling and analytical methods

All samples were collected in the field using hammers, chisels and a diamond-bladed rock saw. Care was taken to collect samples from locations where the rocks showed no visible or, at the very least, relatively minimal alteration or weathering. Fine- to medium-grained rock samples, consisting of 1–3 kg of least-altered homogeneous material, were collected by hammer from bedrock. Each sample was individually bagged and sealed with tape to avoid contamination. Pegmatite samples (coarse to very coarse grained), collected using a rock saw or hammer, varied in weight from 5 to 15 kg. Where possible, the rock samples were trimmed in the field to remove all weathered surfaces, veins, altered fractures or other inhomogeneities. Some samples were also trimmed by rock saw in the MGS's Midland Sample and Core Library in Winnipeg. The cleaned samples were crushed in a steel-jaw crusher to <5 mm, riffled both manually and mechanically, homogenized by rolling and quartered. A fraction was taken from each quarter and these were crushed together in a mild-steel shatter box and placed in a vibratory-ring pulverizer for milling to <200 mesh. The pulverized sample was quartered, riffled and quartered again to obtain a 20 g sample for analysis. This process was repeated several times for the pegmatite samples due to the large amount of crushed rock.

The whole-rock powders were submitted to Activation Laboratories Ltd. (Actlabs; Ancaster, Ontario) for analysis using the '4Litho' analytical package, which employed a lithium-metaborate/tetraborate fusion followed by nitric-acid digestion. Analysis was by inductively coupled plasma–emission spectrometry (FUS-ICP-ES) for the major elements and selected trace elements (Ba, Be, Sc, Sr, V, Y, Zr), and inductively coupled plasma–mass spectrometry (FUS-ICP-MS) for trace and rare-earth elements. Lithium was analyzed using total-digestion (TD) ICP-MS. For the analyses of F, a fusion with a combination of lithium metaborate and lithium tetraborate was used in an induction furnace to release the fluoride ions from the sample matrix. The fuseate³ was dissolved in dilute nitric acid. Prior to analysis, the solution was complexed and the ionic strength adjusted with an ammonium-citrate buffer. The fluoride-ion electrode was immersed in this solution to measure the fluoride-ion activity directly. An automated fluoride analyzer from Mandel Scientific was used for the analysis. To analyze B, samples 1 g in size were encapsulated in a polyethylene vial and placed in a thermalized beam of neutrons produced from a nuclear reactor. Samples were measured for the doppler-broadened prompt gamma ray at 478 KeV using a high-purity GE detector. Samples were compared with the certified reference materials used to calibrate the system.

Selected samples were submitted for assay and were analyzed using the package 1H 'Au+48' and Ultratrace2. The elements Au, As, Ba, Br, Ce, Co, Cr, Cs, Eu, Fe, Hf, Hg, Ir, La, Lu, Na, Nd, Rb, Sb, Sc, Se, Sm, Sn, Ta, Th, Tb, U, W and Yb were determined by instrumental neutron activation analysis (INAA). The remaining elements (Al, Be, Bi, Ca, Cd, Cu, K, Li, Mg, Mn, Mo, P, Pb, S, Sr, Ti, V and Y) were determined by the four-acid technique using a 'near total' digestion employing HF, HClO₄, HNO₃ and HCl to get as much of the sample into solution as possible without fusing. The resulting metals were determined by TD-ICP-ES. The elements Ag, Ni and Zn were run by both INAA and TD-ICP-ES. Depending on the results, the Actlabs system has specially formatted 'mult' schemes that select whether the INAA or the TD-ICP-ES results should be presented (MULT INAA/TD-ICP-ES). Each sample batch included at least one internal standard and one blind duplicate for analytical quality control. Data from the standards and duplicates have been removed and are not presented in Data Repository Item DRI2019001.

Although primary minerals were replaced by middle- to upper-amphibolite–facies metamorphic mineral assemblages, most major elements, high-field-strength elements (HFSE; Ti, Hf, Zr, Nb), rare-earth elements (REE), Th and transition elements are considered to have been immobile during this process (e.g., Pearce and Cann, 1973; Winchester and Floyd, 1977; Wood, 1980; MacLean, 1990; Jenner, 1996). The consistency in compositional trends using both mobile and immobile elements in the volcanic rocks, and their similarities to those of modern igneous rocks, support the interpretation that most

major and trace elements were not significantly affected by alteration or metamorphic processes, and their distributions are therefore interpreted to represent primary magmatic trends.

The chemical composition of granitoid rocks was plotted on discrimination diagrams of Pearce et al. (1984) and Frost (2001). The interpretation of discrimination diagrams of Pearce et al. (1984) must be undertaken with caution because the diagrams might not apply to granitoid rocks older than Phanerozoic (Pearce et al., 1984), which includes all granitoid rocks of the Southern Indian Lake area. The same authors emphasised that their discrimination diagrams offer a guide to the nature of the source regions of granitic magmas that, in conjunction with geological constraints, can add information on the tectonic setting of Phanerozoic (and probably Proterozoic) granitic intrusions. Of the main reasons advanced by Pearce et al. (1984) for exercising caution in using their classification in rocks older than Phanerozoic, the uncertainty regarding degree of partial melting and mantle fractionation and the influence of crustal melting are considered the most significant causes for concern in reliable tectonic-setting interpretations.

In addition to whole-rock lithogeochemical analysis, 37 samples were selected for Sm-Nd isotopic analysis. The samples were submitted to the Radiogenic Isotope Facility at the University of Alberta in Edmonton. The powders were accurately weighed and totally spiked with a known amount of mixed ¹⁵⁰Nd–¹⁴⁹Sm tracer solution; this tracer was calibrated directly against the Caltech mixed Sm/Nd normal described by Wasserburg et al. (1981). Dissolution occurred in mixed 24N HF + 16N HNO₃ media in sealed Teflon™ PFA (perfluoroalkoxy copolymer resin) vessels at 160°C for 6 days. The fluoride residue was converted to chloride with HCl, and Nd and Sm were separated by conventional cation and HDEHP (Bis[2-ethylhexyl] phosphate)–based chromatography. Chemical-processing blanks contained <200 picograms of either Sm or Nd, and were insignificant relative to the amount of Sm or Nd contained in any rock sample. Further details can be found in Creaser et al. (1997) and Unterschutz et al. (2002).

The isotopic composition of Nd was determined in static mode by multicollector inductively coupled plasma–mass spectrometry (MC-ICP-MS; Schmidberger et al., 2007). All isotope ratios were normalized for variable mass fractionation to a value of ¹⁴⁶Nd/¹⁴⁴Nd = 0.7219 using the exponential fractionation law. The ¹⁴³Nd/¹⁴⁴Nd ratio of samples is presented here relative to a value of 0.511850 for the La Jolla Nd isotopic standard, monitored by use of an in-house Alfa Nd isotopic standard for each analytical session. Samarium isotopic abundances were measured in static mode by MC-ICP-MS and were normalized for variable mass fractionation to a value of 1.17537 for ¹⁵²Sm/¹⁵⁴Sm, also using the exponential fractionation law. The Geological Survey of Japan Nd isotope standard 'Shin Etsu: J-Ndi-1' (Tanaka et al., 2000) was also analyzed

³ The product of lithium-metaborate/tetraborate (or any other type of) fusion.

using the same isotopic analysis and normalization procedures, and gave a $^{143}\text{Nd}/^{144}\text{Nd}$ value of 0.512107 ± 7 relative to a LaJolla $^{143}\text{Nd}/^{144}\text{Nd}$ value of 0.511850, when normalized to $^{146}\text{Nd}/^{144}\text{Nd} = 0.7219$. The value of $^{143}\text{Nd}/^{144}\text{Nd}$ determined for the J-Ndi-1 standard during the analysis of the samples reported here was 0.512100 ± 7 (2SE); the long-term average value is 0.512098 ± 10 (1σ , $n = 102$, past 8 years). Using the mixed $^{150}\text{Nd}/^{149}\text{Sm}$ tracer, the measured $^{147}\text{Sm}/^{144}\text{Nd}$ ratios for the international rock standard BCR-1 range from 0.1380 to 0.1382, suggesting reproducibility for $^{147}\text{Sm}/^{144}\text{Nd}$ of approximately $\pm 0.1\%$ for real rock powders. The value of $^{147}\text{Sm}/^{144}\text{Nd}$ determined for BCR-1 is within the range of reported literature values by isotope-dilution methods.

Analytical results

Geochemical and Sm-Nd isotopic data are presented for Archean orthogneiss and each of the volcanic assemblages, sedimentary units and felsic intrusive rock units, in order of decreasing known or inferred age. Because there are only two samples from the Churchill River assemblage, these data were plotted together with results from the Pukatawakan Bay assemblage. A full geochemistry dataset for the Churchill River assemblage is available for only one sample, but trace-element geochemistry is available for both samples; therefore, some diagrams have two points plotted for the Churchill River assemblage, whereas others have only one point. Discrimination diagrams in Figures 16 to 22 show geochemical data for the entire sample suite, separated according to the different assemblages or map units. Representative results are shown in Table 2. Samarium-neodymium isotopic data are provided in Table 3. All major and trace elements are included in Data Repository Item DRI2019001. Lithogeochemical data for the Thorsteinson monzogranite, and pegmatites from South Bay, Southern Indian Lake and Partridge Breast Lake can be found in Data Repository Item DRI2014001.

Archean rocks (unit 1)

A late Neoarchean to early Paleoproterozoic granodiorite gneiss sample (CXA-01-D56) has negative ϵ_{Nd} values and a model age of 2.83 Ga (Table 3). This result suggests interaction with older crustal components. Similar results were also found for orthogneiss sample 107-09-252 from an isolated island west of the Missi Falls Control Structure. Based on Sm-Nd isotopic data, rocks from both locations were assigned to unit 1.

Churchill River assemblage (unit 4)

Basalt from the Churchill River assemblage plots in the basalt field on the $\text{Na}_2\text{O} + \text{K}_2\text{O}$ vs. SiO_2 diagram (Figure 16a) and has Zr/Ti and Nb/Y ratios around 0.01 and 0.1, respectively, suggesting a subalkaline affinity (Figure 16b). The sample plots at the edge of the basalt and Fe-tholeiite fields on the cation (Al_2O_3 vs. $\text{FeO} + \text{TiO}_2$ vs. MgO) diagram of Jensen and Pyke (1982; Figure 16c) and in the tholeiitic field on the immobile trace-

element (Th/Yb vs. Zr/Y) diagram (Figure 16d). One basalt sample from the Churchill River assemblage contains 44.74 wt. % SiO_2 , 15.38 wt. % Fe_2O_3 and 2.93 wt. % TiO_2 , and has a Mg number of 37. Two samples of basalt contain 140 ppm (for both) and 30 and 130 ppm Ni. The basalt samples have relatively flat profiles on the chondrite-normalized extended-element diagram (Figure 17a), showing a slight enrichment in the light rare-earth elements (LREE). On the normal mid-ocean-ridge basalt (N-MORB)-normalized extended-element diagram, the Churchill River basalt shows unfractionated LREEs and heavy rare-earth elements (HREEs), with negative Nb and Zr anomalies (more pronounced in one of the samples) and weak positive Th and Ti anomalies (Figure 17b).

On the Th vs. Hf/3 vs. Ta trace-element discrimination diagram (Wood, 1980), the Churchill River assemblage basalts plot at the border with and inside the N-MORB field (Figure 18a). On the La/10 vs. Y/15 vs. Nb/8 diagram (Cabaniš and Lecolle, 1989), they plot in the back-arc field and the volcanic-arc tholeiite basalt field (Figure 18b). On the TiO_2/Yb vs. Nb/Yb diagram (Figure 18c; Pearce, 2008), they plot above the shallow-melting asthenospheric array, indicating that the basalt may have originated from a low degree of melting at greater depth, likely with minor residual garnet (Pearce, 2008). On the Th/Yb vs. Nb/Yb diagram of Pearce and Peate (1995), they plot at the edge of the N-MORB array (Figure 18d) and just above it in the oceanic-arcs field, indicating lack of continental-crust involvement via contamination or subduction (Pearce, 2008). Low Nb/Yb ratios indicate a strongly depleted mantle source, which favours an oceanic rather than continental-arc setting (Pearce and Peate, 1995; Pearce 2008). The samples have ϵ_{Nd} values of 4.3 and 4.6 at 1.9 Ga (Table 3), corroborating the interpretation that these rocks were derived from a juvenile-mantle source and that their interaction with isotopically evolved crustal material must have been minor. Churchill River assemblage basalt could have been erupted in a back-arc basin-like tectonic environment (Pearce and Stern, 2006), comparable to the modern analogue back-arc basin of the Mariana arc (samples from the Churchill River assemblage and the Mariana arc plot in the same field on the Ba/Yb vs. Nb/Yb diagram, not shown). The data presented above also suggest that the tectonic environment for the Churchill River assemblage could have been a restricted or isolated basin with minor interaction with the forming advancing arc.

Geochemical data for the arkose associated with the basalt of the Churchill River assemblage (not shown) reveal enrichment in LREE and a relatively flat pattern for the HREE on the chondrite-normalized extended-element diagram. The primitive mantle-normalized extended-element diagram shows distinct Nb and Ti anomalies, and a slight Eu anomaly, similar to what would be expected for calcalkaline felsic rocks and thus suggesting a continental source for these arkosic rocks.

It is worth emphasizing that outcrops of the Churchill River assemblage are limited in the study area (see 'Churchill River assemblage (unit 4)' section), so the available geochemical data

Table 2: Lithogeochemical data for representative samples of lithological units in the Southern Indian Lake area.

Sample:	107-08-598A	107-08-81A	107-08-96	107-08-107A	107-08-222	107-08-447	107-08-559A	107-08-150	107-08-186	107-08-265	107-09-37A	107-09-9	107-09-47B	107-14-059	113-16-158	113-16-162	113-14-1112	113-14-1115	107-14-051	113-15-018	113-15-056B
Assemblage:	CR	Puk	Puk	Puk	Puk	Puk	Puk	Puk	Puk	PBL	PBL	PBL	PBL	PBL	PBL	PBL	NIL	Unit 18	Chip.	Chip.	Unit 21
Rock type:	Basalt	MORB	MORB	Peridotite	Basalt	Basalt	Volc.	Gabbro	Gabbro	Basalt	Basalt	Felsic volc.	Felsic volc.	Felsic tuff	Gabbro	Gabbro	Grano	Grano	Granite	granite	monzo
Parameter																					
(wt. %)																					
SiO ₂	44.74	49.61	48.11	40.94	49.31	50	59.48	53.93	50.67	47.28	61.4	65.94	76.95	77.13	45.51	57.89	62.96	71.49	69.7	65.93	71.73
Al ₂ O ₃	17.31	16.68	13.96	5.11	12.99	14.26	16.22	14.87	14.61	14.67	14.49	14.64	10.89	12.46	14.47	14.34	16.77	15.68	14.74	15.62	13.76
Fe ₂ O ₃	15.38	9.57	13.18	10.81	17.97	14.22	11.49	9.86	12.21	13.3	8.32	5.22	2.71	2.3	19.84	12.25	5.02	2.21	3.46	3.96	2.55
MnO	0.232	0.167	0.222	0.129	0.276	0.222	0.147	0.115	0.126	0.202	0.123	0.123	0.047	0.049	0.345	0.215	0.084	0.028	0.06	0.048	0.024
MgO	4.61	5.93	9.4	28.32	4.61	6.11	3.95	4.31	4.36	4.94	3.56	1.14	0.72	0.43	3.18	1.7	2.61	0.71	1.2	0.94	0.38
CaO	10.67	14.51	10.78	4.35	9.36	9.68	3.67	6.59	7.91	9.28	6.11	2.36	0.66	1.6	8.8	4.75	5.18	2.95	2.52	2.11	1.5
Na ₂ O	1.84	0.88	2.15	0.22	2.49	2.65	1.77	3.09	2.82	3.08	2.35	4.48	3.45	3.82	3.57	3.52	4.27	4.82	3.3	3.39	2.68
K ₂ O	0.93	0.38	0.16	0.03	0.38	0.77	0.58	3.14	2.41	0.75	1.62	2.83	2.12	2.01	0.71	2.6	2.06	1.82	4.19	5.93	5.6
TiO ₂	2.927	1.032	0.819	0.324	2.544	1.819	1.26	1.537	1.896	2.636	0.37	0.665	0.137	0.335	2.707	1.861	0.527	0.237	0.449	0.556	0.244
P ₂ O ₅	0.17	0.23	0.08	0.03	0.28	0.22	0.06	1.08	2.18	1.65	0.13	0.2	<0.01	0.04	1.28	0.68	0.19	0.1	0.18	0.19	0.07
LOI	0.14	1.03	0.75	10.19	0.36	0.85	0.59	0.83	0.9	0.28	0.97	0.93	0.55	0.48	0.27	0.45	0.66	0.44	0.78	0.46	0.07
Total	98.96	100	99.63	100.5	100.6	100.8	99.22	99.35	100.1	99.57	100.4	99.11	98.53	100.9	100.7	100.3	100.9	100.8	101	99.14	0.53
(ppm)																					
Sc	42	48	54	22	43	43	33	17	19	27	32	14	3	6	61	28	11	1	7	6	2
Be	3	2	1	<1	3	2	3	3	2	3	<1	2	1	2	<1	2	1	1	3	2	2
V	386	351	312	135	557	399	255	204	292	284	189	53	<5	8	41	30	89	27	47	44	19
Ba	733	76	41	9	30	188	316	1948	1205	681	705	878	683	773	362	1770	789	917	1064	2186	1228
Sr	419	101	85	33	155	305	231	1304	946	775	267	248	148	244	604	442	551	682	346	516	193
Y	32.5	20.1	18.9	7.4	43.8	29.1	16.3	21.5	26	42.5	12.7	26.6	55.5	24	18	45	14	3	19	32	8
Zr	155	56	42	23	184	111	190	171	236	206	71	198	131	192	32	401	101	86	181	285	187
Cr	140	170	280	2100	100	110	130	60	60	120	50	<20	<20	<20	<20	<20	60	20	30	<20	<20
Co	55	86	51	97	50	50	31	30	38	46	22	10	<1	2	20	11	16	5	6	5	3
Ni	30	130	60	1630	<20	<20	<20	70	20	<20	<20	<20	<20	<20	<20	<20	40	<20	<20	<20	<20
Cu	70	20	30	<10	90	50	70	40	70	50	150	40	<10	<10	<10	10	10	<10	<10	<10	<10
Zn	180	120	70	90	140	60	90	110	180	560	70	190	40	60	190	180	70	50	60	60	70
Ga	23	16	13	8	22	20	22	20	22	22	12	16	14	14	21	23	20	20	19	20	17
Ge	1.5	1.1	1.3	1.3	1.2	1.5	1.5	1.2	1.2	1.1	1.5	1.6	1.4	2	2	2	1	<1	2	<1	1
As	<5	<5	34	140	<5	<5	<5	<5	<5	<5	<5	<5	<5	<5	<5	<5	<5	<5	<5	<5	<5
Rb	49	13	3	<1	2	16	19	73	65	11	39	65	30	63	11	30	59	39	125	111	143
Nb	3.5	3.4	2.6	1.1	11.5	9.9	12.1	8.2	12.7	15.7	3.7	9.7	6.8	6	3	15	5	2	11	13	7
Mo	<2	<2	<2	<2	<2	<2	<2	<2	<2	<2	<2	<2	<2	<2	<2	3	<2	2	<2	2	<2

Abbreviations: Chip., Chipewyan batholith; CR, Churchill River; Grano, granodiorite; Monzo, monzogranite; MORB, mid-ocean–ridge basalt; NIL, Northern Indian Lake; PBL, Partridge Breast Lake; Puk, Pukatawakan Bay; Volc., volcanioclastic

Table 2 (continued): Lithogeochemical data for representative samples of lithological units in the Southern Indian Lake area.

Sample:	107-08-598A	107-08-81A	107-08-96	107-08-107A	107-08-222	107-08-447	107-08-559A	107-08-150	107-08-186	107-08-265	107-09-37A	107-09-9	107-09-47B	107-14-059	113-16-158	113-16-162	113-14-1112	113-14-1115	107-14-051	113-15-018	113-15-056B
Assemblage:	CR	Puk	Puk	Puk	Puk	Puk	Puk	Puk	Puk	PBL	PBL	PBL	PBL	PBL	PBL	PBL	NIL	Unit 18	Chip.	Chip.	Unit 21
Rock type:	Basalt	MORB	MORB	Peridotite	Basalt	Basalt	Volc.	Gabbro	Gabbro	Basalt	Basalt	Felsic volc.	Felsic volc.	Felsic tuff	Gabbro	Gabbro	Grano	Grano	Granite	granite	monzo
(ppm)																					
Ag	<0.5	<0.5	<0.5	<0.5	<0.5	<0.5	<0.5	1.7	<0.5	<0.5	<0.5	<0.5	<0.5	0.8	<0.5	1.2	0.9	0.8	0.9	<0.5	<0.5
In	<0.1	<0.1	<0.1	<0.1	0.1	<0.1	<0.1	<0.1	<0.1	<0.1	<0.1	<0.1	<0.1	<0.2	<0.2	<0.2	<0.2	<0.2	<0.2	<0.2	<0.2
Sn	1	4	10	1	2	<1	<1	1	2	2	<1	4	7	2	<1	1	1	<1	3	2	<1
Sb	<0.2	<0.2	0.7	4.1	<0.2	1.8	<0.2	1.5	1.7	<0.2	0.8	0.5	<0.2	<0.5	<0.5	0.6	<0.5	<0.5	<0.5	<0.5	<0.5
Cs	7.5	0.9	0.2	0.2	0.4	<0.1	0.9	1.6	1.6	0.2	1	1.3	1.2	2.7	0.7	<0.5	0.9	<0.5	1.2	<0.5	2.8
La	6.04	4.33	3.66	1.57	17.1	19.9	37	78.7	75.2	76.2	14.9	28	25.3	27.7	13.6	39	19.6	12.3	42.4	70.5	44.2
Ce	19.4	10	8.63	3.78	44.2	42.4	71.4	144	149	160	27.6	56.7	51.5	56.4	32.8	95.4	38.8	21.7	83.1	152	86.5
Pr	3.01	1.39	1.17	0.53	6.25	4.95	8.18	17.9	18.4	22.4	3.34	6.97	6.46	6.52	4.56	12.3	4.58	2.25	9.04	17.5	9.23
Nd	16.9	7.84	6.54	2.85	26.1	20.4	24.7	65.5	63.4	77.6	13.3	27.4	26.7	23.8	23.2	56.5	18	7.7	31.9	60.7	30.3
Sm	5.55	2.23	1.9	0.92	6.77	5.02	4.38	13	13	15.6	2.7	5.24	6.37	4.9	5.5	12.5	3.2	1.1	5.6	10.3	4.3
Eu	1.87	0.833	0.761	0.394	2.24	1.64	2.06	3.41	3.13	4.24	0.721	1.19	1.48	0.85	3.22	4.39	0.87	0.49	1.18	1.72	1.45
Gd	6.69	2.86	2.57	1.18	7.43	5.13	3.28	8.7	8.95	12.3	2.34	4.59	6.99	4.4	5.8	11	2.6	0.6	4.4	6.8	2.3
Tb	1.08	0.49	0.46	0.21	1.41	0.82	0.55	0.98	1.07	1.82	0.38	0.73	1.31	0.7	0.7	1.6	0.4	<0.1	0.6	1	0.2
Dy	6.54	3.23	2.96	1.31	8.99	4.92	3.3	4.38	5.09	9.63	2.18	4.42	8.8	4.4	4	8.8	2.2	0.3	3.7	5.6	1
Ho	1.34	0.73	0.67	0.27	1.78	1.04	0.66	0.72	0.92	1.67	0.46	0.91	1.99	0.9	0.7	1.7	0.4	<0.1	0.7	1	0.2
Er	4.07	2.34	2.15	0.82	5.11	3.19	1.98	1.89	2.47	4.42	1.32	2.69	6.14	2.8	1.9	4.6	1.3	0.2	2	2.9	0.4
Tm	0.586	0.368	0.336	0.115	0.734	0.459	0.309	0.246	0.322	0.6	0.217	0.446	1.08	0.43	0.26	0.64	0.2	<0.05	0.3	0.41	0.05
Yb	3.45	2.36	2.17	0.69	4.55	2.89	2.21	1.4	1.8	3.54	1.45	2.92	7.05	2.8	1.5	4.1	1.3	0.2	1.9	2.6	0.3
Lu	0.492	0.347	0.309	0.101	0.655	0.413	0.368	0.181	0.251	0.496	0.216	0.415	1.05	0.44	0.22	0.62	0.2	<0.04	0.28	0.41	0.05
Hf	4.7	1.6	1.4	0.7	5.4	3.3	5.6	3.9	6	5.3	1.7	4.9	3.5	4.5	0.9	8	2.4	2	4.4	6.6	4.7
Ta	0.23	0.2	0.17	0.08	0.82	0.65	0.95	0.52	0.72	0.86	0.19	0.45	0.28	0.6	0.2	0.9	0.3	0.1	0.6	1	0.6
W	9.1	1.2	<0.5	0.8	1.2	<0.5	0.9	0.9	1.9	1.1	<0.5	<0.5	<0.5	1	<1	<1	<1	1	4	<1	<1
Tl	0.66	0.16	<0.05	<0.05	0.08	<0.05	0.17	0.34	0.51	0.07	0.17	0.14	<0.05	0.4	0.2	0.2	0.4	0.4	0.7	0.7	0.8
Pb	8	10	<5	<5	<5	<5	<5	11	14	<5	6	8	9	15	<5	10	6	8	28	23	21
Bi	0.7	12.4	0.2	12.8	7.3	0.8	3.3	10.1	4.8	3.5	0.2	1.5	<0.1	<0.4	<0.4	<0.4	<0.4	<0.4	<0.4	<0.4	<0.4
Th	0.31	0.25	0.34	0.15	3.48	3.21	6.84	6.64	7.79	1.46	2.62	5.86	3.78	9.1	1.4	0.8	4	2.2	17.8	12.1	15.9
U	0.13	9.9	0.34	0.04	1.34	0.35	1.85	3.63	2.45	0.54	1.09	2.65	3.04	2.9	0.8	0.9	0.6	0.5	3.5	1.2	1

Abbreviations: Chip., Chipewyan batholith; CR, Churchill River; Grano, granodiorite; Monzo, monzogranite; MORB, mid-ocean–ridge basalt; NIL, Northern Indian Lake; PBL, Partridge Breast Lake; Puk, Pukatawakan Bay; Volc., volcanioclastic

Table 3: Samarium-neodymium isotopic data for rock samples from the Southern Indian Lake area.

Sample number	Geologist	Location	UTM (Zone 14, NAD 83)		Rock type	Sm (ppm)	Nd (ppm)	¹⁴⁷ Sm/ ¹⁴⁴ Nd	¹⁴³ Nd/ ¹⁴⁴ Nd	Err. (2σ)	T _{DM} (Ga)	T (Ma)	ε _{Nd}
			Easting	Northing									
Archean crust													
107-09-252	Kremer	West of Missi Falls	540621	6352839	Orthogneiss	7.64	43.07	0.1072	0.51119	0.00001	2.81	1850	-7.1
CXA-01-D56	Corrigan	Southern Indian Lake	520463	6325770	Diorite gneiss	7.46	41.02	0.1100	0.51122	0.00001	2.83	1850	-7.1
Gneisses of unknown age (unit 2)													
107-08-452A	Kremer	Pukatawakan Bay	521114	6327271	Orthogneiss	4.55	31.53	0.0872	0.51138	0.00001	2.14	1900	2.3
Churchill River assemblage													
107-08-598-A	Kremer	Lower Churchill River	559625	6359639	Basalt	5.537	17.46	0.1917	0.51279	0.00001		1900	4.3
CXA-01-D102a	Corrigan	Southern Indian Lake	559641	6359673	Mafic volcanic	5.74	17.87	0.1944	0.51284	0.00001	N/A	1800	4.6
Pukatawakan Bay assemblage													
107-09-095A	Kremer	Budgie Island	542798	6349112	Orthogneiss	7.67	44.00	0.1054	0.51143	0.00001	2.43	1850	-1.9
107-08-222	Kremer	Southern Indian Lake	505823	6327929	Pillow basalt	6.366	23.63	0.1629	0.51214	0.00002		1900	-1.5
107-08-566-A	Kremer	Southern Indian Lake	511812	6330611	Basalt	3.478	8.660	0.2429	0.51345	0.00001		1900	4.7
107-09-208B	Kremer	Turtle Island	547270	6350082	Basalt	3.74	12.39	0.1827	0.51259	0.00001	N/A	1850	2.5
107-08-157	Kremer	Southern Indian Lake	507263	6322070	Basalt	2.690	9.177	0.1772	0.51245	0.00001		1900	1.0
107-08-243	Kremer	Southern Indian Lake	517962	6325167	Pillow basalt	3.180	10.70	0.1798	0.51249	0.00001		1900	1.3
107-09-095B	Kremer	Budgie Island	542798	6349112	Basaltic dike	7.46	35.14	0.1283	0.51190	0.00001	2.24	1850	1.9
107-08-100	Kremer	Southern Indian Lake	508226	6325697	Amphibolite (massive basalt)	3.017	10.47	0.1743	0.51250	0.00001		1900	2.7
CXA-01-45a1	Corrigan	Southern Indian Lake	510139	6326027	Meta-andesite	7.01	31.86	0.1331	0.51191	0.00001	2.35	1880	1.2
CXA-01-45b	Corrigan	Southern Indian Lake	510140	6326028	Mafic volcanic	2.59	8.05	0.1945	0.51271	0.00001	N/A	1905	2.0
CXA-01-D28b	Corrigan	Southern Indian Lake	517933	6325139	Mafic volcanic	3.61	12.22	0.1784	0.51252	0.00001	N/A	1905	2.2
CXA-01-32b	Corrigan	Southern Indian Lake	519238	6327761	Mafic volcanic	0.97	3.84	0.1522	0.51223	0.00001	N/A	1905	3.0
Northern Indian Lake pluton													
113-14-1112	Martins	Northern Indian Lake	600887	6362683	Granodiorite	3.03	16.2	0.1129	0.51171	0.00001	2.18	1890	2.3
Turtle Island complex													
CXA-01-N1	Corrigan	Southern Indian Lake	547812	6351095	Turtle Island diorite	2.56	13.36	0.1157	0.51141	0.00001	2.71	1855	-4.7

Abbreviation: N/A, not available

Table 3 (continued): Samarium-neodymium isotopic data for rock samples from the Southern Indian Lake area.

Sample number	Geologist	Location	UTM (Zone 14, NAD 83)		Rock type	Sm (ppm)	Nd (ppm)	¹⁴⁷ Sm/ ¹⁴⁴ Nd	¹⁴³ Nd/ ¹⁴⁴ Nd	Err. (2σ)	T _{DM} (Ga)	T (Ma)	ε _{Nd}
			Easting	Northing									
Partridge Breast Lake assemblage													
107-09-293	Kremer	Long Point	540998	6335029	Pillow basalt	2.80	9.06	0.1865	0.51271	0.00001	N/A	1850	3.9
107-08-265	Kremer	Southern Indian Lake	518146	6320912	Mafic volcanic rock (amygdaloidal)	13.97	77.43	0.1091	0.51138	0.00001	2.58	1900	-3.2
113-16-224	Martins	Southern Indian Lake	533855	6338018	Paragneiss	10.7	58.9	0.1100	0.51151	0.00001	2.42	1900	-0.8
CXA-01-P60a	Corrigan	Southern Indian Lake	553073	6357996	Metapelite	5.63	31.22	0.1091	0.51123	0.00000	2.79	1800	-7.2
107-09-047B	Kremer	Partridge Breast Lake	570926	6351825	Felsic volcanic	6.325	26.74	0.1430	0.51195	0.00001	N/A	1850	-0.8
107-14-059	Kremer	Northern Indian Lake	606810	6350887	Felsic tuff	4.87	25.3	0.1163	0.51175	0.00001	2.20	1900	2.3
107-09-041F	Kremer	Northern Indian Lake	606677	6357674	Orthogneiss	7.305	45.70	0.0967	0.51129	0.00001	2.43	1850	-2.5
CXA-01-N3	Corrigan	Southern Indian Lake	560351	6359262	Metapsammite	5.18	27.49	0.1138	0.51160	0.00001	2.38	1800	-1.1
Chipewyan batholith													
107-14-051	Kremer	Northern Indian Lake	604536	6365763	Megacrystic granite	5.61	31.8	0.1064	0.51147	0.00001	2.39	1900	-0.8
Granodiorite (unit 18a)													
113-14-1028	Martins	Northern Indian Lake	597643	6355496	Granite	0.906	6.37	0.0860	0.51136	0.00001	2.15	1900	2.0
CXA-01-N20a	Corrigan	Southern Indian Lake	531319	6366219	Granitic orthogneiss	8.64	46.17	0.1132	0.51154	0.00000	2.45	1800	-2.1
CXA-01-N2	Corrigan	Southern Indian Lake	558099	6359186	Leucogranite	0.45	2.25	0.1198	0.51165	0.00001	2.45	1890	-0.7
1829 Ma monzogranite													
CXA-01-D40(rpt)	Corrigan	Southern Indian Lake	513897	6321537	Monzodiorite	7.18	39.85	0.1089	0.51158	0.00001	2.29	1855	0.3
CXA-01-D51(rpt)	Corrigan	Southern Indian Lake	517450	6321100	Megacrystic granite	17.48	78.88	0.1340	0.51187	0.00001	2.47	1855	-0.1

Abbreviation: N/A, not available

are very limited. The results from only two samples of basalt suggest an overall characteristic MORB signature and minor subduction components. The basalt is dominantly juvenile and shows very little evidence of interaction with crustal material. Intervening arkosic layers were presumably derived from older crust, most likely from the Hearne craton; U-Pb geochronological data from this unit (sample 107-08-598C) reveal predominant zircon detrital modes at 2630 and 2655 Ma, with an early Proterozoic zircon dated at 2437 ± 9 Ma, which is interpreted as a maximum age of sedimentation (Kremer et al., 2009b).

Pukatawakan Bay assemblage

These volcanic rocks are exclusively mafic except for a few outcrops of volcanoclastic rocks at Pine Lake. Based on whole-rock lithogeochemistry data, the volcanic rocks of this assemblage have been subdivided into ocean-floor and juvenile-arc subtypes.

Volcanic rocks of the Pukatawakan Bay assemblage contain 47.73–59.48 wt. % SiO_2 , 9.57–18.26 wt. % Fe_2O_3 and 0.82–2.55 wt. % TiO_2 . Chromium ranges from 60 to 360 ppm and Ni ranges from below detection limit to 130 ppm. Magnesium numbers are low to moderate, ranging from 34 to 59. One sample is distinguished by its higher values of 2100 ppm Cr and 1630 ppm Ni, and high Mg number of 84, indicating a more primitive origin. This ultramafic rock was mapped as peridotite and is considered part of the Pukatawakan Bay assemblage, based on outcrop interpretations and similarities in REE profiles to the mafic rocks of this assemblage.

The compositions of both subtypes of mafic volcanic rocks overlap and range from basalt to basaltic andesite on major-element diagrams, with the single intermediate volcanoclastic sample from Pine Lake plotting in the andesite field (Figure 16a). Major-element and immobile trace-element discrimination diagrams indicate a subalkaline affinity for the

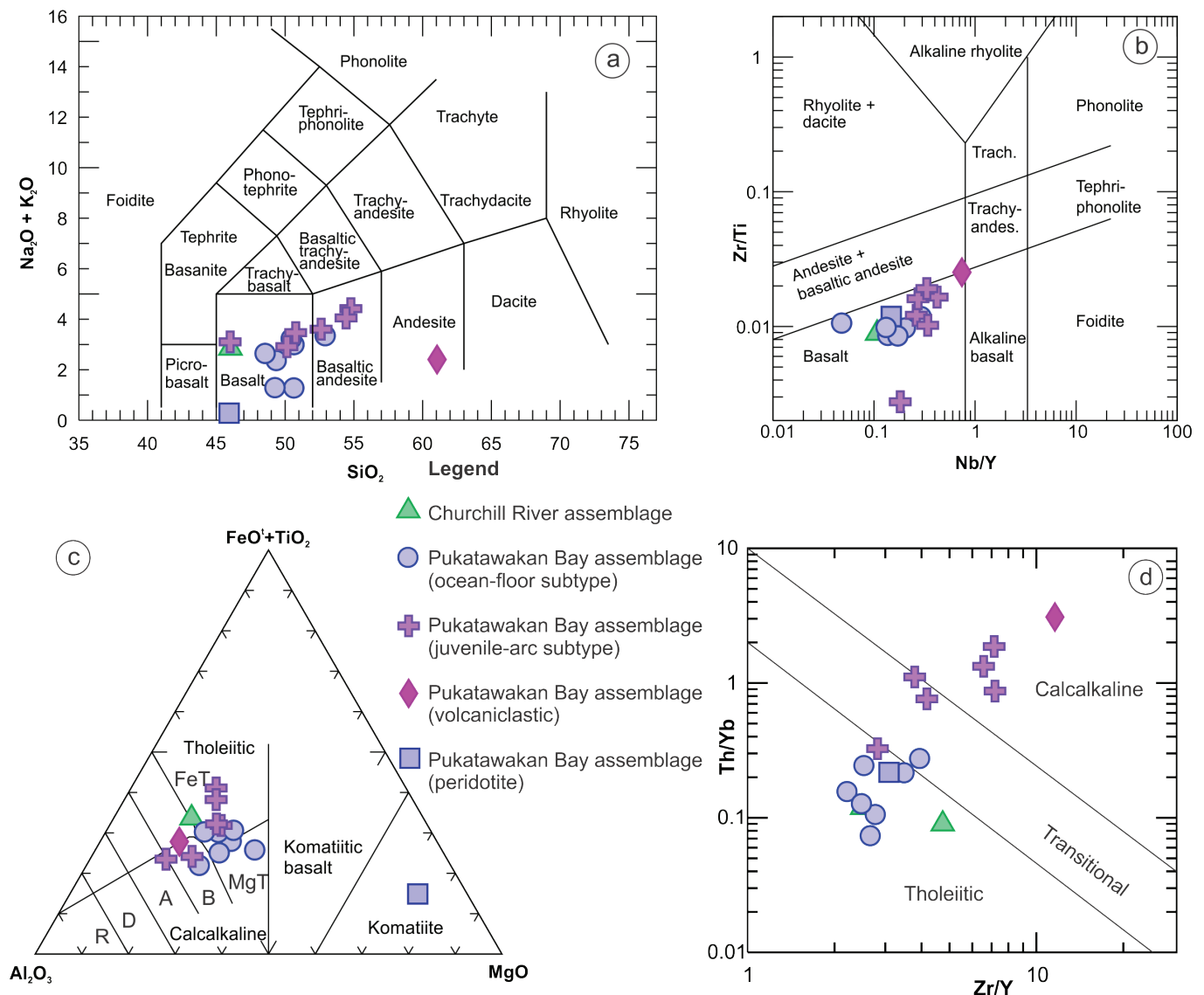


Figure 16: Major-element and immobile trace-element discrimination diagrams for basalt from the Churchill River and Pukatawakan Bay assemblages: **a)** $\text{Na}_2\text{O} + \text{K}_2\text{O}$ vs. SiO_2 diagram normalized to 100 (after Le Bas et al., 1986); **b)** Zr/Ti vs. Nb/Y diagram (after Pearce, 1996); **c)** Al_2O_3 vs. $\text{FeO} + \text{TiO}_2$ vs. MgO cation diagram (after Jensen and Pyke, 1982); **d)** Th/Yb vs. Zr/Y diagram (Ross and Bédard, 2009). Abbreviations: A, andesite; Andes., andesite; B, basalt; D, dacite; FeT, Fe tholeiite; MgT, Mg tholeiite; R, rhyolite; Trach., trachyte.

volcanic and associated intrusive rocks of the Pukatawakan Bay assemblage (Figure 16b). On trace-element discrimination diagrams, the samples plot in the basalt field and have low Zr/Ti values (0.002–0.012) and low Nb/Y values (0.05–0.42), suggesting a subalkaline affinity, whereas the volcanoclastic sample has slightly elevated Nb/Y, suggestive of a mildly alkaline affinity (Figure 16b). On the Jensen and Pyke (1982) diagram, the basaltic rocks cluster in the basalt and the Fe and Mg tholeiitic fields, with a couple of outliers plotting in the calcalkaline fields (Figure 16c).

The mafic rocks considered part of the ocean-floor subtype have relatively flat REE patterns on the chondrite-normalized extended-element diagram (Figure 17a), characteristic of mafic volcanic rocks in a modern MORB setting. When plotted on the N-MORB-normalized extended-element diagram, samples from this subtype have relatively flat profiles with weakly

fractionated LREE, unfractionated heavy HREE and negative Nb anomalies (Figure 17b). Immobile trace-element ratios indicate that the rocks identified as part of the ocean-floor subtype are tholeiitic, with one sample plotting in the transitional field (Figure 16d). On the Th vs. Hf/3 vs. Ta diagram (Wood, 1980), the MORB-affinity samples cluster close to the N-MORB basalt field (Figure 18a) and, on the La/10 vs. Y/15 vs. Nb/8 diagram (Cabanis and Lecolle, 1989), they plot in the back-arc basin and N-MORB fields (Figure 18b). On the Th/Nb vs. La/Sm diagram (Anderson, 2013), the MORB samples show a weakly vertical trend (Figure 18e), indicating subduction input. On the TiO₂/Yb vs. Nb/Yb diagram of Pearce (2008), the samples straddle the N-MORB and E-MORB fields (Figure 18c). On the Th/Yb vs. Nb/Yb diagram of Pearce and Peate (1995), the data plot just above the MORB array, defining a parallel trend (Figure 18d).

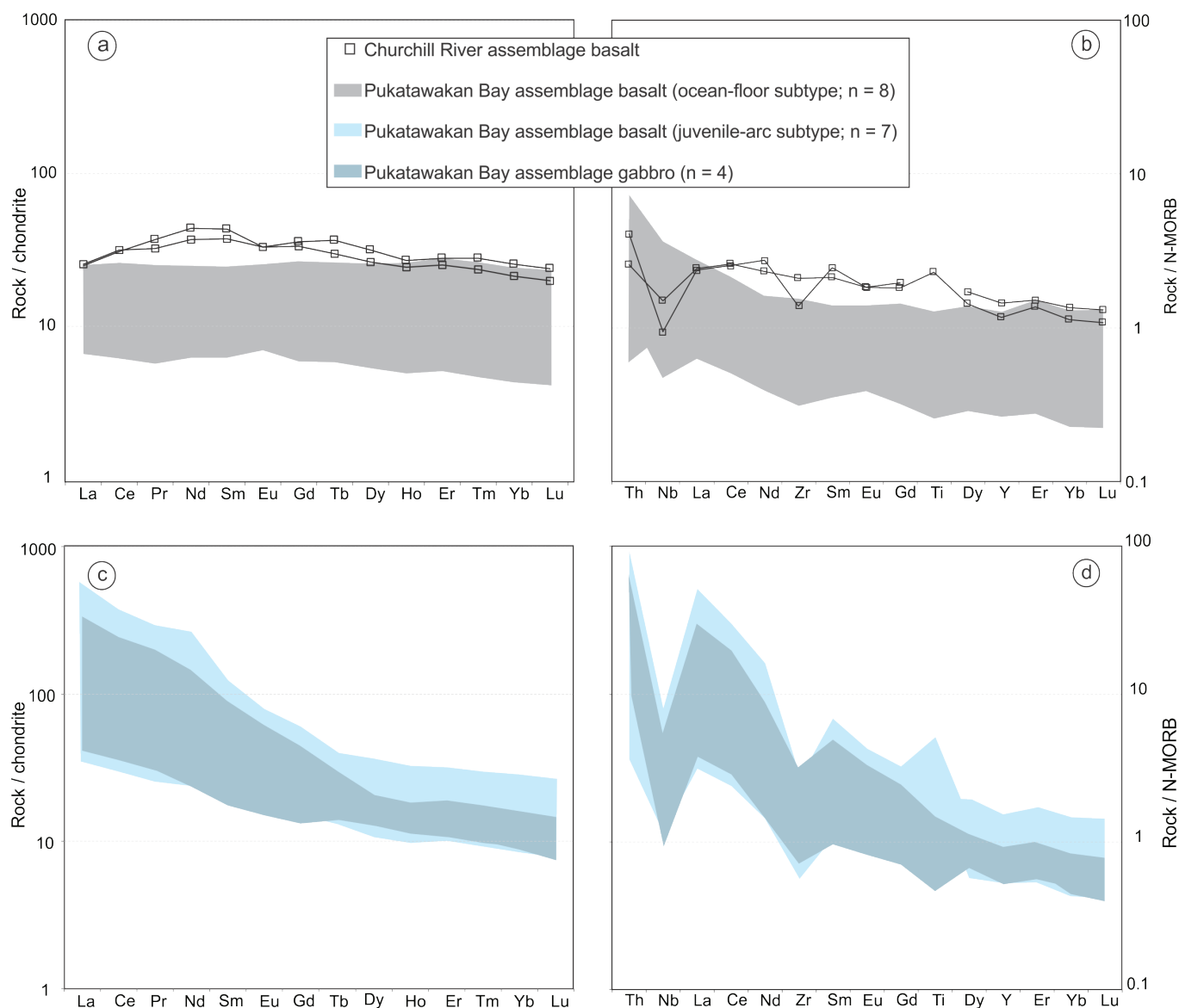
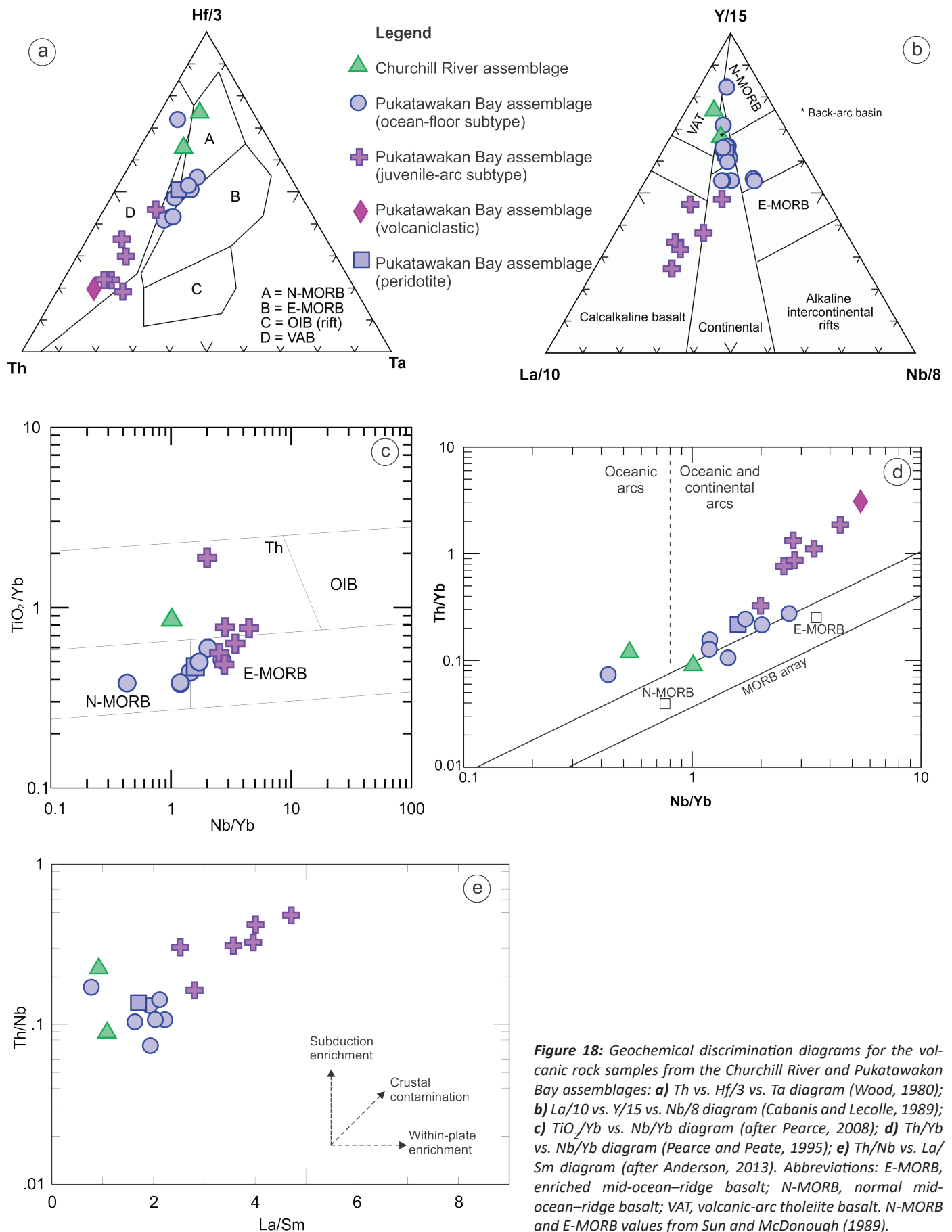


Figure 17: Chondrite-normalized extended-element diagrams (left) and N-MORB normalized extended-element diagrams (right) for: **a)** and **b)** Churchill River assemblage and Pukatawakan Bay assemblage (ocean-floor subtype) basalt; **c)** and **d)** Pukatawakan Bay assemblage (juvenile-arc subtype) basalt and gabbro. Normalizing values for chondrite and primitive mantle are from McDonough and Sun (1995) and normalizing values for N-MORB are from Sun and McDonough (1989). Abbreviation: N-MORB, normal mid-ocean-ridge basalt.



In comparison, the group of rocks considered part of the juvenile-arc subtype have slightly enriched LREE patterns on the chondrite-normalized extended-element diagram (Figure 17c). When plotted on the N-MORB-normalized extended-element diagram, data from the juvenile-arc subtype show enriched and fractionated LREE and negative Nb, Zr and Ti anomalies (Figure 17d); a negative Nb anomaly is characteristic of the volcanic-rifted margin basalt and results from magma-crust interaction (Pearce, 2008). On immobile trace-element diagrams, these samples plot in the transitional or calcalkaline fields, with only one exception plotting in the tholeiitic field (Figure 16d). On the Th vs. Hf/3 vs. Ta diagram (Wood, 1980), they fall in the volcanic-arc basalt field (Figure 18a) and, on the La/10 vs. Y/15 vs. Nb/8 diagram (Cabanis and Lecolle, 1989), most samples plot in the calcalkaline basalt field, with one sample plotting in the continental field (Figure 18b). On the TiO_2/Yb vs. Nb/Yb diagram of Pearce (2008), the samples straddle the E-MORB and tholeiitic fields (Figure 18c). On the Th/Yb vs. Nb/Yb diagram of Pearce and Peate (1995), they scatter above the MORB array, suggesting an input of a high Th/Yb crustal component (Figure 18d). On the Th/Nb vs. La/Sm diagram (Anderson, 2013), these arc-affinity samples show a diagonal trend (Figure 18e), suggestive of crustal contamination.

Eleven samples collected from the Pukatawakan Bay assemblage were submitted for Sm-Nd isotopic analysis. Values of ϵ_{Nd} for basalt samples with MORB compositions vary between 1.0 and 4.7 (at 1.9 Ga; Table 3), whereas those for basalt samples with a juvenile-arc signature vary between -1.5 and 1.9. More positive ϵ_{Nd} values are indicative of a more juvenile-mantle source with little to no interaction with older crustal material, as is the case for basalt samples with MORB composition. More negative ϵ_{Nd} values, on the other hand, are commonly indicative of increased interaction with older crustal rocks, as is somewhat indicated by the samples with juvenile-arc signature.

Combined lithogeochemical and Sm-Nd data suggest that the volcanic rocks of the Pukatawakan Bay assemblage could have formed in different tectonic environments. The juvenile-arc subtype samples, with strong depletions in high-field-strength elements, could have erupted in an oceanic volcanic arc (Kelemen et al., 1990; Saunders et al., 1991). Their ϵ_{Nd} values (-1.5 to 1.9) corroborate the interpretation of some interaction with older crustal material. The MORB-signature rocks, with positive ϵ_{Nd} values (1.0 and 4.7), could be associated with a back-arc basin. Alternatively, the volcanic rocks of the juvenile-arc subtype could be unconformably overlying the MORB-signature rocks.

Lithogeochemical results for the gabbroic rocks associated with the Pukatawakan Bay assemblage indicate an origin similar to that of the mafic juvenile-arc volcanic rocks, based on extended-element profiles (Figure 17c, d).

Partridge Breast Lake assemblage

On the basis of major-element and immobile trace-element discrimination diagrams, the rocks from this assemblage have a bimodal distribution of volcanic and associated intrusive rock compositions characterized by a broadly linear trend from basalt to rhyolite (Figure 19a). The results also show a linear trend from medium to elevated Zr/Ti values (0.010–0.301) at low Nb/Y values (0.16–0.37), suggesting a subalkaline affinity (Figure 19b). On the Jensen and Pyke (1982) diagram, they define a continuous trend from Fe-tholeiitic basalt to rhyolite (Figure 19c). Immobile trace-element ratios indicate a trend from tholeiitic to calcalkaline (Figure 19d).

Mafic rocks

Basaltic rocks from the Partridge Breast Lake assemblage contain 47.28–59.32 wt. % SiO_2 , 0.37–2.64 wt. % TiO_2 , 6.2–13.3 wt. % FeO^t and Mg numbers of 42–66. Chromium ranges from below detection limit to 581 ppm (average of 133 ppm) and Ni ranges from below detection limit to 60 ppm (average of 29 ppm). All data have negative slopes when plotted on chondrite-normalized extended-element diagrams, with fractionated and enriched LREE and moderately enriched HREE, except for a few samples that have profiles more similar to a MORB-type basalt (Figure 20a). On an N-MORB normalized diagram, most data display the typical arc signature, with prominent negative Nb and Zr anomalies and moderately negative Ti anomaly (Figure 20b). Thorium, Ti, Nb and Yb show well-defined linear trends when plotted against Ce or Zr (not shown) as indices of fractionation, suggesting a crystal fractionation control for these elements. The profiles of the basalt samples that are more similar to MORB-type basalt are relatively flat with weakly fractionated LREE, unfractionated heavy HREE and negative Nb anomalies (Figure 20b).

With the exception of three outliers, the mafic volcanic rocks of the Partridge Breast Lake assemblage show strong depletion of Nb and weak depletion of Zr and Ti, indicative of subduction influence on the generation of the magmas in a volcanic-arc setting (Perfit et al., 1980; Saunders and Tarney, 1984; Kelemen et al., 1990; Saunders et al., 1991). The Th vs. Hf/3 vs. Ta diagram (Figure 21a; Wood, 1980) shows the majority of data plotting in the volcanic-arc-basalt field, with a few exceptions plotting in the N-MORB and E-MORB fields. On the La/10 vs. Y/15 vs. Nb/8 diagram (Figure 21b; Cabanis and Lecolle, 1989), the majority of samples fall in the calcalkaline basalt field, typical of a volcanic-arc environment, with a few exceptions plotting in the back-arc basin field. Most of the samples fall in the continental-arc field on the Pearce (1983) Zr/Y vs. Zr diagram (Figure 21c). On the Th/Yb vs. Nb/Yb diagram, the samples plot above the MORB array, indicating a significant input of high-Th/Yb crustal material and a variably enriched mantle source and/or variable degrees of partial melting (Figure 21d; Pearce and Peate, 1995; Pearce, 2008). The samples define a sloped trend on the plot of Th/Nb vs.

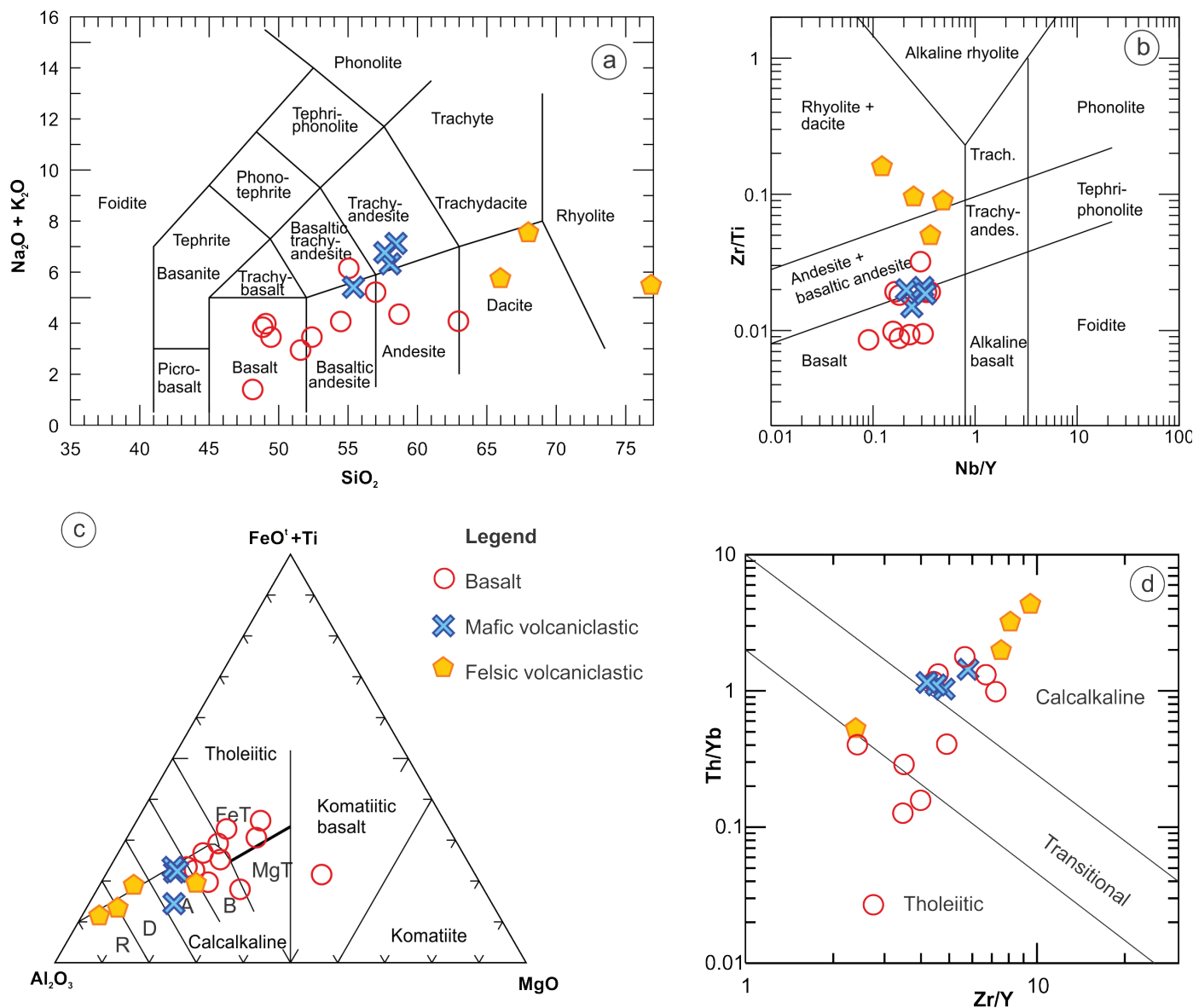


Figure 19: Major-element and immobile trace-element discrimination diagrams for volcanic rocks of the Partridge Breast Lake assemblage: **a)** Na₂O+K₂O vs. SiO₂ diagram normalized to 100 (after Le Bas et al., 1986); **b)** Zr/Ti vs. Nb/Y diagram (after Pearce, 1996); **c)** Al₂O₃ vs. FeO⁺+TiO₂ vs. MgO diagram (after Jensen and Pyke, 1982); **d)** Th/Yb vs. Zr/Y diagram (Ross and Bédard, 2009). Abbreviations: A, andesite; Andes., andesite; B, basalt; D, dacite; FeT, Fe tholeiite; MgT, Mg tholeiite; R, rhyolite; Trach., trachyte.

La/Sm (Figure 21e; Anderson, 2013), which implicates crustal contamination during their petrogenesis.

Two samples of mafic volcanic rocks from the Partridge Breast Lake assemblage yielded ϵ_{Nd} values of -1.5 and -3.2 at 1.90 Ga, and depleted-mantle model ages up to 2.58 Ga (Table 3), indicating interaction with and/or recycling of Archean continental crust in a subduction-zone setting, corroborating the lithogeochemical interpretations. In comparison, a mafic volcanic sample with MORB-like signature yielded an ϵ_{Nd} value of 3.9, indicative of juvenile-mantle derivation.

Lithogeochemical results for the gabbroic rocks of the Partridge Breast Lake assemblage show patterns on chondrite- and N-MORB-normalized extended-element diagrams similar to those of mafic volcanic rocks, suggesting a cogenetic relationship.

Felsic rocks

Felsic (66–77 wt. % SiO₂) volcanoclastic rocks from the Partridge Breast Lake assemblage outcrop predominantly south of Partridge Breast Lake. On the chondrite-normalized extended-element diagram, data for felsic volcanoclastic samples show sloping profiles with LREE enrichments and fractionation, moderately negative Eu anomalies and enriched HREE (Figure 20c). On the primitive-mantle-normalized extended-element diagram, the data show negative Nb and Ti anomalies with slightly positive Zr anomalies (Figure 20d; one sample has a slightly negative Zr anomaly). The Zr/Y ratios are moderate (2.4–9.4) and Cr and Ni contents are below detection limit (one sample has a Cr value of 50 ppm above detection limit). Moderate [La/Yb]_N (3.6–9.9) and Zr/Y (2.4–9.4) ratios, and moderate values of Yb (2.92–7.05 ppm) and Y (24–56 ppm) indicate an affinity to

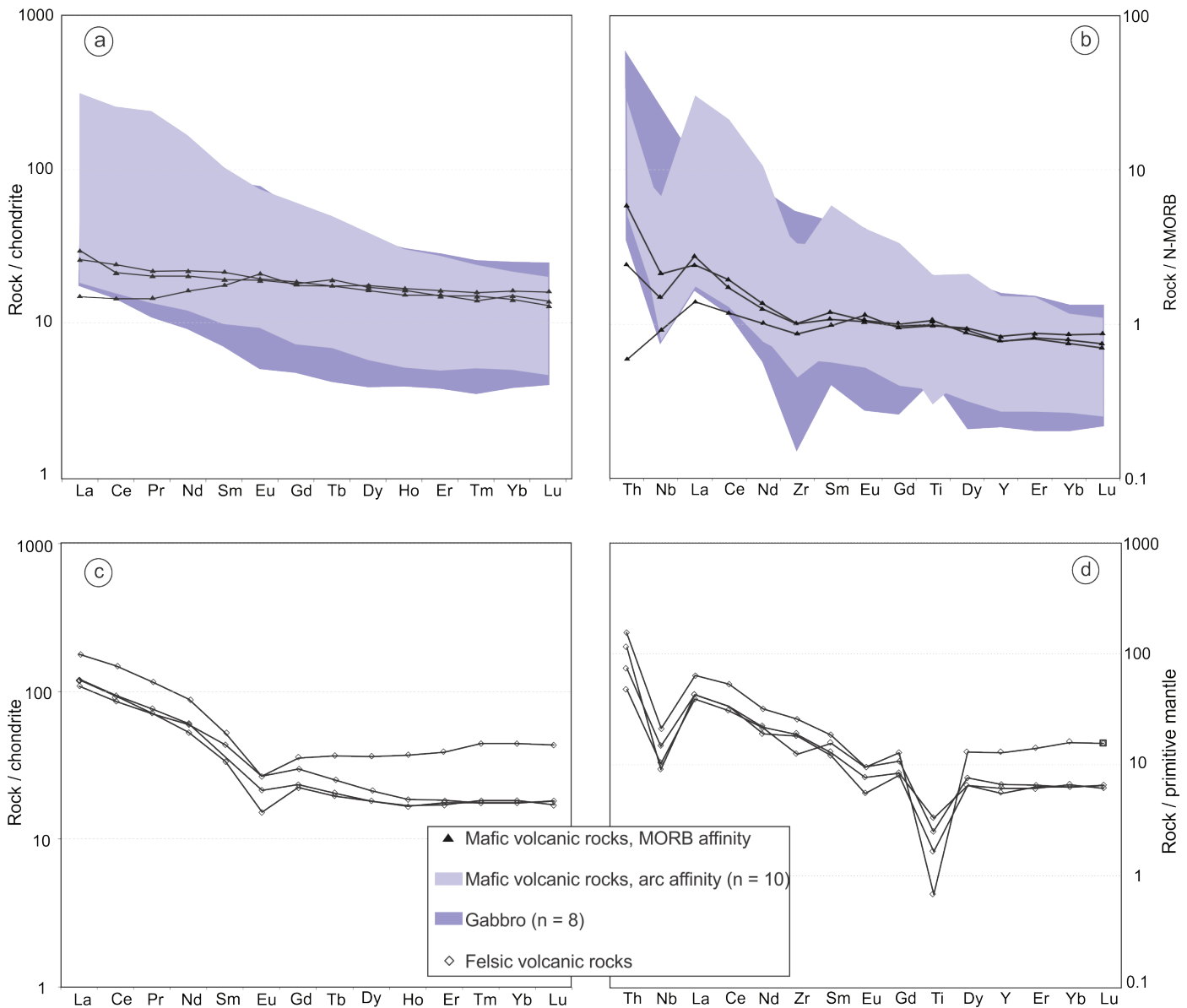


Figure 20: Extended-element diagrams for rocks of the Partridge Breast Lake assemblage: **a)** chondrite-normalized diagram for mafic volcanic rocks and gabbro; **b)** N-MORB-normalized diagram for mafic volcanic rocks and gabbro; **c)** chondrite-normalized diagram for felsic volcanic rocks; **d)** primitive-mantle-normalized diagram for felsic volcanic rocks. Normalizing values for chondrite and primitive mantle are from McDonough and Sun (1995), and those for N-MORB are from Sun and McDonough (1989). Abbreviation: N-MORB, normal mid-ocean-ridge basalt.

FII felsic volcanic rocks in the scheme of Leshner et al. (1986; Figure 21f), and these rocks are consequently interpreted to have formed in a rift-like environment, possibly derived from partial melting of hydrated basaltic crust at midcrustal levels (Hart et al., 2004). Two samples of felsic volcanoclastic rock yielded ϵ_{Nd} values of -0.8 and 2.3 at 1.90 Ga (Table 3), indicating some interaction with an older, isotopically evolved crust.

Granitoid rocks

The diagrams of Pearce et al. (1984) are some of the most widely used trace-element plots for discriminating granitic rocks and attempt to classify these types of rocks according to their tectonic environment. In this report, however, the clas-

sification of Frost et al. (2001) is preferred, mainly because it is a purely chemical classification based on major elements and not founded on judgments as to the origin or the tectonic environment of granitoid rocks. As Frost et al. (2001) pointed out, trace-element compositions of granitoid rocks are, for the most part, not a function of their tectonic environment but vary according to their source rocks and the crystallization history of a melt leading to granitoid magmatism. Furthermore, Pearce et al. (1984) recognized the limitations of their classification scheme applied to rocks older than the Phanerozoic.

Several types of granitoid rocks were described and divided into different units in the Southern Indian Lake area, based on field petrography, textural characteristics, field relationships

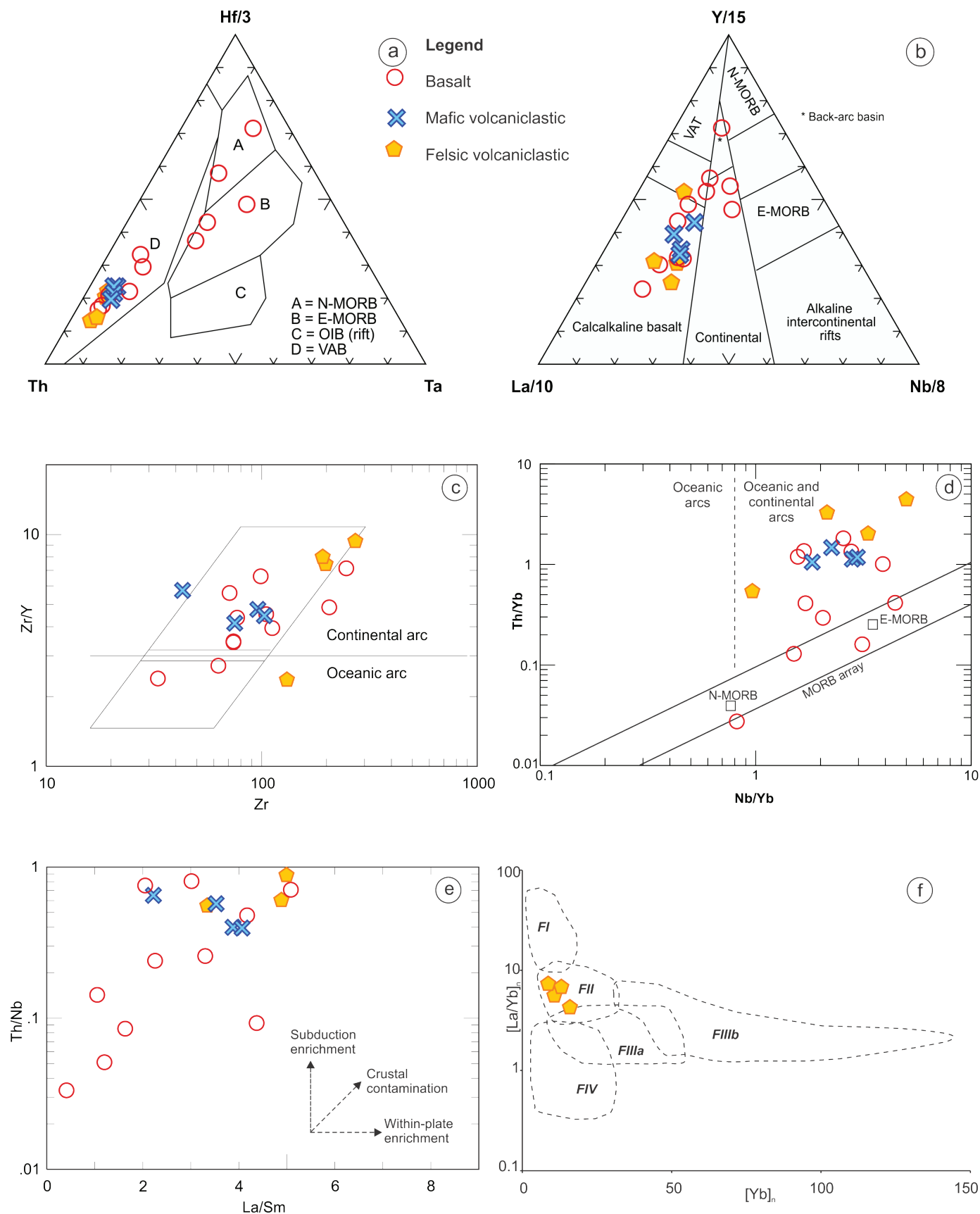


Figure 21: Geochemical discrimination diagrams for rocks of the Partridge Breast Lake assemblage: **a)** Th vs. Hf/3 vs. Ta diagram (Wood, 1980); **b)** La/10 vs. Y/15 vs. Nb/8 diagram (Cabanis and Lecolle, 1989); **c)** Zr/Y vs. Zr diagram (after Pearce, 1983); **d)** Th/Yb vs. Nb/Yb diagram (Pearce and Peate, 1995); **e)** Th/Nb vs. La/Sm diagram (after Anderson, 2013; one felsic volcanoclastic rock sample plots outside the diagram); **f)** $[La/Yb]_N$ vs. $[Yb]_N$ diagram, showing the fields for FI-FIV rhyolite (after Hart et al., 2004). Abbreviations: E-MORB, enriched mid-ocean-ridge basalt; N-MORB, normal mid-ocean-ridge basalt; VAT, volcanic-arc tholeiite basalt. N-MORB and E-MORB values are from Sun and McDonough (1989).

and age (ranging from 1896 to 1829 Ma; see 'U-Pb Geochronology' section). These felsic intrusive rocks are predominantly biotite and hornblende bearing, and their composition (based on detailed petrography and point counting), although variable, falls mainly within the granodiorite, granite and monzogranite fields of Streckeisen (1967). In terms of whole-rock geochemistry, an aluminum-silica saturation-index diagram shows that most granitoid rocks plot in the peraluminous and metaluminous fields (Figure 22a). Trace-element geochemical data indicate that these rocks have a typical arc signature, with HFSE depletion and LREE enrichment when plotted on the chondrite-normalized extended-element diagram (not shown). On the primitive-mantle-normalized extended-element diagram (not shown), the data reveal prominent Nb and Ti anomalies. On the Rb vs. Yb+Ta diagram (Pearce et al., 1984), the majority of samples plot in the volcanic-arc granite field (Figure 22b). Other discrimination diagrams from the same author (not shown) also place the granitoid units in similar tectonic environments. On the Fe^* vs. SiO_2 diagram (Figure 22c) of

Frost et al. (2001), the majority of samples plot in the field of Cordilleran granites (equivalent to the volcanic-arc granite field of Pearce et al., 1984) and in the magnesian and ferroan fields. In a modified alkaline-lime index (Na_2O+K_2O+CaO vs. SiO_2) of Frost et al. (2001), the samples plot predominantly in the calcalkaline and alkaline-calcic fields, with a few samples falling in the calcic and alkaline fields (Figure 22d).

These data suggest a close affinity to relatively hydrous, oxidizing magmas and source regions (Frost and Lindsley, 1991), consistent with a subduction-related origin (Frost et al., 2001). Both classification schemes (Pearce et al., 1984; Frost et al., 2001) seem to suggest that the granitoid rocks were probably formed in a tectonic regime dominated by collision and subduction.

The granitoid plutons from the study area have moderately juvenile ϵ_{Nd} compositions, as well as some slightly negative ϵ_{Nd} values varying from -1.22 to 3.05 (Figure 23). The Nd isotopic data suggest that there was minor to no involvement

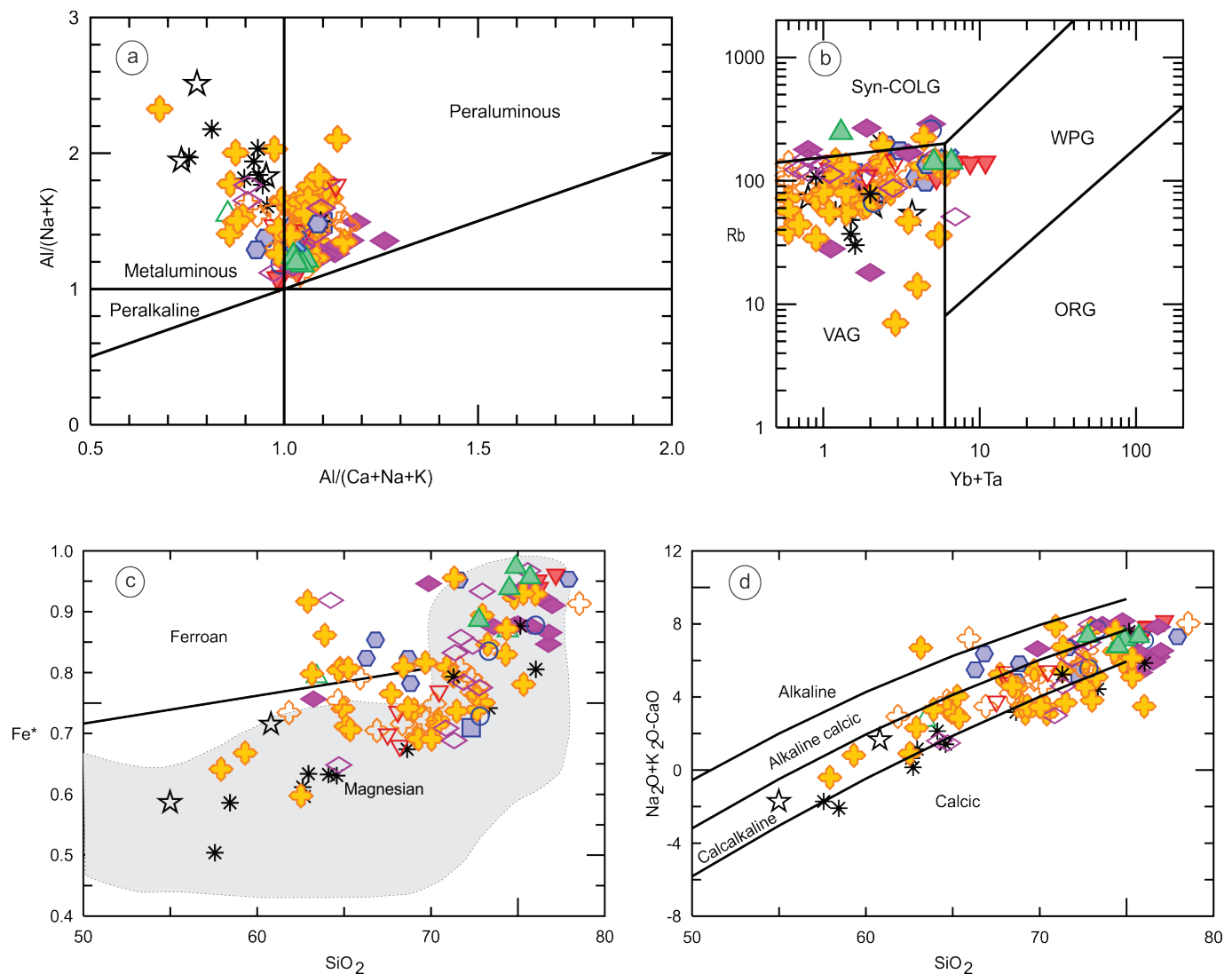


Figure 22: Geochemical discrimination diagrams for granitoid rocks: **a)** $Al/(Na+K)$ vs. $Al/(Ca+Na+K)$ diagram; **b)** Rb vs. Yb+Ta diagram of Pearce et al. (1984); **c)** Fe^* vs. SiO_2 , where $Fe^* = [FeO]/([FeO]+[MgO])$; grey field represents Cordilleran granites (after Frost et al., 2001); **d)** modified alkaline-lime index (Na_2O+K_2O+CaO vs. SiO_2) of Frost et al. (2001). Abbreviations: ORG, ocean-ridge granites; Syn-COLG, syncollisional granites; VAG, volcanic-arc granites; WPG, within-plate granites.

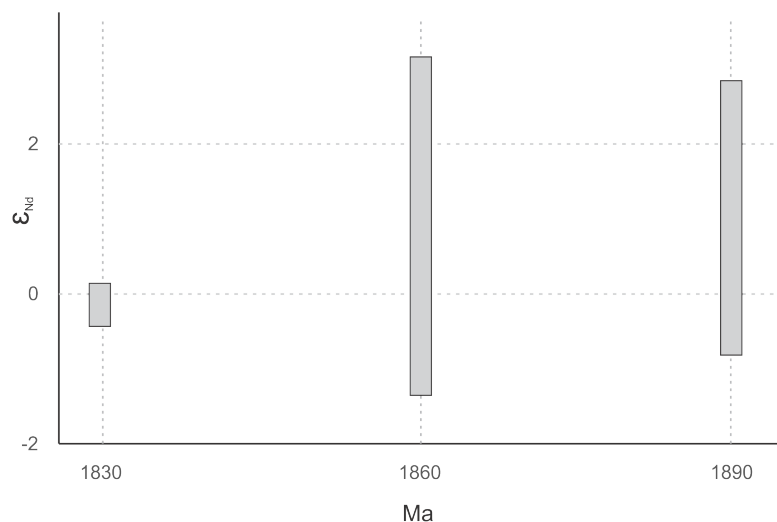


Figure 23: Range of values of ϵ_{Nd} for granitoid rocks from the Southern Indian Lake area plotted against their determined or inferred U-Pb age.

of older crustal components in the generation of these plutons. This is somewhat unexpected since most of these granitoids intrude mainly Paleoproterozoic crust, with input of Archean-age material in rocks of the Pukatawakan Bay and Partridge Breast Lake assemblages. Overall the ϵ_{Nd} data seem to suggest that the felsic plutons show a shift to slightly more evolved ϵ_{Nd} values with decreasing age (Figure 23), which could indicate a change in composition or amount of subducted sediments (e.g., White and Dupré, 1986); alternatively, this could reflect a slight increase in crustal contamination. However, there is no clear evidence for either a spatial or a compositional control on variations in the Nd-isotopic signatures of the ca. 1890–1829 Ma plutons.

U-Pb geochronology

Twenty-two samples were collected from key map units for geochronological analysis in order to better constrain the ages of volcanism, sedimentation and plutonism in the Southern Indian domain. Only unpublished ages are included in this report: five samples analyzed by the GSC using SHRIMP, three samples analyzed by the Radiogenic Isotope Facility at the University of Alberta using laser-ablation multicollector inductively coupled plasma–mass spectrometry (LA-MC-ICP-MS), and one sample analyzed also by LA-MC-ICP-MS at the University of New Brunswick. Partial results from the geochronological studies were published by Rayner and Corrigan (2004), Kremer et al. (2009b), Rayner (2013) and Martins and McFarlane (2016a, b). Complete unreleased U-Pb geochronology data can be found in DRI2019001.

Methodology

A 10–15 kg sample of each selected unit was collected in the field with hammers or a rock saw from locations where little to no discernible alteration was present. All weathered surfaces were removed from the samples, and cleaned samples were individually bagged and put in plastic rock pails before

being shipped to the appropriate facilities for mineral separation and analysis. For a pegmatite sample, polished thin sections were cut and used for in situ U-Pb study.

Sensitive high-resolution ion microprobe (SHRIMP)

Uranium-lead geochronology was carried out using the SHRIMP at the GSC in Ottawa. Analytical procedures followed those described by Stern (1997), with standards and U-Pb calibration methods following Stern and Amelin (2003). The internal features of the zircons (such as zoning, structures, alteration, etc.) were characterized in backscattered electron mode (BSE) using a Zeiss Evo 50 scanning electron microscope. Analyses were carried out over three separate analytical sessions, the details of which are found in DRI2019001. Analyses of secondary standard z1242 were interspersed through the analytical sessions and the measured $^{207}\text{Pb}/^{206}\text{Pb}$ ages compared and corrected with the accepted standard age determined by thermal ionization mass spectrometry (2679.7 Ma; B. Davis, pers. comm.). Isoplot versions 3.00 (Ludwig, 2003) and 3.70 (Ludwig, 2008) were used to generate concordia plots and calculate weighted means. All errors reported in the text are given at the 2σ uncertainty level.

Laser-ablation, multicollector, inductively coupled plasma–mass spectrometry (LA-MC-ICP-MS)

Analysis of detrital zircons by LA-MC-ICP-MS at the University of Alberta for U-Pb dating followed the procedures outlined by Simonetti et al. (2005). Samples were crushed and pulverized, and underwent mineral separation by heavy-liquid techniques followed by sorting of the concentrates using a Frantz isodynamic separator. Zircon separates were hand picked, mounted in epoxy and polished to half-section thickness for analysis. All analyses were performed on a Nu Plasma MC-ICP-MS coupled to a frequency-quintupled Nd: YAG laser-ablation system. Ion-counting detectors were used to measure ^{207}Pb , ^{206}Pb and ^{204}Pb , whereas U was measured on

Faraday collectors. The procedures for determining the Faraday ion-counter factor and the Faraday multiplier calibration, and for correcting the measured Pb isotope ratios for instrumental mass bias, have been described by Simonetti et al. (2005). Common Pb corrections utilized the projected age of the zircons and the corresponding initial Pb isotopic compositions from the two-stage evolution model of Stacey and Kramers (1975). The resulting U-Pb isotopic data are presented in DRI2019001 and plotted on concordia diagrams. All reported errors are quoted at 1σ and were calculated by numerical propagation of all known sources of uncertainty. Concordia diagrams were generated using the Isoplot version 3.70 application of Ludwig (2008), and the error ellipses are shown at 2σ . For the purposes of interpretation, the results were filtered to include only the most concordant ($\geq 90\%$) and precise (1σ analytical errors ≤ 20 Ma) $^{207}\text{Pb}/^{206}\text{Pb}$ ages.

Columbite-tantalite group minerals were analyzed in situ at the Department of Earth Sciences, University of New Brunswick. Selected grains were dated using an Australian Scientific Instruments (formerly Resonetics) RESOLUTION Series M-50-LR 193 nm excimer laser-ablation system coupled with an Agilent 7700x quadrupole ICP-MS equipped with dual external rotary pumps. Columbite-tantalite grains were analyzed with a crater size of 24 μm , 3.5 Hz repetition rate and 30 s ablation time following 30 s of background collection. The grains were ablated with a laser fluence of ~ 3 J/ cm^2 . An ablation sequence, comprising 16 analyses of NIST610 reference glasses throughout the sequence and at least 15 well-characterized U-Pb age standards, was distributed so as to bracket blocks of five to ten unknowns. Columbite-tantalite standards originated from the 1060 Ma Kragero pegmatite, Bamble sector, southeastern Norway; the 2570–2550 Ma Moose II pegmatite, Yellowknife pegmatite suite; the 500 Ma Ipe mine, Minas Gerais, Brazil; and the 270 Ma Amelia tantalite from the Morefield pegmatite, Winterham, Virginia. Ablated aerosols were carried out in the Laurin Technic S-155 two-volume sample cell using pure He at a flow rate of 300 mL/min. This was mixed with 930 mL/min of Ar carrier gas and 2.0 mL/min of N_2 , which was used to enhance ionization efficiency in the ICP-MS plasma. Before entering the ICP-MS torch, the combined gas stream passed through a smoothing device (Laurin Technic ‘squid’). The Agilent 7700x ICP-MS was operated at an RF power of 1550 W with ion lenses tuned to obtain $<0.3\%$ ThO^+/Th^+ and U^+/Th^+ of ~ 1.05 , as measured on NIST610 reference glasses. One sweep of the ICP-MS quadrupole comprised a rapid (0.01 s) measurement of guide masses (^{93}Nb and ^{181}Ta), followed by ^{204}Pb (0.04 s), ^{206}Pb (0.05 s), ^{207}Pb (0.07 s), ^{208}Pb (0.01 s), ^{232}Th (0.01 s), and ^{238}U (0.02 s). This gave a total measurement time of ~ 0.25 s per sweep or ~ 120 measurements per 30 s ablation. The ICP-MS datafile (data as counts/sec) and laser-sequence log file were combined offline in Lolite v. 3.32 and ages were calculated using the VizualAge U-Pb geo-

chronology data-reduction scheme described by Petrus et al. (2012).

SHRIMP results

Garnet-sillimanite greywacke, Pukatawakan Bay assemblage (unit 5; sample 107-09-050A)

A sample of well-bedded, isoclinally folded, garnet-sillimanite greywacke was collected from the southwestern shore of Partridge Breast Lake. The sample was originally thought to represent part of the Partridge Breast Lake assemblage. Sixty-three detrital zircons, characterized by oscillatory zoning, prismatic to elongate habit and variable degrees of roundedness, were recovered and analyzed. Results are similar to those published by Rayner (2013) for sample 107-09-207A, with zircons ranging in age from ca. 3.4 to 1.95 Ga. The dominant detrital mode was found at 2.52 Ga, but a significant number of results fall in the 2.4–2.3 Ga range (Figure 24a). Replicate analyses on the youngest detrital zircon yielded an age of 1950 ± 11 Ma (weighted mean $^{207}\text{Pb}/^{206}\text{Pb}$ age, $n = 3$, $\text{MSWD}^4 = 1.8$), interpreted as the maximum age of deposition of the greywacke. The results suggest that these particular sediments at Partridge Breast Lake are part of the Pukatawakan Bay assemblage rather than the Partridge Breast Lake assemblage, as originally thought.

Rhyolite, Partridge Breast Lake assemblage (subunit 13b; sample 107-09-047A)

A sample of massive to locally fragmental, quartz- and feldspar-phyric rhyolite was collected from south of Partridge Breast Lake to provide the age of volcanism for the Partridge Breast Lake assemblage. Nine very small and variably fractured, altered and/or resorbed zircons were recovered from the sample, on which no duplicate analyses could be done. All zircons were of different ages, ranging from ca. 2.8 to 2.3 Ga (Figure 24b). These ages are consistent with the documented inherited and detrital zircon ages in the area. Samples of the Partridge Breast Lake assemblage have Sm-Nd isotopic signatures (Table 3) that indicate interaction with, or contamination by, an older crustal component. On this basis, all zircons recovered from the rhyolite are interpreted to be inherited; therefore, the sample provides no constraints on the age of volcanism for the Partridge Breast Lake assemblage, other than it being younger than ca. 2.3 Ga.

Garnet greywacke gneiss, Partridge Breast Lake assemblage (subunit 11b; sample 107-09-295A)

A sample of garnetiferous greywacke was collected from the eastern extremity of Long Point. The sample consists of variably migmatitic, garnet greywacke gneiss, generally with

⁴ Mean square of weighted deviates

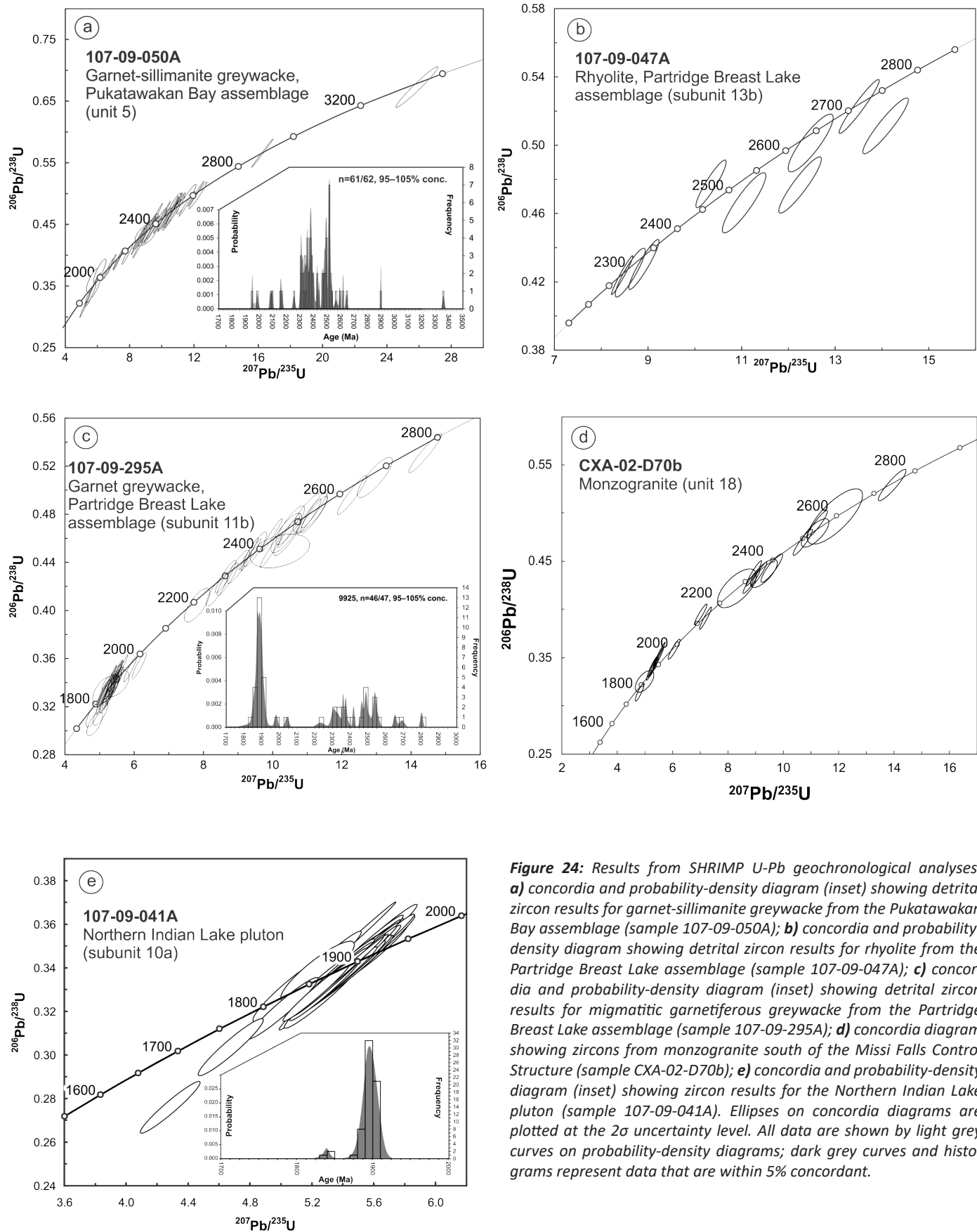


Figure 24: Results from SHRIMP U-Pb geochronological analyses: **a)** concordia and probability-density diagram (inset) showing detrital zircon results for garnet-sillimanite greywacke from the Pukatawakan Bay assemblage (sample 107-09-050A); **b)** concordia and probability-density diagram showing detrital zircon results for rhyolite from the Partridge Breast Lake assemblage (sample 107-09-047A); **c)** concordia and probability-density diagram (inset) showing detrital zircon results for migmatitic garnetiferous greywacke from the Partridge Breast Lake assemblage (sample 107-09-295A); **d)** concordia diagram showing zircons from monzogranite south of the Missi Falls Control Structure (sample CXA-02-D70b); **e)** concordia and probability-density diagram (inset) showing zircon results for the Northern Indian Lake pluton (sample 107-09-041A). Ellipses on concordia diagrams are plotted at the 2σ uncertainty level. All data are shown by light grey curves on probability-density diagrams; dark grey curves and histograms represent data that are within 5% concordant.

<5% mobilize, which was avoided during sample collection. The abundant zircons recovered from the sample are typically pale brown, rounded prismatic grains with few inclusions or fractures. The majority of the grains exhibit high-U overgrowths in the BSE images. The U-Pb results range from 2802 to 1822 Ma (Figure 24c). Seven of the youngest nine analyses have distinctly low Th/U ratios, and two of these young analyses are from high-U overgrowths. The weighted mean $^{207}\text{Pb}/^{206}\text{Pb}$ age of 1839 ± 5 Ma for these seven analyses is interpreted to represent an episode of metamorphism and possibly migmatization. In addition, it provides a minimum age of deposition of the sediment. The remaining 47 analyzed zircons are interpreted as detrital. The dominant mode is centred at 1.9 Ga, similar to that in the dacitic tuff within the same assemblage (sample 107-08-649; Kremer et al., 2009b). Replicates on the youngest zircon yielded a mean age of 1883 ± 24 Ma, which constrains the maximum age of deposition. Older detrital zircon ages are sporadically distributed between 2.8 and 2.0 Ga, with the majority between 2.55 and 2.3 Ga. The migmatized metasedimentary rocks mapped on Long Point, and their inferred extension into the Partridge Breast Lake area, do not represent an older sedimentary suite and instead are interpreted to have been deposited between 1883 and 1839 Ma as part of the Partridge Breast Lake assemblage.

Monzogranite, south of the Missi Falls Control Structure (unit 18; sample CXA-02-D70b)

This sample of monzogranite was collected south of the Missi Falls Control Structure. The zircons recovered yielded a span of concordant zircon ages from 2740 to 1763 Ma (Figure 24d). The weighted mean $^{207}\text{Pb}/^{206}\text{Pb}$ age of 1849 ± 10 Ma of five analyses is interpreted to represent the crystallization age. Although this age is only constrained by five analyses, this unit likely represents plutonism associated with the Chipewyan-Wathaman batholith with an inherited component.

Northern Indian Lake pluton (subunit 10a; sample 107-09-041A)

Sample 107-09-041A was collected at Northern Indian Lake, where the best exposure of the boundary between the Chipewyan-Wathaman batholith and the Southern Indian domain was observed. Initially interpreted as a fragmental paragneiss, exposures of the Northern Indian Lake pluton were thought to represent the metamorphosed equivalent of a polymictic conglomerate or possibly a fragmental volcaniclastic rock. The population of zircons is composed of variably fractured, stubby to elongate prisms with slightly resorbed/rounded facet edges. Sixty of the 63 zircons analyzed fall within a single population with a weighted mean $^{207}\text{Pb}/^{206}\text{Pb}$ age of 1896 ± 2 Ma ($n=65$, MSWD = 1.6). Three zircons (grains 27, 37 and 64 in DRI2019001) give distinctly younger ages, which yield a combined weighted mean $^{207}\text{Pb}/^{206}\text{Pb}$ age of 1839

± 5 Ma ($n = 7$, MSWD = 1.1; Figure 24e). These younger zircons do not have distinctly different Th/U or U abundance than the 1.89 Ga zircon population, nor are they different in morphology or zoning patterns.

Based on these results, the older zircons are interpreted to represent the age of the Northern Indian Lake pluton at ca. 1890 Ma, consistent with the observations of Martins and McFarlane (2016a), whereas the few younger zircons could represent an episode of high-strain deformation, metamorphism and possibly migmatization. At this location, Kremer and Martins (2014a) described the boundary between the Southern Indian and the Chipewyan domains as being marked by a localized increase in strain in both the supracrustal and felsic plutonic rocks of the Southern Indian domain and the Chipewyan-Wathaman batholith, possibly attributed to forceful intrusion of the Chipewyan-Wathaman batholith into rocks of the Southern Indian domain. This high strain makes it difficult to differentiate the various units present in the outcrop.

LA-MC-ICP-MS results

Orthogneiss, Northern Indian Lake (subunit 10a; sample 107-09-041B)

Sample 107-09-041B is from the same outcrop as sample 107-09-041A (see above) and was selected for analysis because of the possibility that it represents late Archean to early Paleoproterozoic gneissic crust identified at Southern Indian lake (Kremer et al., 2009b). The population of zircons is colourless to light tan and varies in size and morphology from prismatic to round. A total of 110 grains was analyzed; the ages range from 1916 to 1853 Ma, with a few around 1830 Ma (Figure 25a). One possible interpretation of these zircon-age results is that this sample may be a highly deformed, ca. 1867 Ma granitoid rock. Alternatively, this could be a highly deformed paragneiss with contributions from sediments derived from the different ages and provenances of rocks in the Southern Indian domain. At this outcrop, unit interpretation and correlation with rock units mapped elsewhere in the Southern Indian domain is hindered by very high levels of strain, as described by Kremer and Martins (2014a).

Polymictic conglomerate, Strawberry Island assemblage (subunit 19a; sample 107-09-164)

A sample of polymictic conglomerate was collected from the eastern shore of Southern Indian Lake, south of the Missi Falls Control Structure. This sample was thought to represent the younger orogenic sediments of the Whyme Bay assemblage and was collected to help determine the extent of these rocks (previously thought to occur only as xenoliths in the young monzogranite pluton at Whyme Bay; Kremer, 2008a, b). The sample yielded a zircon population composed of euhedral and rounded grains that vary in size and colour from colourless to Fe stained. The U-Pb results range from 2496 to 1809 Ma

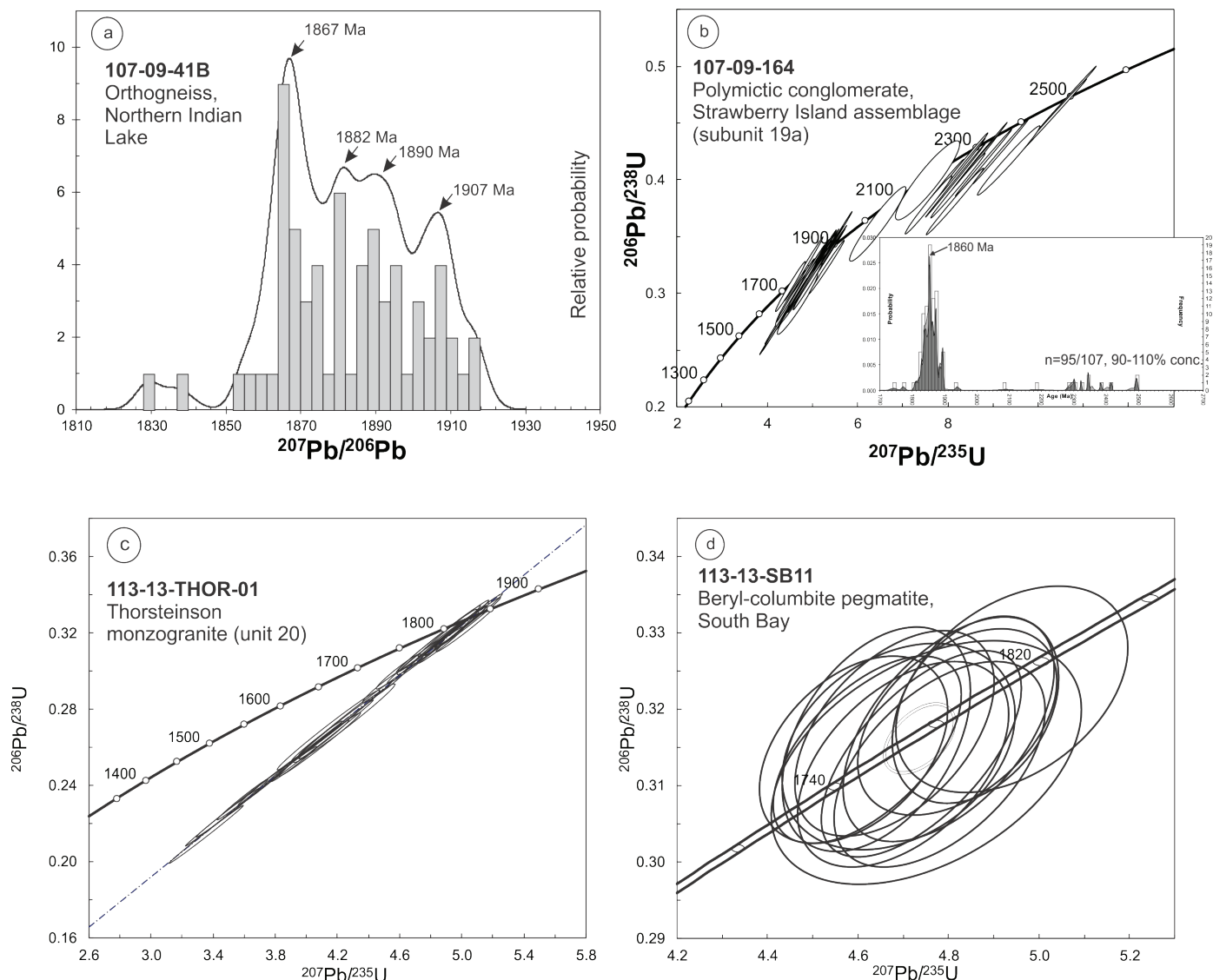


Figure 25: Results from LA-MC-ICP-MS U-Pb geochronological analyses: **a)** relative probability diagram showing zircon results for orthogneiss from Northern Indian Lake (sample 107-09-41B); **b)** concordia and probability-density diagram (inset) showing zircon results for polymictic conglomerate from the Strawberry Island assemblage (sample 107-09-164); **c)** concordia showing zircon results for the Thorsteinson monzogranite (sample 113-13-THOR-01); **d)** concordia showing zircon results for the beryl-columbite pegmatite from the South Bay pegmatite field (outside of the current map area). Ellipses on concordia diagrams are plotted at the 2σ uncertainty level. All data are shown by light grey curves on probability-density diagrams; dark grey curves and histograms represent data that are within 5% concordant.

(Figure 25b). Older, detrital zircon ages are distributed mainly between 2.5 and 2.3 Ga. The dominant mode is centred around 1860 Ma, which best constrains the maximum age of deposition. This unit is cut by the monzogranite intrusion south of the Missi Falls Control Structure dated at ca. 1849 Ma, suggesting that the conglomerate was formed in a basin that developed over a period of <11 m.y.

Thorsteinson monzogranite (unit 20; sample 113-13-THOR-01)

This sample was collected in the summer of 2013 from an outcrop on the southwest end of the southern tip of Thorsteinson Lake (south of the present map area). It consists of undeformed, medium-grained, fluorite-bearing monzogran-

ite. It was selected for geochronological analysis because it was thought to be a younger intrusion in the Southern Indian Lake area and related to an anorogenic setting (Halden et al., 1990). The previous Rb-Sr whole-rock age (Halden et al., 1990) is poorly constrained, so the objective was to provide a new, robust age of crystallization for this granitic body. The samples yielded a population of zircons that vary in size and range in morphology from euhedral (prismatic) to anhedral (rounded) grains with concentric zoning. A few grains have inclusions and exhibit a rim overgrowth. Analyses of 30 grains yielded $^{207}\text{Pb}/^{206}\text{Pb}$ ages ranging from 1855 to 1815 Ma (Figure 25c). Linear regression of the concordant or moderately discordant analyses resulted in a concordia upper-intercept age of 1829 ± 5.5 Ma (MSWD = 4.3), interpreted as the crystal-

lization age of the monzogranite. Although younger than other major plutons in the area, it is not the youngest intrusion in the Southern Indian Lake area (the youngest intrusive bodies are the ca. 1773 Ma beryl-columbite pegmatites) and has an age similar to that of the 1829 ± 1 Ma monzogranite intrusion in Pukatawakan Bay (Rayner and Corrigan, 2004).

Beryl-columbite pegmatite, South Bay pegmatite field

Minerals of the columbite-tantalite group from a beryl-columbite pegmatite in the South Bay pegmatite field, located southwest of the map area (Martins and Kremer, 2013), were used to estimate the time of emplacement of the pegmatite swarm. The columbite-tantalite minerals were described in detail by Martins (2014, 2016c): grains range in size from 20 μm to 5 mm, are subhedral to euhedral and occur disseminated in the groundmass of both the aplitic- and pegmatitic-textured portions of the beryl-columbite pegmatite. Backscattered-electron imagery revealed relatively simple zonation, usually with a Nb-enriched core surrounded by a rim with higher Ta content (Martins, 2016c). Thirteen analyses yielded a concordant age of 1773 ± 9.1 Ma (MSWD = 0.16; Figure 25d). This is interpreted as the crystallization age of the pegmatite, given that crystallization of the columbite-tantalite group minerals is considered synchronous with that of the primary silicate phases, based on petrographic observations (Martins, 2016c).

Summary of U-Pb data

Pukatawakan Bay assemblage (>1988 to 1890 Ma)

The U-Pb data presented in this report, together with data released by previous authors (Rayner and Corrigan, 2004; Kremer et al., 2009b; Rayner, 2013), indicate that the Pukatawakan Bay assemblage was deposited during a time interval of less than a 100 m.y. Epiclastic and associated volcanic rocks from this assemblage yielded a youngest detrital zircon grain, with an age of 1988 ± 11 Ma (sample 107-09-207A), and are intruded by the Turtle Island intrusive complex, with a reported age of 1889 ± 11 Ma (Rayner and Corrigan, 2004), the latter providing a minimum age of deposition. The garnet-sillimanite greywacke sample presented in this report has a dominant detrital zircon mode centred around 2.6–2.3 Ga. A possible source for these zircons is the Hearne craton, although it is also possible that a crust equivalent in age to the Sask craton was the source of zircon in these epiclastic rocks (Corrigan et al., 2007). Compared to the Partridge Breast Lake assemblage, the rocks belonging to the Pukatawakan Bay assemblage are older and have a higher proportion of detrital ages of 2.6–2.3 Ga. This could indicate either proximity to the Archean source and increased degree of derivation from such crustal material in the depositional basin, or higher levels of erosion at the time of deposition. Results presented in this report further show that rocks from the Pukatawakan Bay assemblage are not restricted to the Pukatawakan Bay area and Pine Lake, as initially though

(Kremer, 2008a, b), but also outcrop elsewhere in the Southern Indian domain, namely in the Partridge Breast Lake area and on Turtle Island, southwest of the Missi Falls Control Structure.

Partridge Breast Lake assemblage (>1883 to 1860 Ma)

Age constraints for the Partridge Breast Lake assemblage, although not well defined, suggest that this assemblage was deposited during a relatively narrow interval of up to about 30 m.y. Maximum age of deposition for one of the units is ca. 1883 Ma, with detrital zircons mainly at ca. 1.9 Ga and minor, older components varying between 2.5 and 2.3 Ga. The ca. 1.9 Ga peak likely represents input from the Turtle Island complex and the Northern Indian Lake pluton, both of which are dated at ca. 1890 Ma (this study; Rayner and Corrigan, 2004; Martins and McFarlane, 2016b). The event dated at ca. 1839 Ma is interpreted as metamorphism and/or migmatization, possibly associated with the intrusion of granitoid bodies of similar age within the Southern Indian domain. The Partridge Breast Lake assemblage is cut by the K-feldspar megacrystic Chipewyan-Wathaman batholith, thus providing a minimum age of disposition of 1.86–1.85 Ga (Corrigan et al., 2000). Detrital ages of 2.55–2.30 Ga are similar to but less abundant than those of rocks of the Pukatawakan Bay assemblage. This could indicate source contribution from a late Archean to early Paleoproterozoic crust into the depositional basin. Alternatively, the older zircons originated from reworked Pukatawakan Bay assemblage sediments, as the Partridge Breast Lake assemblage unconformably overlies the Pukatawakan Bay assemblage.

Strawberry Island assemblage (>1860 to 1849 Ma)

This group of sedimentary rocks, initially thought to be part of the younger Whyme Bay assemblage, has U-Pb zircon ages mainly around 1860 Ma, which fits the age range of plutonism associated with the Chipewyan-Wathaman batholith (Corrigan et al., 2001; Rayner and Corrigan, 2004). This assemblage could have been deposited in a foreland-basin environment where most of the sediments were derived from the uplifted and eroded Chipewyan-Wathaman batholith, with minor contribution of ca. 2.5–2.3 Ga crust. The Strawberry Island assemblage unconformably overlies the Partridge Breast Lake assemblage and is cut by a monzogranite body dated at ca. 1849 Ma, indicating that this basin developed over a relatively short period of time.

Whyme Bay assemblage (>1832 to 1829 Ma)

This assemblage is represented by sedimentary rocks that occur as xenoliths within the monzogranite intrusion in the Whyme Bay area (Kremer, 2008a, b) and north of Loon Island (Martins, 2015a, b, 2016a, b). Uranium-lead zircon data for the Whyme Bay assemblage present a uniform zircon population centred at ca. 1832 Ma (Kremer et al., 2009b). The sediments could have been sourced from proximal plutonic rocks of this

age. This assemblage appears to have been deposited in a short period of time (<3 m.y.) and is interpreted to unconformably overlie the Strawberry Island assemblage. The Whyne Bay assemblage shares temporal links with the Sickie Group arkosic rocks, dated at ca. 1830 Ma, in the Lynn Lake belt (Beaumont-Smith et al., 2006).

Tectonic implications

The rocks of the Southern Indian domain discussed in this report collectively span a period of approximately 750 m.y., from crystallization of granodiorite at ca. 2520 Ma (Kremer et al., 2009b) to crystallization of the beryl-columbite pegmatites at ca. 1773 Ma. Field relationships, lithogeochemistry and U-Pb age constraints indicate that the several phases of crustal growth involved a systematic progression from oceanic volcanism and magmatism, and possible back-arc volcanism; through continental-arc volcanism and magmatism, synorogenic sedimentation, accretion and voluminous arc magmatism, and regional metamorphism; to emplacement of peraluminous granitic bodies and granitic pegmatites.

The record is not continuous. A major peak of activity around 1890 Ma is marked by a phase of juvenile volcanism and associated marine sediments (Pukatawakan Bay assemblage), as well as plutonism leading to the formation of the Turtle Island complex and Northern Indian pluton. A later phase of arc volcanism and associated continental-arc rocks (Partridge Breast Lake assemblage) was followed by accretion of supracrustal sequences and associated voluminous plutonism around 1860 Ma (Chipewyan-Wathaman batholith); development of fore-arc or foredeep basins (Strawberry Island and Whyne Bay assemblages); and continuous plutonic events, such as the various intrusions dated at ca. 1849 and 1829 Ma (Rayner and Corrigan, 2004) and pegmatite bodies dated at ca. 1773 Ma, the youngest recorded igneous activity in the Southern Indian domain.

The geodynamic evolution of the Southern Indian domain presented below was divided into several time intervals, such as was done for the Trans-Hudson orogen (THO) by Corrigan et al. (2009). The time intervals also take into account the formation and accumulation of the distinct supracrustal assemblages identified in the study area and/or significant additions of new crust.

Circa 2.5 Ga

Zircon from a granodiorite gneiss mapped south of Long Point (Figure 1; Map GR2019-1-2) was dated at 2520 ± 6 Ma, which is interpreted as the crystallization age of this unit (Kremer et al., 2009b). Zircon rims reveal a younger age of 2385 Ma, interpreted to be consistent with a metamorphic event (Kremer et al., 2009b). This gneissic unit is interpreted to represent basement rocks for the Southern Indian domain but was only identified on a few isolated islands. However, the age range of its zircon population mimics the dominant and

subdominant detrital zircon populations in most Paleoproterozoic assemblages in the area, indicating it may have served as a major source for the supracrustal rocks of the Southern Indian domain, and that it may be more extensive than its limited exposure would suggest (Rayner and Corrigan, 2004; Kremer et al., 2009b). Ages ranging between 2.55 and 2.30 Ga overlap with known ages for the Sask craton (Rayner et al., 2005) but were also identified in plutons from the southern Hearne craton (Card et al., 2018). The late Neoarchean to early Paleoproterozoic orthogneiss at Southern Indian Lake could represent a window, or fault-bounded tectonic fragment, of Hearne craton in the Reindeer zone of the THO. Alternatively, it may represent a fragment of older, exotic continental crust, analogous to the Sask craton (e.g., Corrigan et al., 2007). Regardless of the affinity of this late Neoarchean to early Paleoproterozoic orthogneiss, its presence indicates involvement of older crust in the formation and evolution of the Southern Indian domain.

Circa 1.98–1.89 Ga

This time interval is best represented by rocks of the Pukatawakan Bay assemblage and possibly also rocks assigned to the Churchill River assemblage. It represents a period of crustal growth recorded by the volcano-sedimentary rocks that is characterized by juvenile oceanic volcanism with coeval deposition of supracrustal rocks in oceanic settings. During this time period, it is thought that closure of the Paleoproterozoic Manikewan ocean (Stauffer, 1984) was ongoing and that initial development of juvenile volcanic arcs, back arcs and associated sedimentary basins took place (e.g., Corrigan et al., 2007, 2009).

The Pukatawakan Bay assemblage represents the rocks associated with intraoceanic, juvenile volcanic-arc complexes and related basin sedimentation associated with the Southern Indian domain. The sedimentary rocks from this package yielded zircon ages in the 2.8–2.3 Ga range, indicating that crust of this age was eroding and was a major contributor to the sediments entering the basin at this time. By ca. 1890 Ma, widespread continental-arc volcanic complexes intruded the volcano-sedimentary sequence of the Pukatawakan Bay assemblage, namely the mafic to intermediate Turtle Island complex and the felsic Northern Indian Lake pluton. These intrusions provide a minimum age constraint for the rocks of the Pukatawakan Bay assemblage.

During this time interval (1.98–1.89 Ga), it is also possible that the MORB basalts from the Churchill River assemblage formed in association with the development of a back-arc basin related with the intraoceanic, juvenile volcanic-arc complexes. Coeval with these basalts would have been the deposition of marine ocean-floor sediments, presumably sourced from the Hearne craton or other Archean crust. Alternatively, the rocks from the Churchill River assemblage represent a relic of the Manikewan ocean and the coeval sediments could represent a passive-margin sedimentary sequence on the Hearne margin. Given the limited data and outcrop exposure of these rocks, it

is very difficult to determine with certainty the environment in which this assemblage was formed.

Circa 1.89–1.87 Ga

This time interval in the Southern Indian domain was recorded by the arc-derived volcano-sedimentary sequence of the Partridge Breast Lake assemblage. The time-interval constraints for this assemblage are defined by two intrusions: the older age bracket is defined by the intrusion of the Turtle Island complex (ca. 1890 Ma) and the younger age limit corresponds to the earlier stages of oceanic, arc-type magmatic activity that led to the formation of the Chipewyan-Wathaman batholith (ca. 1865 Ma).

The data for the rocks of the Partridge Breast Lake assemblage in this report suggest that this assemblage could have formed in a molasse-type, a fore-arc or a foredeep basin. This fits the model from Corrigan et al. (2009) that described increased accretionary activity in pericratonic and intraoceanic settings during this time interval. Molasse-type deposits, such as the sediments from the Partridge Breast Lake assemblage, could have formed along or were accreted to the southeastern margin of the Hearne craton (Corrigan et al., 2009) during this time frame. Accretion of the volcano-sedimentary-arc complexes (such as those of the Pukatawakan Bay and Partridge Breast Lake assemblages) to the southeastern margin of the Hearne craton is thought to have happened after 1.88 Ga and was ongoing until 1.865 Ga (Corrigan et al., 2009).

A similar detrital input is also observed in psammitic rocks from the Crew Lake belt (MacLachlan et al., 2004) and the Park Island assemblage (Corrigan et al., 2007) of the Rottenstone domain in Saskatchewan. These rocks have been interpreted as fore-arc basin deposits north of the La Ronge volcanic arc (MacLachlan et al., 2004; Corrigan et al., 2007).

Also attributed to this time period is a penetrative deformation in the form of early tight folds and layer-parallel foliation (D_1) recorded in protoliths younger than ca. 1.88 Ga that are crosscut by intrusions of Chipewyan-Wathaman age (Corrigan et al., 1998).

Circa 1.87–1.83 Ga

This time period represents an important piece in the evolution of the THO, with the emplacement of voluminous, mainly felsic plutonic rocks in an Andean-type continental-margin setting (e.g., Fumerton et al., 1984; MacHattie, 2001) that is thought to represent a continuous subduction zone along a strike length of at least 2000 km (Corrigan et al., 2009). The Chipewyan batholith in Manitoba is only one example of the many batholiths of this age throughout the THO.

Results from this study and those of other authors indicate the presence of felsic intrusions with similar composition and texture to those of the ca. 1865 Ma Chipewyan-Wathaman batholith in the Southern Indian Lake area but of younger ages (e.g., 1829 Ma; Rayner and Corrigan, 2004). This suggests that

plutonism in the study area, although intermittent, took place for at least 36 m.y. and that not all granitic rocks in Manitoba with Chipewyan-Wathaman-like textures formed in the time interval 1865–1855 Ma. This can create difficulties for tectonic interpretations. For example, this report used the age 1.86–1.85 Ga (a commonly accepted age for the Chipewyan-Wathaman batholith) to limit the time interval during which the Partridge Breast Lake assemblage was deposited. However, it is possible that the supracrustal rocks of the Partridge Breast Lake assemblage were instead intruded by a younger granitoid body (as young as ca. 1829 Ma).

Based on the available information, this report favours the interpretation of the Chipewyan-Wathaman batholith as a complex, multiphase granitic body that was intruded by different pulses of magmatism taking place at different periods of time extending from ca. 1865 Ma to ca. 1829 Ma. Multiphase granitic bodies of different ages are reported elsewhere: the Coast Mountains batholith in British Columbia (over a span of 160 m.y.; Ducea et al., 2015a, b) and the Newry igneous complex in Northern Ireland (Anderson et al., 2016, 2017). It is now recognized that many intrusions can be constructed over periods of several million years as a series of distinct magma pulses (e.g., Annen, 2011; Barboni et al., 2013), and this could have been the case for the Chipewyan batholith in Manitoba. Alternatively, the felsic rocks of similar composition and texture to the Chipewyan batholith that are observed in the Southern Indian domain may have formed independently at various times and are not associated with it. The age constraints on the Chipewyan batholith in Manitoba clearly require further investigation.

It is interpreted that the convergence between the Archean Superior and Hearne cratons was ongoing after 1865 Ma. This collision resulted in the development of a foreland, or possibly a foredeep basin (Hoffman, 1987), where sediments from the uplifted Chipewyan-Wathaman batholith mountain chain accumulated; at Southern Indian Lake, this resulted in the deposition of the Strawberry Island assemblage. Geochronological results reveal that the majority of zircons present in the rocks from this assemblage have ages centred around ca. 1.86 Ga, with a minor population of 2.5–2.3 Ga zircons that possibly came from early Paleoproterozoic crust or from the erosion of the Pukatawakan Bay assemblage or Partridge Breast Lake assemblage that were already accreted onto the Hearne margin.

Other events during this time period include the intrusion of ca. 1842 Ma seriate granite (Rayner and Corrigan, 2004) and granitoid rocks of similar age in the Southern Indian domain. Deformation D_2 is interpreted to have occurred at 1843 Ma (Kremer et al., 2009b), and metamorphism in supracrustal successions is interpreted to have peaked during this time period as well.

The most significant events around 1.83 Ga recorded in the study area are the intrusion of megacrystic monzogranite, dated at ca. 1829 Ma (Rayner and Corrigan, 2004), and the

F-bearing Thorsteinson monzogranite, dated at ca. 1829 Ma. Deposition and rapid burial of fluvial-alluvial orogenic sediments of the Whyne Bay assemblage also occurred around 1.83 Ga.

Less than 1.83 Ga

Terminal collision of the THO with the Superior craton took place at ca. 1.83–1.80 Ga (Bleeker, 1990; Ellis and Beaumont, 1999; Ashton et al., 2005), but records of this terminal collision are not common in the Southern Indian domain or were not documented during this study. It is possible, however, that late intrusions of granitic pegmatite at ca. 1773 Ma in the South Bay area (southwest of the present map area) are related to the THO terminal collision.

Economic considerations

The Southern Indian Lake area has historically seen little exploration activity, despite the targets identified in the 1960s through early 1980s and the recent work developed by the GSC and the MGS. Several assessment files from the 1960s through 1980s demonstrate the existence of several conductors and mineral showings (e.g., Assessment Files 90165, 90176, 93051, Manitoba Growth, Enterprise and Trade, Winnipeg). One of the last reports praises the area as a region with excellent potential for hosting a Homestake-type iron-formation Au deposit, indicated by aeromagnetic anomalies over unexplored, magnetite-rich, auriferous iron formation with a strike length of more than 8 km (Assessment File 93051). During the past decade, work by several authors demonstrated that this area has lithotectonic similarities to producing belts in the region, such as the Lynn Lake and Rusty Lake belts (e.g., Corrigan et al., 2007; Kremer et al., 2009b; Martins and MacFarlane, 2016a). These findings indicate that this area has regional economic potential to host several kinds of mineral deposits, such as volcanogenic massive sulphide, magmatic Ni-Cu and Au.

Recent studies on ice-flow indicators in the region suggest a complex ice-flow history (e.g., Hodder, 2015, 2017; Trommelen, 2015), with a likely dominant dispersal trend of glacial detritus toward the southwest (210–244°; Hodder, 2018). This type of information significantly aids in drift exploration in the area.

Volcanogenic massive sulphide

The potential for volcanogenic massive sulphide (VMS) deposits at the regional scale has been established by temporal links between the bimodal arc-volcanic rocks of the Partridge Breast Lake assemblage at Southern Indian Lake and volcanic rocks in the Lynn Lake–Leaf Rapids domain (Corrigan and Rayner, 2002), which host the Ruttan and Fox Lake VMS deposits. Lithogeochemical results from the felsic volcanic rocks of the Partridge Breast Lake assemblage indicate an affinity to FII felsic volcanic rocks (Leshner et al., 1986). This assemblage is interpreted to have formed in a rift environment from partial melting of hydrated basaltic crust at midcrustal levels (Hart et

al., 2004). This genesis is important for the VMS potential of the region because there is a preferential association of VMS deposits with FII, FIII, and FIV felsic volcanic rocks that occurs in a variety of rift-related regimes favourable for formation of these deposits (Hart et al., 2004). It is also worth mentioning that REE diagrams for the felsic rocks of the Partridge Breast Lake assemblage are identical to those of type FII felsic rocks in the Sturgeon Lake area (which host base-metal sulphide deposits), with a pronounced negative Eu anomaly (Figure 20c; Leshner et al., 1986).

Recent geochronological data for early ‘juvenile-arc’ magmatism in the Southern Indian domain (ca. 1890 Ma; this study; Martins and MacFarlane, 2016a) suggest a broadly coeval timing for early magmatism in several volcanic-arc terranes across the Reindeer zone, including the Lynn Lake belt (1892 ±3 Ma and 1886 ±1.5 Ma; Beaumont-Smith and Böhm, 2002) and the Snow Lake belt (e.g., the 1886 +17/–9 Ma Sneath Lake pluton; Bailes et al., 1991), thus supporting a possible correlation of these belts across the THO (Zwanzig and Bailes, 2010).

Base-metal potential is further evidenced by values up to 6.85% Cu reported from garnet-biotite schist with laminated pyrite, pyrrhotite and chalcopyrite stringers at Peanut Lake, just north of Partridge Breast Lake (Assessment File 93051), and assay results of up to 2.2% Cu obtained from a narrow fracture in volcanic rocks of the Whyne Bay area (Frohlinger, 1972). Malachite showings also occur near the base of the clastic sedimentary sequence around Partridge Breast Lake (Kremer et al., 2009b), and Martins (2015a) identified a gossanous outcrop of epidote-altered amphibolite that contained disseminated pyrite, chalcopyrite and pyrrhotite, and returned assay values of 476 ppm Cu and 152 ppm Zn.

Magmatic Ni-Cu-platinum-group elements (PGE)

Sulphidic and graphitic sedimentary horizons on the northwestern shore of Turtle Island contain up to 70% pyrite and pyrrhotite with minor chalcopyrite (Kremer et al., 2009b). This sequence is intruded by the sulphide-bearing, ultramafic to intermediate Turtle Island intrusive complex, which shows evidence of multiple injections in a fluidly dynamic magma chamber. The host sedimentary rocks may have provided the source of sulphur to the intruding magma, which would have allowed for the fractionation of magmatic Ni-Cu-PGE sulphides. This occurrence fits the ideal scenario for one of the main types of primary magmatic Ni-Cu-PGE mineralization in mafic-ultramafic rocks (Arndt et al., 2005).

Gold mineralization

Mineralized outcrops on the southeast shore on Peanut Lake consist of disseminated and laminated pyrrhotite, pyrite and chalcopyrite hosted in a garnet-quartz-hornblende-biotite-magnetite gneiss, interpreted as iron formation, that has undergone amphibolite-grade metamorphism (e.g., Assessment Files 90165, 93051). Stratabound and crosscutting white

quartz veins up to 1.2 m (4 feet) thick also occur within the mafic gneiss and are frequently mineralized with disseminated sulphides. Preliminary sampling of the Peanut Lake trenches during the summer of 1986 yielded representative grab samples from iron formation that assayed up to 3.77 g/t (0.11 oz./ton) Au and 6.85% Cu. Exploration work in the late 1960s and late 1980s identified similarities to gneiss-hosted auriferous iron-formation lode-Au deposits from the Puffy and Nokomis properties in Manitoba (Assessment File 93051). This mineralization style is similar to what is observed at the Homestake Mine in South Dakota (Poulsen, 1996). Aeromagnetic-anomaly maps indicate that the unexplored magnetite-rich auriferous iron formation has a strike length of more than 8 km (Assessment File 93051).

Unusual polymetallic Be-Au-Zn-Bi mineralization associated with a pegmatite on Turtle Island (central part of Southern Indian Lake; Kremer et al., 2009b; Martins and Kremer, 2013) is restricted to the altered contact zone with the basalt hostrock and occurs as a band (5–10 cm wide) of semimassive to massive pyrite and chalcopryrite within the pegmatite. The semimassive sulphide contains abundant white to pale green beryl crystals (1–3 cm). Samples from this zone returned high values of Be, Au, Ag, Bi, Zn, Nb and Ta (Kremer et al., 2009b; Martins, 2014). Malachite, azurite, bornite and chalcocite were identified in 2015 within a narrow fracture in pink pegmatite (Martins, 2015a). A grab sample of this material yielded values of 4.7 g/t Au, >1% Cu, 4.6 g/t Ag, 2200 ppm Bi, >0.5% Pb and 736 ppm Se. This outcrop is the second Au occurrence on Southern Indian Lake associated with pegmatite, and possibly an example of intrusion-related Au mineralization. The Au-Cu-Ag-Bi geochemical signature of these occurrences is similar to that of other intrusion-related Au systems, such as those in the Fairbanks district of Alaska, namely the Fort Knox and the Pogo deposits, which are also associated with granitoid plutons and pegmatite (Quandt et al., 2008). The Au-Bi association is particularly interesting, given its similarity to that of the Pogo deposit, where mineralized intervals contain elevated Ag, Te, Bi, As, Sb, Cu, Pb, Mo and/or Co, and exhibit a strong correlation between Au and Bi (Smith et al., 1999).

Diamonds

Archean cratons representing old, cold and thick lithospheric crust can be important regional vectors for diamond exploration, especially because that is where kimberlitic economic deposits have been found (Gurney et al., 2005). However, in east-central Saskatchewan, two kimberlite-bearing diamond occurrences are located in areas where there is no exposed Archean crust. Located in the early Paleoproterozoic Glennie domain, the Fort à la Corne kimberlite field occurs on the eastern rim of the Western Canada Sedimentary Basin, with Precambrian basement rocks of the early Paleoproterozoic Glennie domain occurring approximately 700 m below the surface (Kjarsgaard et al., 2009). In addition, the Pikoo kimberlite field occurs near Deschambault Lake (Saskatchewan

Ministry of Energy and Resources, 2018). Both locations are interpreted to be underlain at depth by the mostly buried Archean Sask craton. These two discoveries open exploration potential in other terranes, namely the THO, where Archean crust is not exposed but is thought to occur at depth.

At Southern Indian Lake, the identification of granodiorite gneiss with interpreted crystallization age of ca. 2.5 Ga (Kremer et al., 2009b) was the first known occurrence in the area. A newer sample of orthogneiss from a small island west of the Missi Falls Control Structure (Figure 1; Map GR2019-1-3) yielded an ϵ_{Nd} value of -7.1 , suggesting interaction with older crust, and was interpreted as an additional exposure of Archean crust. The extent of Archean orthogneiss, however, is poorly constrained at Southern Indian Lake, as exposures only occur on two isolated islands on the lake. Orthogneiss could be limited to a relatively small, tectonically interleaved wedge of Archean to earliest Proterozoic crust. Alternatively, the orthogneiss exposures, in addition to common inherited zircons of similar age in intrusive rocks and detrital zircons in sedimentary rocks throughout the Southern Indian Lake area, could indicate that the extent of Archean crust, at least at depth, is much greater than suggested by current models (Corrigan et al., 2007).

Recent reconnaissance-scale sampling for kimberlite-indicator minerals in the Southern Indian Lake area has suggested the presence of kimberlitic detritus (Hodder, 2017). These data add to the growing body of evidence suggesting the presence of pieces of Archean crust in the northwestern flank of the THO internides (Rayner and Corrigan, 2004; Corrigan et al., 2007), and make the Southern Indian domain a good target for diamond exploration.

Other types of mineral deposits

In the Partridge Breast Lake area, the margin of a weakly gossanous tonalitic intrusion cutting a clastic sedimentary sequence yielded anomalous Zn values (1.36%), perhaps indicating potential for sediment-hosted Zn mineralization (Kremer et al., 2009b). Gossanous patches in plagioclase-phyrlic tonalite and supracrustal rocks at several locations in the Southern Indian domain suggest the presence of disseminated sulphides within this unit.

Widespread, late- to post-tectonic plutonism associated with the margins of long-lived Archean cratons is thought to be a prospective setting for Fe-oxide Cu-Au (IOCG)-type mineralization. The presence of locally intense potassic alteration throughout the study area, affecting both plutonic and supracrustal rocks, is also considered a favourable indication, as is the abundant magnetite and pyrite-chalcopryrite identified in late pegmatitic to rapakivi granite on the eastern shore of Southern Indian Lake.

Acknowledgments

The help of several field assistants throughout the years was crucial for the success of this compilation project. E. Ander-

son, N. Brandson and E. Amyotte provided logistical support. Staff and students from the Midland Sample and Core Library (G. Bengier, R. Unruh, V. Varga, C. Epp and C. Stocki) provided sample preparation services. Help from L. Chackowsky with preparing the map figure is greatly appreciated. B. Davie from RnD Technical provided technical editing. Several discussions with C. Couëslan, S. Anderson, T. Corkery and K. MacLachlan were integral in refining the interpretations presented in this report. Critical reviews by C.O. Böhm improved earlier versions of the report. Special thanks are offered to Manitoba Hydro and in particular to C. Boe, who provided logistical support and allowed access to the Missi Falls Control Structure; and to the boat-patrol personnel from O-Pipon-Na-Piwin Cree Nation.

Natural Resources Canada contribution 20190061.

References

- Airbus Defence and Space 2016: SPOT 6 multispectral optical imagery; satellite imagery licensed by Planet Labs Geomatics Corp., URL <<http://geomatics.planet.com>> [2008].
- Anderson, P.E., Cooper, M.R., Stevenson, C.T., Hastie, A.R., Hoggett, M., Inman, J., Meighan, I.G., Hurley, C., Reavy, R.J. and Ellam, R.M. 2016: Zonation of the Newry Igneous Complex, Northern Ireland, based on geochemical and geophysical data; *Lithos*, v. 260, p. 95–106.
- Anderson, P.E., Stevenson, C.T., Cooper, M.R., Meighan, I.G., Reavy, R.J., Hurley, C., Inman, J. and Ellam, R.M. 2017: Refined model of incremental emplacement based on structural evidence from the granodioritic Newry igneous complex, Northern Ireland; *GSA Bulletin*, v. 130, p. 740–756.
- Anderson, S.D. 2013: Geology of the Garner–Gem lakes area, Rice Lake greenstone belt, southeastern Manitoba (parts of NTS 52L11, 14); *Manitoba Mineral Resources*, Manitoba Geological Survey, Geoscientific Report GR2013-1, 135 p.
- Annen, C. 2011: Implications of incremental emplacement of magma bodies for magma differentiation, thermal aureole dimensions and plutonism-volcanism relationships; *Tectonophysics*, v. 500, p. 3–10.
- Arndt, N., Leshner, C.M.G. and Czamanske, K. 2005: Mantle-derived magmas and magmatic Ni-Cu-(PGE) deposits; *Economic Geology*, 100th Anniversary Volume, p. 5–24.
- Ashton, K.E., Lewry, J.F., Heaman, L.M., Stauffer, M.R. and Hartlaub, R.P. 2005: The Pelican Thrust Zone: basal detachment between the Archean Sask Craton and Paleoproterozoic Flin Flon–Glenie Complex, western Trans-Hudson Orogen, Canada; *Canadian Journal of Earth Sciences*, v. 42, p. 403–419.
- Bailes, A.H., Hunt, P.A. and Gordon, T.M. 1991: U-Pb zircon dating of possible synvolcanic plutons in the Flin Flon belt at Snow Lake, Manitoba; *in* Radiogenic Age and Isotopic Studies, Report 4, Geological Survey of Canada, Current Research, Paper 90-2, p. 35–43.
- Barboni, M., Schoene, B., Ovtcharova, M., Bussy, F., Schaltegger, U. and Gerdes, A. 2013: Timing of incremental pluton construction and magmatic activity in a back-arc setting revealed by ID-TIMS U/Pb and Hf isotopes on complex zircon grains; *Chemical Geology*, v. 342, p. 76–93.
- Beaumont-Smith, C.J. and Böhm, C.O. 2002: Structural analysis and geochronological studies in the Lynn Lake greenstone belt and its gold-bearing shear zones (NTS 64C10, 11, 12, 14, 15 and 16), Manitoba; *in* Report of Activities 2002, Manitoba Industry, Trade and Mines, Manitoba Geological Survey, p. 159–170.
- Beaumont-Smith, C.J., Machado, N. and Peck, D.C. 2006: New uranium-lead geochronology results from the Lynn Lake greenstone belt, Manitoba (NTS 64C11–16); *Manitoba Science, Technology, Energy and Mines*, Manitoba Geological Survey, Geoscientific Paper GP2006-1, 11 p.
- Bleeker, W. 1990: New structural-metamorphic constraints on Early Proterozoic oblique collision along the Thompson Nickel Belt, Manitoba, Canada; *Geological Association of Canada, Special Paper 37*, p. 57–73.
- Cabanis, B. and Lecolle, M. 1989: Le diagramme La/10–Y/15–Nb/8: un outil pour la discrimination des series volcaniques et la mise en evidence des processus de mélange et/ou de contamination crustale; *Comptes Rendus de l'Academie des Sciences*, v. 309, p. 2023–2029.
- Campbell, F.H.A. 1972: Stratigraphic and structural studies in the Granville Lake–Lynn Lake region; *Manitoba Department of Mines, Resources and Environmental Management, Mines Branch, Publication 71-2A*, 40 p.
- Card, C.D., Bethune, K.M., Rayner, N. and Creaser, R.A. 2018: Characterising the southern part of the Hearne Province: a forgotten part of Canada's shield revisited; *Precambrian Research*, v. 307, p. 51–65.
- Chiarenzelli, J.R., Aspler, L.B., Villeneuve, M. and Lewry, J.F. 1998: Early Proterozoic evolution of the Saskatchewan craton and its allochthonous cover, Trans-Hudson orogeny; *Journal of Geology*, v. 106, p. 247–267.
- Clark, G.S. 1981: Rubidium-strontium geochronology of the major tectonic domains in the Churchill structural province, northern Manitoba, a preliminary report; *in* University of Manitoba, Centre for Precambrian Studies, Annual Report for 1980, p. 22–28.
- Corkery, M.T. 1993: Supracrustal rocks of the Partridge Breast Lake area (parts of NTS 64H/4, 5 and 64G/1, 8); *in* Report of Activities 1993, Manitoba Energy and Mines, Geological Services, p. 11–12.
- Corkery, M.T. 1995: Partridge Breast Suite volcanic and volcanoclastic derived gneissic rocks in the Pukatawakan area of Southern Indian Lake; *in* Report of Activities 1995, Manitoba Energy and Mines, Geological Services, p. 17–18.
- Corkery, M.T. and Lenton, P.G. 1990: Geology of the lower Churchill River region; *Manitoba Energy and Mines; Geological Services, Geological Report GR85-1*, 7 colour maps at 1:100 000 scale, 2 at 1:250 000 scale.
- Corkery, M.T. and Lenton, P.G. 1993: Partridge Breast Lake area (parts of NTS 64H/4, 5 and 64G/1, 8); *Manitoba Energy and Mines, Preliminary Map 1993L-1*, 1 map at scale 1:50 000 scale.
- Corrigan, D. and Rayner, N. 2002: Churchill River–Southern Indian Lake Targeted Geoscience Initiative (NTS 64B, 64C, 64G, 64H), Manitoba: update and new findings; *in* Report of Activities 2002, Manitoba Industry, Trade, and Mines, Manitoba Geological Survey, p. 144–158.
- Corrigan, D., Galley, A.G. and Pehrsson, S. 2007: Tectonic evolution and metallogeny of the southwestern Trans-Hudson Orogen; *in* Mineral Deposits of Canada: a Synthesis of Major Deposit-Types, District Metallogeny, the Evolution of Geological Provinces, and Exploration Methods, W.D. Goodfellow (ed.), Geological Association of Canada, Mineral Deposits Division, Special Publication 5, p. 881–902.
- Corrigan, D., MacHattie, T.G. and Chakungal, J. 2000: The nature of the Wathaman Batholith and its relationship to the Archean Peter Lake Domain along the Reindeer Lake transect, Saskatchewan; *Geological Survey of Canada, Current Research 2000-C13*, 10 p.

- Corrigan, D., Maxeiner, R.O., Bashforth, A. and Lucas, S. 1998: Preliminary report on the geology and tectonic history of the Trans-Hudson Orogen in the northwestern Reindeer Zone, Saskatchewan; *in* Current Research, 1998-C, Geological Survey of Canada, Paper, p. 95–106.
- Corrigan, D., Maxeiner, R.O. and Harper, C.T. 2001: Preliminary U-P results from the La Ronge–Lynn Lake Bridge project; *in* Summary of Investigations 2001, Volume 2, Saskatchewan Geological Survey, Saskatchewan Energy Mines, Miscellaneous Report 2001-4.2.
- Corrigan, D., Pehrsson, S., MacHattie, T.G., Piper, L., Wright, D., Lassen, B. and Chakungal, J. 1999: Lithotectonic framework of the Trans-Hudson Orogen in the northwestern Reindeer Zone, Saskatchewan: an update from recent mapping along the Reindeer Lake transect; *in* Current Research 1999-C, Geological Survey of Canada, p. 169–178.
- Corrigan, D., Pehrsson, S., Wodicka, N. and de Kemp, E. 2009: The Palaeoproterozoic Trans-Hudson Orogen: a prototype of modern accretionary processes; *in* Ancient Orogens and Modern Analogues; J.B. Murphy, J.D. Keppie and A.J. Hynes (ed.), Geological Society of London, Special Publications, v. 327, p. 457–479.
- Corrigan, D., Theriault, A. and Rayner, N. 2002: Preliminary results from the Churchill River–Southern Indian Lake transect, Northern Manitoba Targeted Geoscience Initiative; Geological Survey of Canada, Current Research 2002-C25, 11 p.
- Coyle, M. and Kiss, F. 2008: Partridge Breast Lake aeromagnetic survey, Manitoba; Geological Survey of Canada, Open Files 5922 to 5929 and Manitoba Science, Technology, Energy and Mines, Manitoba Geological Survey, Open Files OF2008-15 to OF2008-30, scale 1:50 000.
- Cranstone, J.R. 1972: Geology of the Southern Indian Lake area, north-eastern portion; Manitoba Department of Mines, Resources and Environmental Management, Mines Branch, Publication 71-2J, 82 p.
- Creaser, R.A., Erdmer, P.R., Stevens, A. and Grant, S.L. 1997: Tectonic affinity of Nisutlin and Anvil assemblage strata from the Teslin tectonic zone, northern Canadian Cordillera: constraints from neodymium isotope and geochemical evidence; *Tectonics*, v. 16, p. 107–121.
- Ducea, M.N., Paterson, S.R. and DeCelles, P.G. 2015a: High-volume magmatic events in subduction systems; *Elements*, v. 11, p. 107–112.
- Ducea, M.N., Saleeby, J.B. and Bergantz, G. 2015b: The architecture, chemistry, and evolution of continental magmatic arcs; *Annual Review of Earth and Planetary Sciences*, v. 43, no. 1, p. 299–331.
- Ellis, S. and Beaumont, C. 1999: Models of convergent boundary tectonics: implications for the interpretation of LITHOPROBE data; *Canadian Journal of Earth Sciences*, v. 36, p. 1711–1741.
- Froehlinger, T.G. 1972: Geology of the Southern Indian Lake area, central portion; Manitoba Department of Mines, Resources and Environmental Management, Mines Branch, Publication 71-2I, 91 p.
- Frost, B. and Lindsley, D.H. 1991: Occurrence of iron-titanium oxides in igneous rocks; *Reviews in Mineralogy and Geochemistry*, v. 25, p. 433–468.
- Frost, B.R., Barnes, C.G., Collins, W.J., Arculus, R.J., Ellis, D.J. and Frost, C.D. 2001: A geochemical classification for granitic rocks; *Journal of Petrology*, v. 42, p. 2033–2048.
- Fumerton, S.L., Stauffer, M.R. and Lewry, J.F. 1984: The Wathaman batholith: largest known Precambrian pluton; *Canadian Journal of Earth Sciences*, v. 21, p. 1082–1097.
- Gurney, J.J., Helmstaedt, H.H., LeRoex, A.P., Nowicki, T.E., Richardson, S.H. and Westerlund, K.J. 2005: Diamonds: crustal distribution and formation processes in time and space and an integrated deposit model; *Economic Geology 100th Anniversary Volume*, p. 143–177.
- Halden, N.M., Clark, G.S., Corkery, M.T., Lenton, P.G. and Schledewitz, D.C.P. 1990: Trace-element and Rb-Sr whole-rock isotopic constraints on the origin of the Chipewyan, Thorsteinson, and Baldock batholiths, Churchill Province, Manitoba; *in* The Early Proterozoic Trans-Hudson Orogen of North America, J.F. Lewry and M.R. Stauffer (ed.), Geological Association of Canada, Special Paper 37, p. 201–214.
- Hart, T.R., Gibson, H.L. and Leshner, C.M. 2004: Trace element geochemistry and petrogenesis of felsic volcanic rocks associated with volcanogenic massive Cu-Zn-Pb sulfide deposits; *Economic Geology*, v. 99, p. 1003–1013.
- Hodder, T.J. 2015: Ice-flow mapping and till sampling in the northern area of Southern Indian Lake, north-central Manitoba (parts of NTS 64G7-10); *in* Report of Activities 2015, Manitoba Mineral Resources, Manitoba Geological Survey, p. 124–130.
- Hodder, T.J. 2017: Kimberlite-indicator-mineral results derived from glacial sediments (till) in the Southern Indian Lake area of north-central Manitoba (parts of NTS 64B15, 64G1, 2, 7, 8); Manitoba Growth, Enterprise and Trade, Manitoba Geological Survey, Open File OF2017-2, 6 p.
- Hodder, T.J. 2018: Ice-flow history and till composition of the Southern Indian Lake area, north-central Manitoba (parts of NTS64G1, 2, 7–10, 64B15); Manitoba Growth, Enterprise and Trade, Manitoba Geological Survey, Open File OF2018-1, 21 p.
- Hoffman, P.F. 1981: Autopsy of Athapuscow Aulacogen: a failed arm affected by three collisions; *in* Proterozoic Basins of Canada, F.H.A. Campbell (ed.), Geological Survey of Canada, Paper 81-10, p. 97–101.
- Hoffman, P.F. 1987: Early Proterozoic foredeeps, foredeep magmatism, and Superior-type iron-formations of the Canadian Shield; *in* Proterozoic Lithospheric Evolution, A. Kroner (ed.), American Geophysical Union, Geodynamics Series, v. 17, p. 85–98.
- Hoffman, P.F. 1988: United plates of America, the birth of a craton: early Proterozoic assembly and growth of Laurentia; *Annual Review of Earth and Planetary Sciences*, v. 16, p. 543–603.
- Jenner, G.A. 1996: Trace element geochemistry of igneous rocks: geochemical nomenclature and analytical geochemistry; *in* Trace Element Geochemistry of Volcanic Rocks: Applications for Massive Sulfide Exploration, D.A. Wyman (ed.), Geological Association of Canada, Short Course Notes, v. 12, p. 51–77.
- Jensen, L.S. and Pyke, D.R. (1982): Komatiites in the Ontario portion of the Abitibi belt; *in* Komatiites, N.T. Arndt and E.G. Nisbet (ed.), George Allen and Unwin, London, p. 147–157.
- Kelemen, P.B., Johnson, K.T.M., Kinzler, R.J. and Irving, A.J. 1990: High-field-strength element depletions in arc basalts due to mantle–magma interaction; *Nature*, v. 345, p. 521–52.
- Kjarsgaard, B.A., Harvey, S., McClintock, M., Zonneveld, J.P., Du Plessis, P., McNeil, D. and Heaman, L. 2009: Geology of the Orion South kimberlite, Fort à la Corne, Canada; *Lithos*, v. 112S, p. 600–617.
- Kremer, P.D. 2008a: Bedrock geology of the Pukatawakan Bay area, Southern Indian Lake, Manitoba (part of NTS 64G2); Manitoba Science, Technology, Energy and Mines, Manitoba Geological Survey, Preliminary Map PMAP2008-3, scale 1: 25 000.
- Kremer, P.D. 2008b: Geological investigations of the Pukatawakan Bay belt, Southern Indian Lake, Manitoba (part of NTS 64G2); *in* Report of Activities 2008, Manitoba Science, Technology, Energy and Mines, Manitoba Geological Survey, p. 87–98.
- Kremer, P.D. and Martins, T. 2014a: Bedrock geology of the Northern Indian Lake area, Manitoba (parts of NTS 64H3, 5, 6); *in* Report of Activities 2014, Manitoba Mineral Resources, Manitoba Geological Survey, p. 131–139.

- Kremer, P.D. and Martins, T. 2014b: Geology of the Northern Indian Lake area, Manitoba (parts of NTS 64H3, 5, 6); Manitoba Mineral Resources, Manitoba Geological Survey, Preliminary Map PMAP2014-6, scale 1:50 000.
- Kremer, P.D., Corkery, M.T. and Lenton, P.G. 2009a: Bedrock geology of the Partridge Breast Lake belt, Manitoba (parts of NTS 64G1, 2, 8, 64H4, 5); Manitoba Innovation, Energy and Mines, Manitoba Geological Survey, Preliminary Map PMAP2009-2, scale 1:50 000.
- Kremer, P.D., Rayner, N. and Corkery, M.T. 2009b: New results from geological mapping in the west-central and northeastern portions of Southern Indian Lake, Manitoba (parts of NTS 64G1, 2, 8, 64H4, 5); *in* Report of Activities 2009, Manitoba Innovation, Energy and Mines, Manitoba Geological Survey, p. 94–107.
- Kretz, R. 1967: Granite and pegmatite studies at Northern Indian Lake, Manitoba; Geological Survey of Canada, Bulletin 148, 42 p.
- Le Bas, M.J., Le Maitre, R.W., Streckeisen, A. and Zanettin, B. 1986: A chemical classification of volcanic rocks based on the total alkali silica diagram; *Journal of Petrology*, v. 27, p. 745–750.
- LeCheminant, A.N. and Heaman, L.M. 1989: Mackenzie igneous events, Canada: Middle Proterozoic hotspot magmatism associated with ocean opening; *Earth and Planetary Science Letters*, v. 96, p. 38–48.
- Lenton, P.G. and Corkery, T. 1981: The Lower Churchill River project (interim report); Manitoba Energy and Mines, Mineral Resources Division, Geological Services, Open File Report OF81-3, 23 p. plus 2 maps at 1:250 000 scale and 7 maps at 1:100 000 scale.
- Leshner, C.M., Goodwin, A.M., Campbell, I.H. and Gorton, M.P. 1986: Trace-element geochemistry of ore-associated and barren, felsic metavolcanic rocks in the Superior Province, Canada; *Canadian Journal of Earth Sciences*, v. 23, p. 222–237.
- Lewry, J.F., Stauffer, M.R. and Fumerton, S.L. 1981: A Cordilleran-type batholithic belt in the Churchill Province in Northern Saskatchewan; *Precambrian Research*, v. 14, no. 3–4, p. 277–313.
- Ludwig, K.R. 2003: Isoplot 3.00: a geochronological toolkit for Microsoft® Excel®; Berkeley Geochronology Center, Special Publication 4, 71 p.
- Ludwig, K.R. 2008: Isoplot 3.70: a geochronological toolkit for Microsoft® Excel®; Berkeley Geochronology Center, Special Publication 4, 76 p.
- MacHattie, T.G. 2001: Petrogenesis of the Wathaman batholith and La Ronge domain plutons in the Reindeer Lake area, Trans-Hudson Orogen, Saskatchewan; M.Sc. thesis, Memorial University, St. John's, Newfoundland and Labrador.
- MacLachlan, K. 2005: A tale of two transects: distribution of 2.38 to 2.55 Ga versus juvenile 1.89 to 1.86 Ga detritus in the Rottenstone Domain; *in* Summary of Investigations 2005, Volume 2, Saskatchewan Geological Survey, Saskatchewan Industry and Resources, Miscellaneous Report 2005-4.2, CD-ROM, Paper A-7, 19 p.
- MacLachlan, K., Rayner, N., Dunning, G. and Leugner, C. 2004: New results and ideas from the Rottenstone Domain project; *in* Summary of Investigations 2004, Volume 2, Saskatchewan Geological Survey, Saskatchewan Industry and Resources, Miscellaneous Report 2004-4.2, CD-ROM, Paper A-3, 21 p.
- MacLean, W.H. 1990: Mass change calculations in altered rock series; *Mineralium Deposita*, v. 25, p. 44–49.
- Martins, T. 2014: Whole-rock geochemical data from pegmatites at South Bay, Southern Indian Lake and Partridge Breast Lake, and fluorine-bearing granite at Thorsteinson Lake, Manitoba (parts of NTS 64G3–6, 8, 9, 64B11); Manitoba Mineral Resources, Manitoba Geological Survey, Data Repository Item DRI2014001, Microsoft® Excel® file.
- Martins, T. 2015a: Bedrock geology of the northern basin of Southern Indian Lake, north-central Manitoba (parts of NTS 64G7, 8, 9, 10); Manitoba Mineral Resources, Manitoba Geological Survey, Preliminary Map PMAP2015-4, scale 1:50 000.
- Martins, T. 2015b: Geological mapping in the northern basin of Southern Indian Lake, north-central Manitoba (parts of NTS 64G7, 8, 9, 10); *in* Report of Activities 2015, Manitoba Mineral Resources, Manitoba Geological Survey, p. 79–88.
- Martins, T. 2016a: Bedrock geology of central Southern Indian Lake, Manitoba (parts of NTS 64G1, 2, 7, 8); Manitoba Growth, Enterprise and Trade, Preliminary Map PMAP2016-6, scale 1:50 000.
- Martins, T. 2016b: Geological investigations at central Southern Indian Lake, north-central Manitoba (parts of NTS 64G1, 2, 7, 8); *in* Report of Activities 2016, Manitoba Growth, Enterprise and Trade, Manitoba Geological Survey, p. 126–134.
- Martins, T. 2016c: Rare metals in Manitoba: South Bay pegmatite field; Manitoba Growth, Enterprise and Trade, Manitoba Geological Survey, URL <<http://www.manitoba.ca/iem/geo/raremetals/pdfs/southbay.pdf>> [May 2018].
- Martins, T. and Kremer, P.D. 2013: Rare-metals scoping study of the Trans-Hudson orogen, Manitoba (parts of NTS 64G3–6, 8, 9, 64B11); *in* Report of Activities 2013, Manitoba Mineral Resources, Manitoba Geological Survey, p. 114–122.
- Martins, T. and McFarlane, C.R.M. 2016a: Evidence of juvenile-arc magmatism at Northern Indian Lake: implications for base-metal exploration in north-central Manitoba (parts of NTS 64H3, 5, 6); *in* Report of Activities 2016, Manitoba Growth, Enterprise and Trade, Manitoba Geological Survey, p. 135–141.
- Martins, T. and McFarlane, C.R.M. 2016b: U-Pb data for the Northern Indian Lake pluton, north-central Manitoba (parts of NTS 64H3, 5, 6); Manitoba Growth, Enterprise and Trade, Manitoba Geological Survey, Data Repository Item DRI2016006, Microsoft® Excel® file.
- Maxeiner, R.O., Corrigan, D., Harper, C.T., MacDougall, D.G. and Ansdell, K. 2005: Paleoproterozoic arc and ophiolitic rocks on the northwest-margin of the Trans-Hudson Orogen, Saskatchewan, Canada: their contribution to a revised tectonic framework for the orogen; *Precambrian Research*, v. 136, p. 67–106.
- McDonough, W.F. and Sun, S.-s. 1995: The composition of the Earth; *Chemical Geology*, v. 120, p. 223–253.
- McInnes, W. 1909: Explorations on the Churchill River and South Indian Lake, Saskatchewan and Manitoba; *in* Geological Survey of Canada, Summary Report, 1908, p. 87–94.
- McInnes, W. 1913: The basins of the Nelson and Churchill Rivers; Geological Survey of Canada, Memoir 30, 146 p. and accompanying map.
- McRitchie, W.D. 1978: Northern Indian Lake (Regional Correlation Program, 64H); *in* Report of Field Activities 1978, Manitoba Energy and Mines, Minerals Division, p. 24–36.
- Meyer, M.T. 1987: Geochronology and geochemistry of the Wathaman Batholith, the remnant of an Early Proterozoic continental arc in the Trans-Hudson orogen, Saskatchewan, Canada; M.Sc. thesis, University of Kansas, Lawrence, Kansas.
- Meyer, M.T., Bickford, M.E. and Lewry, J.F. 1992: The Wathaman Batholith: an Early Proterozoic continental arc in the Trans-Hudson orogenic belt, Canada; *Geological Society of America Bulletin*, v. 104, p. 1073–1085.
- Natural Resources Canada 1984: Northern Indian Lake; *in* Geoscience Data Repository for Geophysical Data, Magnetic-Radiometric-EM, Natural Resources Canada, URL <<http://gdr.aggr.nrcan.gc.ca/gdrdap/dap/search-eng.php>> [April 2015].
- Pearce, J.A. 1983: Role of the sub-continental lithosphere in magma genesis at active continental margins; *in* Continental Basalts and Mantle Xenoliths, C.J. Hawkesworth and M.J. Norry (ed.), Shiva Press, Nantwich, United Kingdom, p. 230–249.
- Pearce, J.A. 2008: Geochemical fingerprinting of oceanic basalts with applications to ophiolite classification and the search for Archean oceanic crust; *Lithos*, v. 100, p. 14–48.

- Pearce, J.A. and Cann, J.R. 1973: Tectonic setting of basic volcanic rocks determined using trace element analyses; *Earth and Planetary Science Letters*, v. 19, p. 290–300.
- Pearce, J.A. and Peate, D.W. 1995: Tectonic implications of the composition of volcanic arc magmas; *Annual Review of Earth and Planetary Sciences*, v. 23, p. 251–285.
- Pearce, J.A. and Stern, R.J. 2006: Origin of back-arc basin magmas: trace element and isotope perspectives; in *Back-Arc Spreading Systems: Geological, Biological, Chemical, and Physical Interactions*, D.M. Christie, C.R. Fisher, S-M. Lee and S. Givens (ed.), American Geophysical Union, Geophysical Monograph Series, v. 166, p. 63–86.
- Pearce, J.A., Harris, N.B.W. and Tindle, A.G. 1984: Trace element discrimination diagrams for the tectonic interpretation of granitic rocks; *Journal of Petrology*, v. 25, p. 956–983.
- Perfit, M.R., Gust, D.A., Bence, A.E., Arculus, R.J. and Taylor, S.R. 1980: Chemical characteristics of island arc basalts: implications for mantle sources; *Chemical Geology*, v. 30, p. 227–256.
- Petrus, J.A. and Kamber, B.S. 2012: VizualAge: a novel approach to laser ablation ICP-MS U-Pb geochronology data reduction; *Geo-standards and Geoanalytical Research*, v. 36, p. 247–280.
- Poulsen, K.H. 1996: Lode gold; in *Geology of Canadian Mineral Deposit Types*, O.R. Eckstrand, W.D. Sinclair and R.I. Thorpe (ed.), Geological Survey of Canada, Geology of Canada, no. 8, p. 323–328.
- Quandt, D., Ekstrom, C. and Triebel, K. 2008: Technical report for the Fort Knox mine; Kinross Gold Corporation, URL <<http://www.kinross.com/pdf/operations/Technical-Report-Fort-Knox.pdf>> [September 2015].
- Quinn, H.A. 1960: Big Sand Lake, Manitoba; Geological Survey of Canada, Map 45-1959, scale 1:253 440.
- Ray, G.E. and Wanless, R.K. 1980: The age and geological history of the Wollaston, Peter Lake and Rottenstone domains in northern Saskatchewan; *Canadian Journal of Earth Sciences*, v. 17, p. 333–347.
- Rayner, N. 2013: Geochronological data for sample 107-09-207a, Southern Indian Lake, Manitoba (part of NTS 64G08); Manitoba Innovation, Energy and Mines, Manitoba Geological Survey, Data Repository Item DRI2013001, Microsoft® Excel® file.
- Rayner, N. and Corrigan, D. 2004: Uranium-lead geochronological results from the Churchill River–Southern Indian Lake transect, northern Manitoba; Geological Survey of Canada, Current Research 2004-F1, 14 p.
- Rayner, N., Stern, R.A. and Bickford, M.E. 2005: Tectonic implications of new SHRIMP and TIMS U-Pb geochronology of rocks from the Sask Craton, Peter Lake Domain, and Hearne margin, Trans-Hudson Orogen, Saskatchewan; *Canadian Journal of Earth Sciences*, v. 42, p. 635–657.
- Ross, P.-S. and Bédard, J.H. 2009: Magmatic affinity of modern and ancient subalkaline volcanic rocks determined from trace-element discriminant diagrams; *Canadian Journal of Earth Sciences*, v. 46, p. 823–839.
- Saskatchewan Ministry of Energy and Resources (2018): Saskatchewan Mineral Deposit Index file number 5341, URL <<http://www.economy.gov.sk.ca/dbsearch/MinDepositQuery/default.aspx?ID=5341>> [April 2018].
- Saunders, A.D. and Tarney, J. 1984: Geochemical characteristics of basaltic volcanism in back-arc basins, in *Marginal Basin Geology: Volcanic and Associated Sedimentary and Tectonic Processes in Modern and Ancient Marginal Basins*, B.P. Kokelaar and M.F. Howells (ed.), Geological Society of London, Special Publications, v. 16, p. 59–76.
- Saunders, A.D., Norry, M.J., and Tarney, J. 1991: Fluid influence on the trace element composition of subduction zone magmas; *Philosophical Transactions of the Royal Society of London*, v. 335, p. 377–392.
- Schmidberger, S.S., Heaman, L.M., Simonetti, A., Creaser, R.A. and Whiteford, S. 2007: Lu-Hf, in-situ Sr and Pb isotope and trace element systematics for mantle eclogites from the Diavik diamond mine: evidence for Paleoproterozoic subduction beneath the Slave craton, Canada; *Earth and Planetary Science Letters*, v. 254, p. 55–68.
- Simonetti, A., Heaman, L.M., Hartlaub, R.P., Creaser, R.A., MacHattie, T.G. and Böhm, C. 2005: U-Pb zircon dating by laser ablation-MC-ICP-MS using a new multiple ion counting Faraday collector array; *Journal of Analytical Atomic Spectrometry*, v. 20, p. 677–686.
- Smith, M., Thompson, J.F.H., Bressler, J., Layer, P., Mortensen, J.K., Abe, I. and Takaoka, H. 1999: Geology of the Liese zone, Pogo property, east-central Alaska; *Society of Economic Geologists, Newsletter* 38, p. 1–21.
- Stacey, J.S. and Kramers, J.D. 1975: Approximation of terrestrial lead isotope evolution by a 2-stage model; *Earth and Planetary Science Letters*, v. 26, no. 2, p. 207–221.
- Stauffer, M.R. 1984: Manikewan and early Proterozoic ocean in central Canada, its igneous history and orogenic closure; *Precambrian Research*, v. 25, p. 257–281.
- Steeves, M.A. and Lamb, C.F. 1972: Geology of the Issett-Opachuanau-Pemichigamau-Earp Lakes area; Manitoba Department of Mines, Resources and Environmental Management, Mines Branch, Publication 71-2F.
- Stern, R.A. 1997: The GSC sensitive high resolution ion microprobe (SHRIMP): analytical techniques of zircon U-Th-Pb age determinations and performance evaluation; in *Radiogenic Age and Isotopic Studies*, Report 10; Geological Survey Canada, Current Research 1997-F, p. 1–32.
- Stern, R.A. and Amelin, Y. 2003: Assessment of errors in SIMS zircon U-Pb geochronology using a natural zircon standard and NIST SRM 610 glass; *Chemical Geology*, v. 197, no. 1–4, p. 111–142.
- Streckeisen, A. 1967: Classification and nomenclature of igneous rocks: final report of an inquiry; *Newes Jahrbuch fur Mineralogie, Abhandlungen*, v. 107, p. 144–204.
- Sun, S.-s. and McDonough, W.F. 1989: Chemical and isotopic systematics of oceanic basalts: implications for mantle composition and processes; in *Magmatism in the Ocean Basins*, A.D. Saunders and M.J. Norry (ed.), Geological Society of London, Special Publications, v. 42, p. 313–345.
- Tanaka, T., Togashi, S., Kamioka, H., Amakawa, H., Kagami, H., Hamamoto, T., Yuhara, M., Orihashi, Y., Yoneda, S., Shimizu, H., Kunimaru, T., Takahashi, K., Yanagi, T., Nakano, T., Fujimaki, H., Shinjo, R., Asahara, Y., Tanimizu, M. and Dragusanu, C. 2000: JNdi-1: a neodymium isotopic reference in consistency with LaJolla neodymium; *Chemical Geology*, v. 168, p. 279–281.
- Thomas, K.A. 1972: Geology of the Southern Indian Lake area, southwestern portion; Manitoba Department of Mines, Resources and Environmental Management, Mines Branch, Publication 72-2H, 20 p.
- Trommelen, M.S. 2015: Till composition and glacial history, Gauer Lake–Wishart Lake area, Manitoba (NTS 64H4, 5, 12, 13); Manitoba Mineral Resources, Manitoba Geological Survey, Geoscientific Paper GP2014-1, 32 p. plus 14 appendices.
- Unterschutz, J.L.E., Creaser, R.A., Erdmer, P.R., Thompson, I. and Daughtry, K.L. 2002: North American margin origin of Quesnel terrane strata in the southern Canadian Cordillera: inferences from geochemical and Nd isotopic characteristics of Triassic metasedimentary rocks; *Geological Society of America Bulletin*, v. 114, p. 462–475.
- Van Schmus, W.R. and Schledewitz, D.C.P. 1986: U-Pb zircon geochronology of the Big Sand Lake area, northern Manitoba; in *Report of Field Activities 1986*, Manitoba Energy and Mines, Minerals Division, p. 207–210.

- Whalen, J.B. and Chappell, B.W. 1988: Opaque mineralogy and mafic mineral chemistry of I-and S-type granites of the Lachlan fold belt, southeast Australia; *American Mineralogist*, v. 73, p. 281–296.
- Wasserburg, G.J., Jacobsen, S.B., DePaolo, D.J., McCulloch, M.T. and Wen, T. 1981: Precise determination of Sm/Nd ratio, Sm, Nd isotopic abundances in standard solutions; *Geochimica et Cosmochimica Acta*, v. 45, p. 2311–2323.
- Winchester, J.A. and Floyd, P.A. 1977: Geochemical discrimination of different magma series and their differentiation products using immobile elements; *Chemical Geology*, v. 20, p. 325–343.
- White, W.M. and Dupré, B. 1986: Sediment subduction and magma genesis in the Lesser Antilles: isotopic and trace element constraints; *Journal of Geophysical Research*, v. 91, p. 5927–5941.
- Wood, D.A. 1980: The application of a Th-Hf-Ta diagram to problems of tectonomagmatic classification and to establishing the nature of crustal contamination of basaltic lavas of the British Tertiary volcanic province; *Earth and Planetary Science Letters*, v. 50, p. 11–30.
- Wright, G.M. 1953: Uhlman Lake map-area, Manitoba (preliminary account); *Geological Survey of Canada, Paper 53-12*, 5 p.
- Zwanzig, H.V. and Bailes, A.H. 2010: Geology and geochemical evolution of the northern Flin Flon and southern Kisseynew domains, Kississing–File lakes area, Manitoba (parts of NTS 63K, N); Manitoba Innovation, Energy and Mines, Manitoba Geological Survey, Geoscientific Report GR2010-1, 135 p.